博士論文

The study on proliferation, differentiation and maintenance of functional expressions of human hepatocytes *in vitro*

ヒト肝細胞の *in vitro* における増殖、分化、機能発現メカニズムに関する研究

山崎　ちひろ

山口大学大学院創成科学研究科

CONTENTS

Publication of the thesis

(1) Chihiro Yamasaki, Chise Tateno, Akio Aratani, Chimoto Ohnishi, Shigeru Katayama, Toshihiko Kohashi, Hiroshi Hino, Hiroyuki Marusawa, Toshimasa Asahara and Katsutoshi Yoshizato: Growth and Differentiation of Colony-forming human hepatocytes *In vitro*. Journal of hepatology 2006, 44: 749-757.

(2) Chihiro Yamasaki, Miho Kataoka, Yumiko Kato, Masakazu Kakuni, Sadakazu Usuda, Yoshihiro Ohzone, Sunao Matsuda, Yasuhisa Adachi, Shin-ichi Ninomiya, Toshiyuki Itamoto, Toshimasa Asahara, Katsutoshi Yoshizato and Chise Tateno: *In vitro* evaluation of cytochrome P450 and glucuronidation activities in hepatocytes isolated from liver-humanized mice. Drug Metabolism and Pharmacokinetics 2010, 25: 539-550.

(3) Chihiro Yamasaki, Yuji Ishida, Ami Yanagi, Yasumi Yoshizane, Yuha Kojima, Yuko Ogawa, Yutaka Kageyama, Yumiko Iwasaki, Seiichi Ishida, Kazuaki Chayama, and Chise Tateno: Culture density contributes to hepatic functions of fresh human hepatocytes isolated from chimeric mice with humanized livers: Novel, long-term, functional two-dimensional *in vitro* tool for developing new drugs. PLoS One. 2020 Sep 11;15(9):e0237809. doi: 10.1371/journal.pone.0237809. eCollection 2020. PMID: 32915792

I. General introduction

Hepatocytes, parenchymal cells of the liver, perform important functions such as metabolism, detoxification, and protein synthesis for supporting homeostasis of the body. Hence, human hepatocytes are essential materials for research of drug discovery. However, it is limited to obtain human hepatocytes from liver of brain-dead donors or normal part of tissues excised by surgery, because donors as source of supply are shortage. Furthermore, most of hepatocytes are not able to proliferate and lose metabolic functions *in vitro*. These problems are a bottleneck in research of drug discovery. This study aims to establish a method for obtaining a large number of functional human hepatocytes having drug metabolizing activities for long term *in vitro*.

Generally isolated hepatocytes cannot be maintained as replicating differentiated cells *in vitro*. In the previous study, we reported that small sized hepatocytes isolated from rat or h-livers showed highly proliferative ability under an appropriate culture condition [1-4]. Therefore, in Chapter II, I tried to develop a method for propagating h-hepatocytes *in vitro*. As a result, I demonstrated the presence of colony forming parenchymal hepatocytes (CF-PHs) in humans and characterize them with respect to growth and differentiation potential. In this study, I established a method of propagating primary h-hepatocytes *in vitro*. However, I considered that it is difficult to obtain large amount of differentiated h-hepatocytes using this method, because ratio of CF-PHs was very low (~0.1%) in h-hepatocytes.

In the previous study, our group tried to propagate h-hepatocytes in mouse liver (*in vivo*) in order to obtain them more efficiently than *in vitro* procedure. As a result, we succeeded in producing a chimeric mouse (PXB-mouse) in which 70% or more of the liver was replaced with human hepatocytes by transplanting ch-hepatocytes into the liver of urokinase-type plasminogen activator (uPA)/severe combined immunodeficient (SCID) mice or cDNA-uPA/SCID mice [5, 6]. PXB-mice are considered a useful animal

model for predicting h-drug metabolism, toxicity and efficacy. Transplanted h-hepatocytes were able to proliferate 500 to 1000 times in the host mouse liver. We were able to obtain large amount of fresh h-hepatocytes from PXB-mice (PXB-cells) by a collagenase perfusion method.

In Chapter III –(1) and III-(2), I determined whether the PXB-mouse could serve as a novel source of fresh h-hepatocytes for *in vitro* drug development studies.

In Chapter III-(1), PXB-cells were isolated from PXB-mice, and cytochrome P450 (CYP) 1A2, 2C9, 2C19, 2D6, 2E1, 3A and UDP-glucuronosyltransferase (UGT) activities of PXB-cells were determined and compared with ch-hepatocytes. Effects of cryopreservation of PXB-cells on CYP and UGT activities were also analyzed.

Recently, we demonstrated that cultured PXB-cells were susceptible to HBV infection and that HBV-infected PXB-cells can be maintained for more than 3 weeks when the PXB-cells were cultured on collagen-coated dishes at a high density (2.13×10^5cells/cm^2) [7]. Therefore, PXB-cells have been used for *in vitro* efficacy studies of anti-HBV agents [7]. In those studies, we found that PXB-cells can attach to collagen-coated dishes in high density cultures without the detachment seen in rodent hepatocytes and can be maintained for more than 3 weeks [7].

In Chapter III-(2), we determined CYP, UGT, transporter mRNA expression and the activities of CYP3A and multidrug resistance-associated protein (MRP2) transporter and bile salt export pump (BSEP) in the high density 2D-cultures of PXB-cells for 21 days. I also evaluated differences in donors and individual PXB-mice using ch-hepatocytes isolated from three different donors. Finally, the role of the high density culture condition was determined by microarray analysis of PXB-cells cultured at high and low density.

References

1) Tateno C, Yoshizato K. Long-term cultivation of adult rat hepatocytes that undergo multiple cell divisions and express normal parenchymal phenotypes. Am J Pathol 1996;148:383–392.

2) Tateno C, Yoshizato K. Growth and differentiation in culture of clonogenic hepatocytes that express both phenotypes of hepatocytes and biliary epithelial cells. Am J Pathol 1996;149:1593–1605.

3) Tateno C, Takai-Kajihara K, Yamasaki C, Sato H, Yoshizato K. Heterogeneity of growth potential of adult rat hepatocytes *in vitro*. Hepatology 2000;31:65–74.

4) Hino H, Tateno H, Sato H, Yamasaki C, Katayama S, Kohashi T, et al. A long-term culture of human hepatocytes which show a high growth potential and express their differentiated phenotypes. Biochem Biophys Res Commun 1999;256:184–191

5) Tateno C, Yoshizane Y, Saito N, Kataoka M, Utoh R, Yamasaki C, et al. Near completely humanized liver in mice shows human-type metabolic responses to drugs. Am J Pathol. 2004;165(3):901-12. Epub 2004/08/28. doi: 10.1016/s0002- 52 9440(10)63352-4. PubMed PMID: 15331414; PubMed Central PMCID: PMCPmc1618591

6) Tateno C, Kawase Y, Tobita Y. Hamamura S, Ohshita H, Yokomichi H, et al. Generation of novel chimeric mice with humanized livers by using hemizygous cDNA-uPA/SCID mice. PLoS One. 2015;10(11): e0142145. doi: 10.1371/journal.pone.0142145. PubMed PMID: 26536627.

7) Ishida Y, Yamasaki C, Yanagi A, Yoshizane Y, Fujikawa K, Watashi K, et al. Novel robust *in vitro* hepatitis B virus infection model using fresh human hepatocytes isolated from humanized mice. Am J

Pathol. 2015;185(5):1275-85. doi: 10.1016/j.ajpath.2015.01.028. PubMed PMID: 25791527.

II. Growth and differentiation of colony-forming human hepatocytes *in vitro*

Abstract

Background/Aims: Parenchymal hepatocytes (PHs) of rat contain colony-forming parenchymal hepatocytes (CF-PHs) as a small fraction. We aimed to demonstrate the presence of CF-PHs in humans and characterize them with respect to growth and differentiation potential.

Methods: Human PHs were co-cultured with Swiss 3T3 cells in the medium containing human serum, EGF, nicontinamide, and ascorbic acid 2- phosphate. To examine differentiation potential hepatocytes were cultured on gels of Matrigel Matrix.

Results: Few PHs formed colonies, the colony-forming efficiency being as low as 0.01-0.09%. The CF-PHs could be subcultured up to 7 passages. They showed a liver epithelial cell-like morphology, and immunocytochemically positive for albumin (ALB), cytokeratin (CK) 7, 8, 18, and 19 in a pre- and early phase-confluence, whereas they showed a typical differentiated hepatocyte-like morphology, and positive for α_1-antitrypsin, but negative for CK7 and 19 in condensed regions at confluence. The CF-PHs at late confluence expressed mRNAs of ALB, HNF4, and isoforms of cytochrome P450 at low levels. However, when cultured on Matrigel, these cells expressed them at high levels comparable to those of original PHs.

Conclusions: We concluded that the human liver contains highly replicative hepatic progenitor-like cells as a minute population that retain a normal differentiation potential.

Introduction

Generally, hepatocytes *in vitro* can be maintained as replicating differentiated cells for a limited period. We devised a culture medium, hepatocyte clonal growth medium (HCGM), that supports the growth of rat hepatocytes for a longer period [1-3]. Using HCGM we were able to demonstrate the presence of the colony-forming parenchymal hepatocytes (CF-PHs) as small hepatocytes (SHs) that have a much higher growth potential than conventional PHs [3]. We also showed the presence of replicative human SHs that continue to increase the colony size up to around 35 days when cultured in modified HCGM containing human serum (HS) and Swiss 3T3 cell-conditioned medium (3T3-CM) [4]. However, CF-PHs have not been isolated as a pure fraction and, thus, not been characterized well yet.

The present study was performed, firstly, to determine the occupancy of CF-PHs in the human liver, secondly, to propagate them by serial subculture, and, thirdly, to characterize them in terms of differentiation potential. As a result, we demonstrated the presence of CF-PHs in human PHs and were able to obtain a pure fraction of CF-PHs by serial subcultivation. CF-PHs were characterized in terms of growth potential and differentiation capacity.

Materials and methods

Isolation, cryopreservation, and thawing of human hepatocytes

The present study was performed under the ethical approval of the Hiroshima Prefectural Institute of Industrial Science and Technology Ethics Board. Liver tissues were obtained from 15 donors (Table 1) in hospitals after receiving their consent before operations according to the 1975 Helsinki declaration.

Hepatocytes were isolated as previously [4] with some modifications. Previously we isolated a SH-containing NPC fraction as the centrifugal supernatant at 50 x g for 1 min [4]. In the present study we isolated PHs as the pellets at 50 x g for 2 min, because their colony-forming efficiency (0.063%) was much higher than that (0.013%) at 50 x g for I min. Some of the isolated PHs were cryopreserved and thawed as previously [5]. These cryopreserved and thawed (C-T) PHs were dubbed C-T PHs. The viability of cells was determined by the trypan blue exclusion test. Cells were counted with a hemocytometer. We also used cryopreserved human hepatocytes from a 9-month-old Caucasian boy (IVT079) provided by *In vitro* Technologies Inc.(Baltimore, MD). The hepatocytes were thawed as described above. These hepatocytes were called C-T 9MM.

Culture of PHs

PHs were inoculated at 8 x 10^3 cells/cm^2 in 35-mm dishes (Becton Dickinson Labware, Franklin, NJ) containing 1.8 ml of h-HCGM for cultures and on Sumilon Celldesks (Sumitomo Bakelite, Tokyo, Japan) in 24-well plates (Becton Dickinson Labware) containing 0.4 ml of h-HCGM for immunocytochemical examinations except that PHs isolated from donor No. 16F1 were inoculated at 4 x 10^3 cells/cm^2 in dishes and Celldesks. The ingredients and their concentrations of h-HCGM were identical to the previously

reported HCGM [4] except that 3T3-CM and dimethyl sulfoxide (DMSO) were not incorporated. The cells were cultured at 37˚C in a 5% CO_2-incubator. Swiss 3T3 cells (American Type Culture Collection, Rockville, MD) were treated with mitomycin C [6] and were added at 4 x 10^3 cells /cm^2 to the cultures at the next day after the start of culture and every 10 days during culture. h-HCGM was refilled twice per week during culture.

PHs in primary culture grew and became confluent in 35-mm dishes around 30 days after plating. For serial subculturing, the cells were detached by treating with 0.25% trypsin and 1 mM EDTA, and inoculated at 4 x 10^3 cells/cm^2 in new 35-mm dishes. Swiss 3T3 cells were incorporated into the dishes as above.

The concentration of albumin (ALB) in culture media was determined with Human ALB ELISA Quantitation Kit (Bethyl laboratories Inc., Montgomery, TX). Cellular proteins were quantified with Protein Assay Kit (Bio-Rad, Hercules, CA) as previously [7].

Determination of colony-forming efficiency of PHs

PHs were cultured on Celldesks, fixed in -30˚C ethanol at 20 days, and stained with anti-cytokeratin (CK) 18 mouse monoclonal antibodies (Amersham Pharmacia Biotech, Piscateway, NJ). Hepatocyte colonies were counted as clusters containing more than 8 CK18-positive ($CK18^+$) cells, and the colony-forming efficiency was calculated by dividing the number of colonies by the number of inoculated PHs.

Immunocytochemistry

Cells were fixed in ethanol at -30˚C. The following primary antibodies were used: rabbit antibodies against human ALB (Dakopatts, Glostrup, Denmark), human a_1-antitrypsin (α_1-AT, Dakopatts), human α_1-fetoprotein (AFP, Dakopatts), and mouse monoclonal antibodies against CK8 (Amersham Pharmacia Biotech), CK18, CK7, and CK19 (Progen Biotechnik GmbH, Bretonneux, France). Antibodies were visualized as previously [2].

Culture of cells in spheroids

Matrigel Matrix solution (BD Biosciences, Bedford, MA) was dissolved in DMEM at 5 mg/ml, 2 ml of which was added into each well of 6-well plates. The plates were incubated at 37˚C for 30 min. CF-PHs from donor No. 12M (12M-CF-PHs) at 3 passages in subculture or HepG2 cells were inoculated at 10^5 cells/cm^2 onto the gels, and were cultured at 37˚C ("spheroid culture") in h-HCGM. At 24 h after plating the media were changed to d-HCGM prepared by adding DMSO at 1% to h-HCGM, and removing nicotinamide and HS from it. The d-HCGM was refilled every 3 days during culture. Spheroids were recovered with BD Cell Recovery Solution (BD Biosciences).

Quantification of mRNAs

We examined whether C-T procedures had caused breaks in RNA of PHs. Total RNAs were extracted from fresh and C-T PHs of 3 donors, 51M, 53M2, and 68F, and electrophoresed on agarose gels. There were no significant differences in the banding patterns of 28S and 18S RNA between fresh and the corresponding C-T PHs, which indicated that the C-T procedure did not cause such breaks.

12M-CF-PHs at 3 passages in subculture were divided into two groups. One group was cultured in

dishes as monolayers and the other group was cultured on Matrigel as spheroids. HepG2 cells were similarly treated. Total RNAs were obtained from these 4 different cell preparations. cDNAs were synthesized using 1 μg of total RNA, PowerScript RT (Clontech labolatories, Inc., Palo Alto, CA) and Oligo(dT)12-18 primers according to the manufacturer's instruction. mRNAs of genes indicated in the text were measured by real-time quantitative RT-PCR using the previous primers [5] except those for AFP (forward, 5'-CAGCCAAAGTGAAGAGGGAAGA; reverse, 5'- CAGCTTGTGACAGGTTCTGGA) and a SYBR Green dye [8]. Copy numbers of mRNA in the cDNA samples were calculated as previously [8].

Results

Growth and morphology

C-T 9MM-PHs were thawed, seeded on dishes, and co-cultured with Swiss 3T3 cells up to 20 days (Fig. 1A-H). Some of the attached hepatocytes were marked and monitored for their growth during the culture. A small number of single cells started to divide at 5 days, grew slowly but steadily, and formed colonies. Similarly, freshly isolated 16F2-PHs were cultured up to 33 days for the observation of cell morphology (Fig. 1I and J). The cells showed a liver epithelial cell-like (flat and spread) morphology at 20 days when they were in a growing phase (Fig. 1I). They grew to confluence at 33 days after plating (Fig. 1J). The cells in condensed regions showed a typical hepatocyte-like (cuboidal and densely packed) morphology. PHs were obtained from 11 donors whose age ranged from 3 to 72 years and cultured for 20 days. The colony-forming efficiency was variable from 0.01% to 0.09%, but the efficiency significantly decreased as donors aged (Fig. 2A).

Growth of CF-PHs in subculture

PHs from both younger donors, 3M, 12M, 16F2, and older ones, 63M and 72M1, grew under serial subculture (Fig. 2B). Population doubling time (PDT) at passage 4 of older hepatocytes were larger than that of younger ones. The possible maximum passage number of CF-PHs of younger and older donors was 7 and 5, respectively. These results indicated that the growth potential of CF-PHs is correlated with the age of donor.

Phenotypes of CF-PHs in subculture

The expression of liver-specific marker proteins was determined during subculture of 3M- and 12M-CF-PHs. There were no noticeable differences in their expression profiles between 3M- and 12M-CF-PHs. 3M-CF-PHs at 2 passages were cultured up to 13 days when they were still in a pre-confluence or an early phase of confluence. These cells were $CK8^+$ (Fig. 3A) and $CK18^+$ (data not shown), markers of both hepatocytes and bile duct cells, and $CK7^+$ (data not shown) and $CK19^+$ (Fig. 3B), markers of bile duct cells. 12M-CF-PHs at 3 passages were further cultured up to 27 days when they became confluent. They were ALB^+ (Fig. 3C), a universal hepatocytic marker. Especially, CF-PHs in condensed regions were heavily ALB^+. CF-PHs expressed α_1-AT, a marker of mature hepatocytes, in condensed regions, but not in non-condensed regions (Fig. 3D). These cells were AFP^- (Fig. 3E), a marker of immature or neoplastic hepatocytes. The CF-PHs were also subjected to double immuno-staining for a_1-AT and CK19 (Fig. 3G, H, and I). CF-PHs in condensed regions were strongly α_1-AT^+ (Fig. 3G and I), but $CK19^-$ (Fig. 3H and I). Double immuno-staining of α_1-AT and CK7 showed that the CK7 expression pattern was identical to that of CK19 (data not shown).

Phenotypes of CF-PHs in spheroids

12M-CF-PHs at 3 passages were detached from dishes, and inoculated in dishes (Fig. 4A) or on Matrigel (Fig. 4C), and cultured for 7 days. Similarly, HepG2 cells were cultured as a reference cell (Fig. 4B and D). Both types of cells became confluent at 7 days in dishes (Fig. 4A and B). On Matrigel, both 12M-CF-PHs and HepG2 cells aggregated at 1 day and formed spheroids with diameter of approximately 100 μm at 7 days (Fig. 4C and D). CF-PHs of other donors such as 16F2 were also able to form spheroids.

12M-CF-PHs in spheroids were subjected to double immuno-staining for ALB and CK7 (or CK19). They were both ALB^+ and $CK7^+$ (also $CK19^+$) (data not shown). ALB secretion was quantified during culture (Fig. 5). The secretion level from 4 to 7 days increased 2.6-fold in monolayers as compared to that from 1 to 4 days, whereas the level increased 6.6-fold in spheroids.

The above results suggested that spheroid-culture induces CF-PHs to express differentiated phenotypes. To further demonstrate such effects of spheroid-culture, the expression level of mRNAs of hepatocyte-differentiation marker proteins were compared between monolayer- and spheroid-cultures. This comparative study was performed using C-T PHs. Thus, before such experiments, gene expression profiles of C-T PHs was investigated in relation to those of fresh PHs. Total RNAs were extracted from C-T and fresh PHs of 3 donors, and used for quantifying mRNA of glyceraldehyde-3-phosphate dehydrogenase (GAPDH), ALB, HNF4, and cytochrome P450 isozymes (CYPs) (Fig. 6A). mRNAs of GAPDH, CYP2C9, and CYP2C19 in C-T PHs were expressed at a similar level as in fresh PHs. The expression of CYP2D6 and CYP3A4 in C-T PHs was higher than in fresh ones, whereas that of ALB, HNF4, CYP1A1, and CYP1A2 was lower in C-T PHs.

C-T PHs were prepared from 12M. Aliquots of them were used for total RNA extraction and the remaining was subcultured to 3 passages. CF-PHs at 3 passages and HepG2 cells as a reference cell were cultured in monolayers and spheroids for 7 days, and used for total RNA extraction. These RNAs were used to measure mRNAs of GAPDH, ALB, HNF4, AFP, and CYPs by real-time RT-PCR. The expression level of GAPDH mRNA was similar among monolayer- and spheroid-cultures of both CF-PHs and HepG2 cells, which was higher than that of the original (C-T PHs) level (Fig.6B). CF-PHs in monolayer expressed mRNAs of ALB (Fig. 6C) and HNF4 (Fig. 6D) at low levels as compared to the original level. In contrast,

their expressions were significantly elevated to levels comparable to the original C-T PHs' level when cultured in spheroids. CF-PHs in both of monolayer-and spheroid-culture did not express AFP mRNA as in the case of C-T PHs (Fig. 6E). HepG2 expressed AFP mRNA at a high level. The original C-T PHs variably expressed mRNAs of CYPs (1A1, 1A2, 2C9, 2C19, 2D6, and 3A4) as shown in Fig. 6F. CF-PHs expressed them at very low levels in monolayer- culture. It was noteworthy that CF-PHs gained a mRNA expression profile of CYPs similar to that of the original C-T PHs in spheroid-culture. Such effects of spheroid-culture were not observed on HepG2 cells. They expressed mRNAs of ALB (Fig. 6C), HNF4 (Fig. 6D) and AFP (Fig. 6E) at a high level and expressed mRNAs of CYPs at an extremely low level (Fig. 6F) in both types of culture.

Discussion

Previously, we cultured a human nonparenchymal cell (NPC) fraction in medium containing 3T3-CM, and showed that CF-PHs present in the NPC fraction can grow well [4]. In the present study we made primary cultures of human PHs in the presence of Swiss 3T3 cells and demonstrated the presence of CF-PHs, their occupancy rate being quite low. We were able to propagate them by serial subculturing.

In primary cultures of human PHs, we observed a small number of single cells started to divide at 5 days, grew slowly but steadily, and formed colonies. Such CF-PHs were characterized by phenotyping at earlier time points of culture. Most of the hepatocytes were immunocytochemically ALB^+ and $CK19^-$. The primary hepatocyte population contained ALB^+ and $CK19^+$ cells at an occupancy rate of ~0.02%. The ratio of the number of colonies with ALB^+ and $CK19^+$ cells, and ALB^- and $CK19^+$ to that of total colonies at 4 days of primary culture was 80 and 20%, respectively. The cells in all the colonies observed so far at 7 and 21 days in primary culture were ALB^- and $CK19^+$, strongly suggesting that originally ALB^+ and $CK19^-$ cells became ALB^- and $CK19^+$ in the currently adopted culture conditions. Therefore, it is most likely that the biliary/progenitor cell features of CF-PHs are acquired during the periods of subculture. However, the possibility that ALB^+ and $CK19^+$ cells present at an occupancy rate of ~0.02% at the start expanded during culture can not be completely excluded at present.

Human CF-PHs were able to be subcultured within limited passages. CF-PHs from young donors could be passaged 7 times, PDT at passage 4 being170-220 h, and, then the cells became senescent. CF-PHs from older donors were passaged only 5 times at most. They grew more slowly, their PDT at passage 4 being 650-1200 h. These results suggested that replication potential of human CF-PHs is correlated with the age of donors. It should be emphasized that the cumulative population doubling level (CPDL) of CF-PHs from

younger donors, 3M and 12M, were as high as 19.3 and 24.7 during 300 days, respectively. Gibson-D'Ambrosio et al. serially passaged human PHs 12-15 times [9], using as medium supplemented with insulin, transferrin, hydrocortisone, EGF, and FBS. FBS was prescreened for their subculture, which was said to be important to obtain an optimal growth of the cells. Only 2 of the tested 7 FBS lots supported the growth of normal human PHs. PDT of PHs during subcultures was calculated as ~64 h. These PHs expressed ALB and CK18, but not AFP. At present, it is unclear whether these proliferative hepatocytes are identical to the CF-PHs characterized in the present study. CF-PHs showed a liver epithelial cell-like morphology when they were in the growth phase and in an early phase of confluence, whereas they showed a typical hepatocyte-like morphology in condensed regions at confluence. CF-PHs expressed ALB, and CK7, 19, 8, and 18, but not α_1-AT in the former conditions, indicating that these cells are able to express traits of both hepatocytes and biliary cells. In accordance with the morphological characteristics, CF-PHs in the condensed region expressed hepatocytic traits such as ALB, CK8 and 18, and a_1-AT, but not biliary traits such as CK7 and 19. Thus, the CF-PHs seem to be hepatic progenitor-like cells existing even in the adult liver.

Previously, we devised HCGM as a culture medium that supports the growth of rat PHs [1]. Rat PHs grew in HCGM when co-cultured with NPCs [2] or Swiss 3T3 cells [6]. The growth promoting activity of 3T3 cells was partly replaceable with 3T3-CM. The active principles in 3T3-CM were HGF and pleiotrophin [6, 8]. In the present study we showed that 3T3-CM also supported the growth of human PHs, although its activity was less than that of 3T3 cells (data not shown).

A putative adult rat hepatocyte progenitor cells, Lig-8, elevated the expression of proteins of C/EBPα, ALB, and CYPs when cultured in spheroids [10]. We examined whether human CF-PHs in spheroid culture

elevate differentiation-related genes. The mRNA expression level of ALB, HNF4, and CYPs of CF-PHs were low in monolayer-culture. However, when these CF-PHs were cultured in spheroid, they regained the expression of mRNAs of ALB and HNF4 to a level comparable to that of the original PHs, i.e., the cells before cultivation, and also regained a mRNA expression profile of CYPs of 2C9, 2C19, and 3A4 similar to that of original PHs. On the other hand, HepG2 cells expressed mRNAs of ALB and HNF4 even in monolayers to levels higher than those of PHs or cultured CF-PHs. In spite of such a high expression of HNF4 mRNA, HepG2 cells did not express CYP mRNAs in both monolayer- and spheroid-culture. Using an adenovirus-mediated antisense targeting method, a research group showed that the expression of CYPs in human PHs is regulated by HNF4 [11]. Currently, we suppose that human CF-PHs cultured in spheroids reexpress hepatocyte specific differentiation markers through the up-regulation of HNF4 expression.

In summary, the present study demonstrated the presence of CF-PHs, a highly replicative compartment of human PHs, even in the adult human liver. These CF-PHs can be serially subcultured, retaining their normal hepatocytic characteristics. These cultures should be useful to study the cellular and molecular mechanisms of growth, differentiation, toxicity, metabolism, and carcinogenesis of human hepatocytes.

Acknowledgements

We thank Y. Kodama and K. Watashi for help in the preparation of human liver tissues. This study was supported by grants from Hiroshima Prefecture CREATE, JST and CLUSTER, Japan.

References

1) Tateno C, Yoshizato K. Long-term cultivation of adult rat hepatocytes that undergo multiple cell divisions and express normal parenchymal phenotypes. Am J Pathol 1996;148:383-392.

2) Tateno C, Yoshizato K. Growth and differentiation in culture of clonogenic hepatocytes that express both phenotypes of hepatocytes and biliary epithelial cells. Am J Pathol 1996;149:1593-1605.

3) Tateno C, Takai-Kajihara K, Yamasaki C, Sato H, Yoshizato K. Heterogeneity of growth potential of adult rat hepatocytes *in vitro*. Hepatology 2000;31:65-74.

4) Hino H, Tateno H, Sato H, Yamasaki C, Katayama S, Kohashi T, et al. A long-term culture of human hepatocytes which show a high growth potential and express their differentiated phenotypes. Biochem. Biophys Res Commun 1999;256:184-191.

5) Tateno C, Yoshizane Y, Saito N, Kataoka M, Utoh R, Yamasaki C, et al. Near-completely humanized liver in mice shows human-type metabolic responses to drugs. Am J Pathol 2004;165:901-912.

6) Sato H, Funahashi M, Kristensen DB, Tateno C, Yoshizato K. Pleiotrophin as a Swiss 3T3 cell-derived potent mitogen for adult rat hepatocytes. Exp Cell Res 1999;46:152-164.

7) Xu J, Ma M, Purcell WM. Characterization of some cytotoxic endpoints using rat liver and HepG2 spheroids as *in vitro* models and their application in hepatotoxicity studies. II. Spheroid cell spreading inhibition as a new cytotoxic markers. Toxicol Appl Pharmacol 2003;189:112-119.

8) Asahina K, Sato H, Yamasaki C, Kataoka M, Shiokawa M, Katayama S, et al. Pleiotrophin/heparin-binding growth-associated molecule as a mitogen of rat hepatocytes and its role in regeneration and development of liver. Am J Pathol 2002;160:2191-2205.

9) Gibson-D'Ambrosio RE Crowe DL, Shuler CE D'Ambrosio SM. The establishment and continuous subculturing of normal human adult hepatocytes: expression of differentiated liver functions. Cell Biol Toxicol 1993;4;385-403.

10) Semino CE, Merok JR, Crane GG, Panagiotakos G, Zhang S. Functional differentiation of hepatocyte-like spheroid structures from putative liver progenitor cells in three-dimensional peptide scaffolds. Differentiation 2003;71:262-270.

11) Jover R, Bort R, Gomez-Lechon MJ, Castell JV. Cytochrome P450 regulation by hepatocyte nuclear factor 4 in human hepatocytes: a study using adenovirus-mediated antisense targeting. Hepatology 2001;33:668-675.

Table and figures

Table 1

Sources of liver tissues

Donor No.	Age	Sex	Disease of excised tissues	Wet weight (g)	Viability (%)
3M	3	male	Neuroblastoma	3.4	93.9
12M	12	male	Hepatocellular carcinoma	7.9	91.5
16F1	16	female	Focal nodular hyperplasia	40.4	88.5
16F2	16	female	OTC* deficiency	32.5	94.5
45F	45	female	Metastatic liver tumor	27.4	75.8
51M	51	male	Metastatic liver tumor	29.5	89.5
53M	53	male	Metastatic liver tumor	10.6	91.6
53M2	53	male	Metastatic liver tumor	16.4	93.8
58F	58	female	Cholangioma	6.4	95.5
61F	61	female	Metastatic liver tumor	4.4	80.4
63F	63	female	Metastatic liver tumor	15.7	89.3
63M	63	male	Metastatic liver tumor	5.4	87.3
68F	68	female	Metastatic liver tumor	27.2	92.2
72M1	72	male	Metastatic liver tumor	14.4	40.0
72M2	72	male	Metastatic liver tumor	24.2	93.5

*, Ornithine transcarbamylase

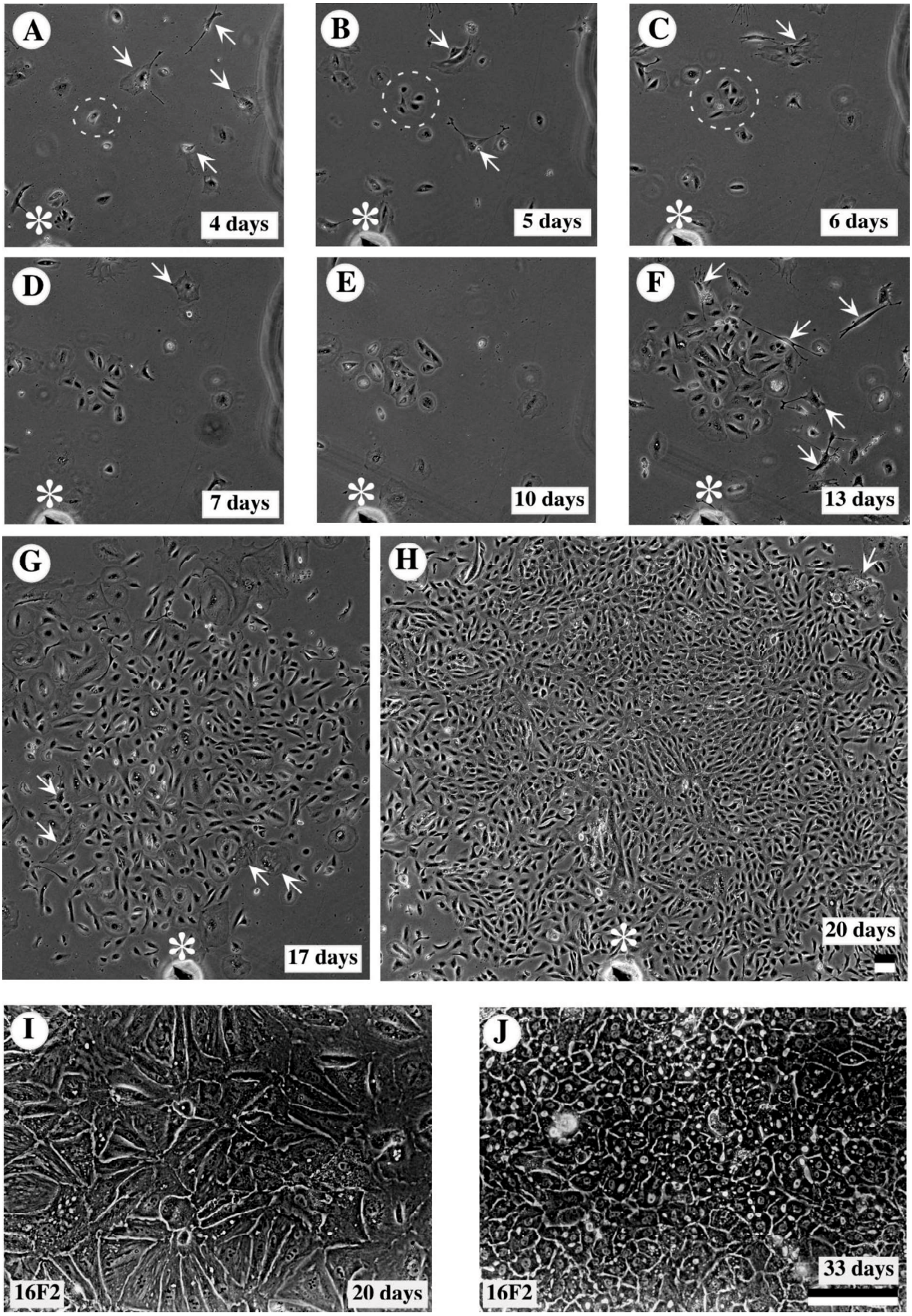
A
4 days
B
5 days
C
6 days
D
7 days
E
10 days
F
13 days
G
17 days
H
20 days
I
16F2
20 days
J
16F2
33 days

Fig. 1. Phase contrast microphotographs of PHs in culture. Thawed 9MM PHs were seeded at 8 x 10^3 cells/cm^2 in 35-mm dishes (growth area, 9.6 cm^2) and co-cultured up to 20 days with 4 x 10^3 Swiss 3T3 cells/cm^2 in h-HCGM (A-H). Freshly isolated 16F2-PHs were seeded at 8 x 10^3 cells/cm^2 in 35-mm dishes, and cultured up to 33 days as in16F1-PHs (I and J). The mark (*) was made on the back surface of the dishes on day 1 of culture to monitor the growth of seeded cells. A cell enclosed by dotted line in A was selected and monitored for the growth through 20 days by periodically taking phase contrast microphotographs. **A**. Day 4. **B**. Day 5. **C.** Day 6. **D.** Day 7. **E.** Day 10. **F.** Day 13. **G.** Day 17. **H.** Day 20. Arrows in A to H point to some of Swiss 3T3 cells. The size of colony increased gradually during culture. The area of colony was 0.0037, 0.0262, and 0.0685 cm^2 at 13, 17 and 20 days, respectively. Magnification of A to G is the same as in H. Bar in H, 100 μm. **I.** PHs at 20 days. **J.** PHs at 33 days. Magnification of I is the same as in J. Bar in J, 100 μm

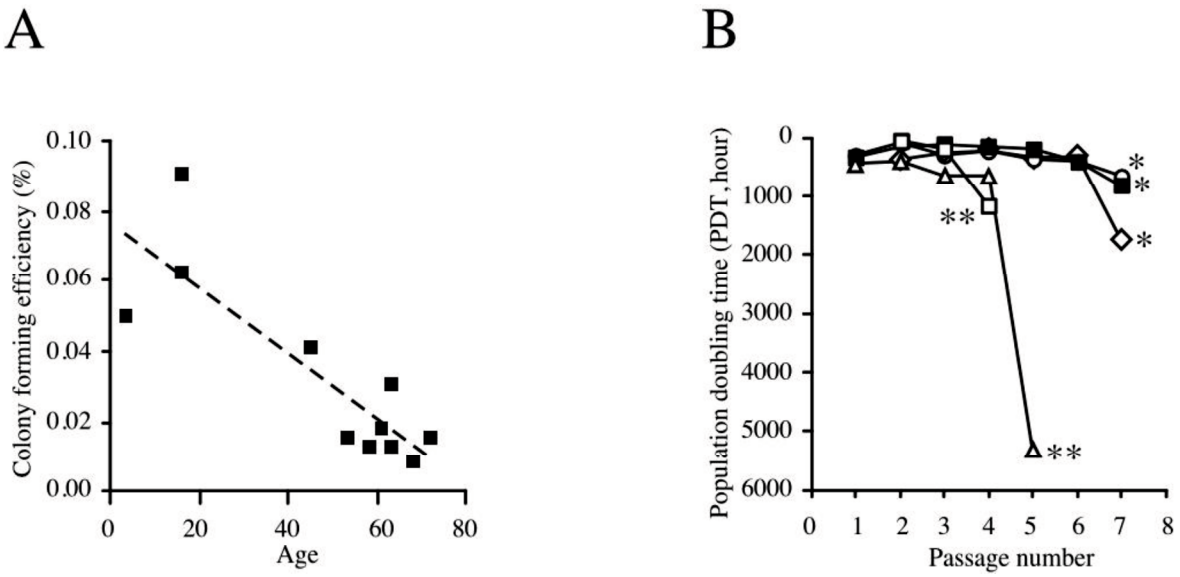

Fig. 2. Growth ability of CF-PHs. **A**. Colony-forming efficiency of PHs in relation to the age of donors. PHs were prepared from 3M, 16F1, 16F2, 45F, 53M, 58F, 61F, 63F, 63M, 68F, and 72M2, and were seeded at the density of 8 x 10^3 cells/cm^2, except PHs from 16F1 which were seeded at 4 x 10^3 cells/cm^2, and cultured for 20 days as in Fig. 1. The colony-forming efficiency was determined as the ratio (%) of number of colonies formed at 20 days of culture to that of the seeded PHs and plotted against the donor's age. The solid line represents the statistically significant regression curve ($y = -0.001x + 0.076$, $r^2 = 0.714$). **B**. Serial subcultivation of CF-PHs. PHs from 5 donors (3M, 12M, 16F2, 63M, and 72M1) were seeded at the density of 8 x 10^3 cells/cm^2, and cultured as in Fig. 1. They were detached as CF-PHs from the dishes at appropriate time points when they became confluent and subjected to subcultures, the seeding density being at 4 x 10^3 cells/cm^2 at each passage. Open rhombuses, 3M-CF-PHs; closed squares, 12M-CF-PHs; open circles, 16F2-CF-PHs; open triangles, 63M-CF-PHs; open squares, 72M1-CF-PHs. PDT at passage 4 of CF-PHs from 3M, 12M, 16F2, 63M, and 72M1 was 220.3, 170.7, 223.6, 649.4, and 1,162.0 h, respectively. Cultures of 3M-, 12M-, and 16F2-CF-PHs were terminated at passages marked by *, because they failed to grow thereafter. Cultures of 63M- and 72M1-CF-PHs were terminated at passages marked by **, because PDT became large thereafter.

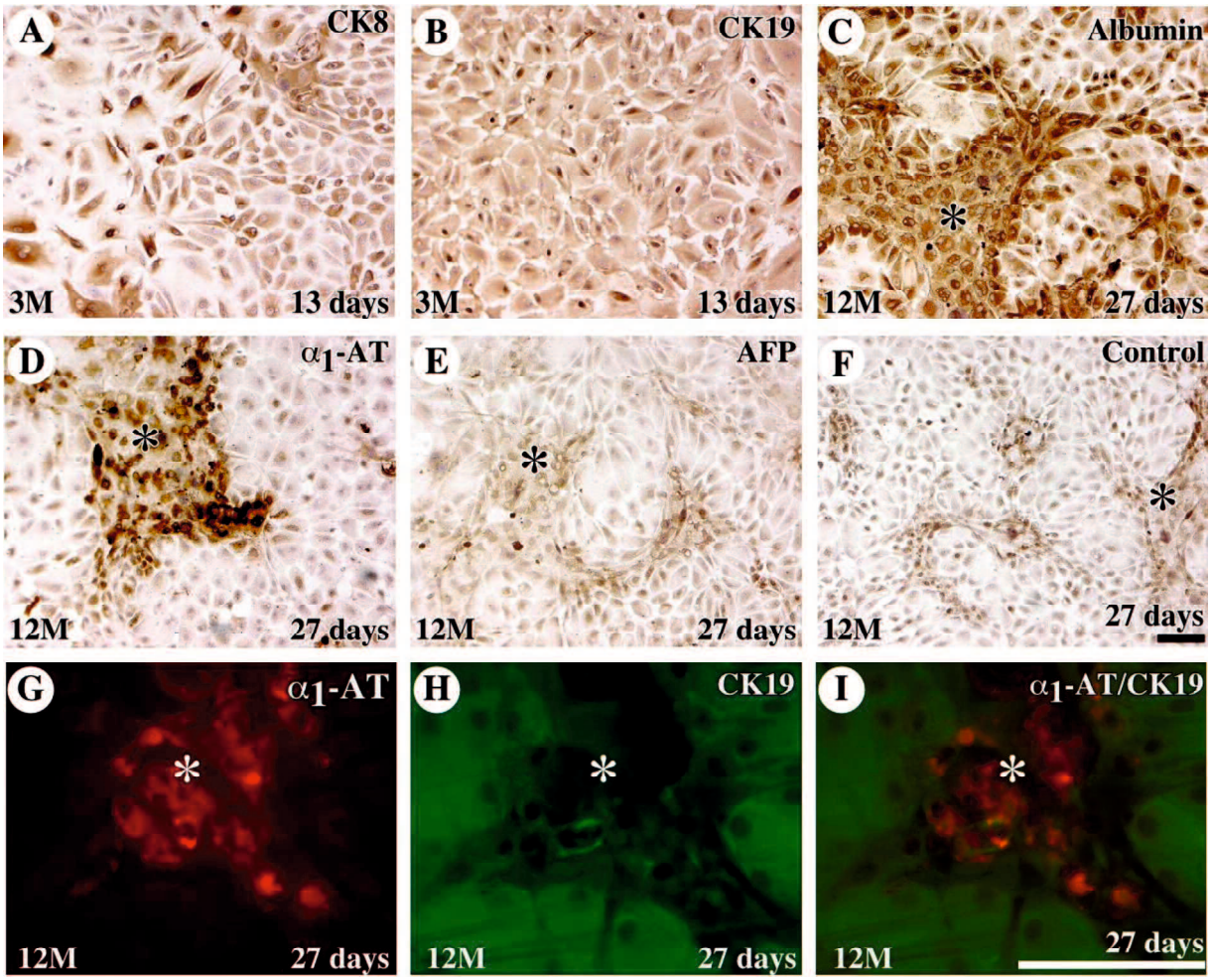

Fig. 3. Phenotypes of CF-PHs. 3M- and 12M-PHs were serially subcultured. 3M-CF-PHs at passage 2 were cultured up to 13 days when the cells were still in pre-confluence and subjected to immunocytochemical staining (A and B). 12M-CF-PHs at passage 3 were cultured for 27 days when the cells were confluent and were subjected to immunocytochemistry (C - I), in which double immunocytochemistry for α_1-AT and CK19 was done in G - I. **A**. CK8-staining. Most cells were $CK8^+$. **B**. CK19-staining. All the cells were $CK19^+$. **C**. ALB-staining. Most cells are ALB^+. Especially hepatocytes in condensed regions indicated with * are strongly positive. * is similarly marked in D - I. **D**. α_1-AT staining. α_1-AT^+ cells are present in condensed regions. **E**. AFP-staining. All the cells were AFP^-. **F**. Negative staining for C, D, and E. Magnification of A to E is the same as in F. Bar in F, 100 μm. **G**. Red color shows anti-human α_1-AT rabbit antibodies visualized by goat Texas red-anti-rabbit IgG. **H**. Green color shows anti-human CK19 mouse antibodies visualized by goat FITC-conjugated anti-mouse IgG. **I**. Photographs of G and H are merged. α_1-AT^+ cells are negative for CK19. Magnification of G and H is the same as in I. Bar in I, 100 μm.

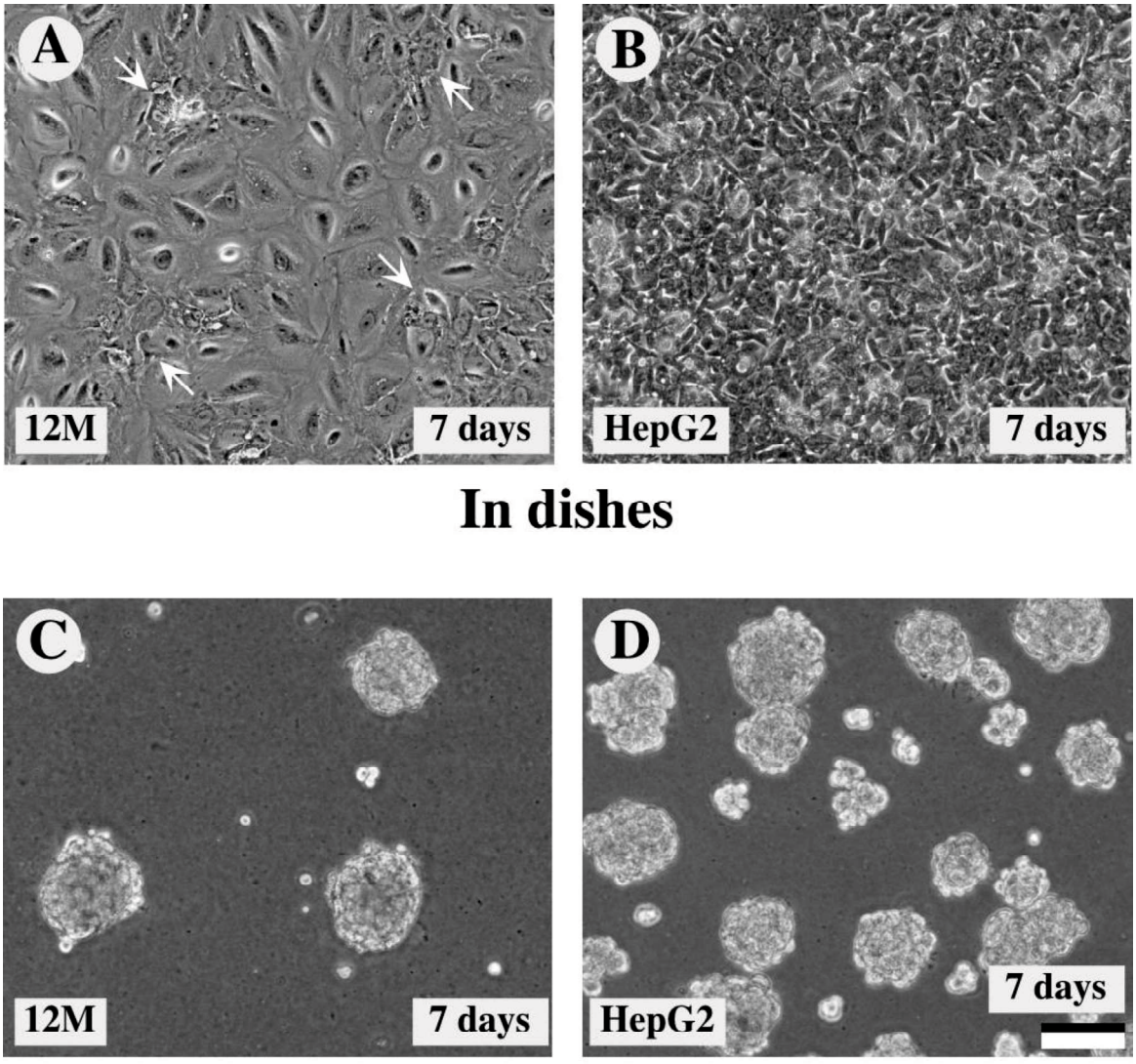

Fig. 4. Phase contrast microphotographs of CF-PHs and HepG2 cultured in monolayers and spheroids. **A**. 12M-CF-PHs at 3 passages were detached from dishes and inoculated at 10^5 cells/cm^2 in 35-mm wells and cultured for 7 days. They showed a typical hepatocyte-like morphology in condensed regions (arrows). **B**. HepG2 cells were similarly cultured in wells as in A. **C.** 12M-CF-PHs at 3 passages similarly cultured as in A, but on Matrigel. **D**. HepG2 cells were similarly cultured as in A, but on Matrigel. Magnification of A through C is the same as in D. Bar in D, 100 μm.

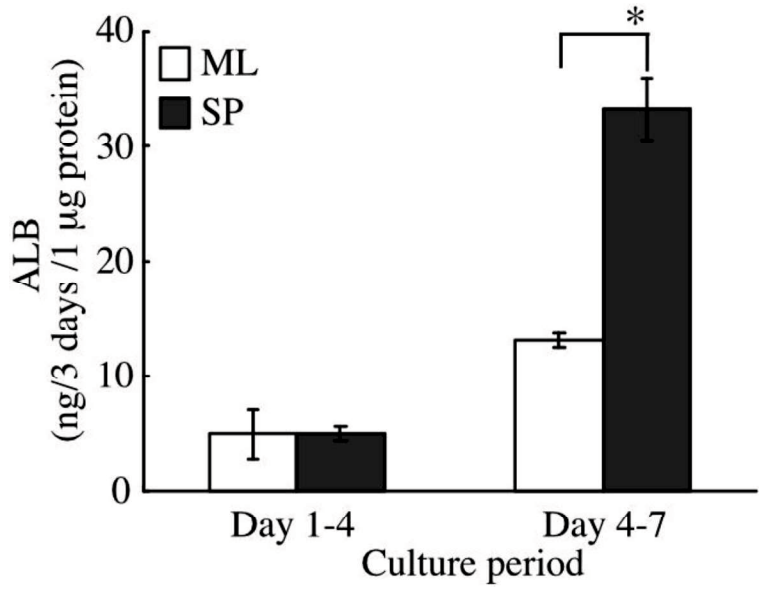

Fig. 5. ALB secretion by CF-PHs in monolayer- and spheroid-culture. 12M-CF-PHs at 3 passages were harvested from dishes at 22-58 days in culture and were cultured in monolayers (ML, open bars) and spheroids (SP, closed bars) as in Fig. 4 up to 7 days. The cells were refilled with fresh media at 1 day and cultured for additional 3 days (Day 1-4). Then, the cells were refilled with fresh media and cultured further for 3 days (Day 4-7). Media were collected at 4 and 7 days, and were used to quantify ALB of Day 1-4 and Day 4-7, respectively. The level of ALB secretion was determined as ALB secreted during 3 days in culture per 1 mg protein of CF-PHs in culture. CF-PHs in monolayer and in spheroid secreted ALB at 5.0 ± 2.2 and 5.0 ± 3.9 ng/3 days/1 μg cell protein through 1 to 4 days, and 13.1 ± 0.6 and 33.2 ± 2.7 ng/3 days/1 μg cell protein through 4 to 7 days, respectively. Each value represents the mean ± S.D. (n=3). * represents the statistical difference at $P<0.05$.

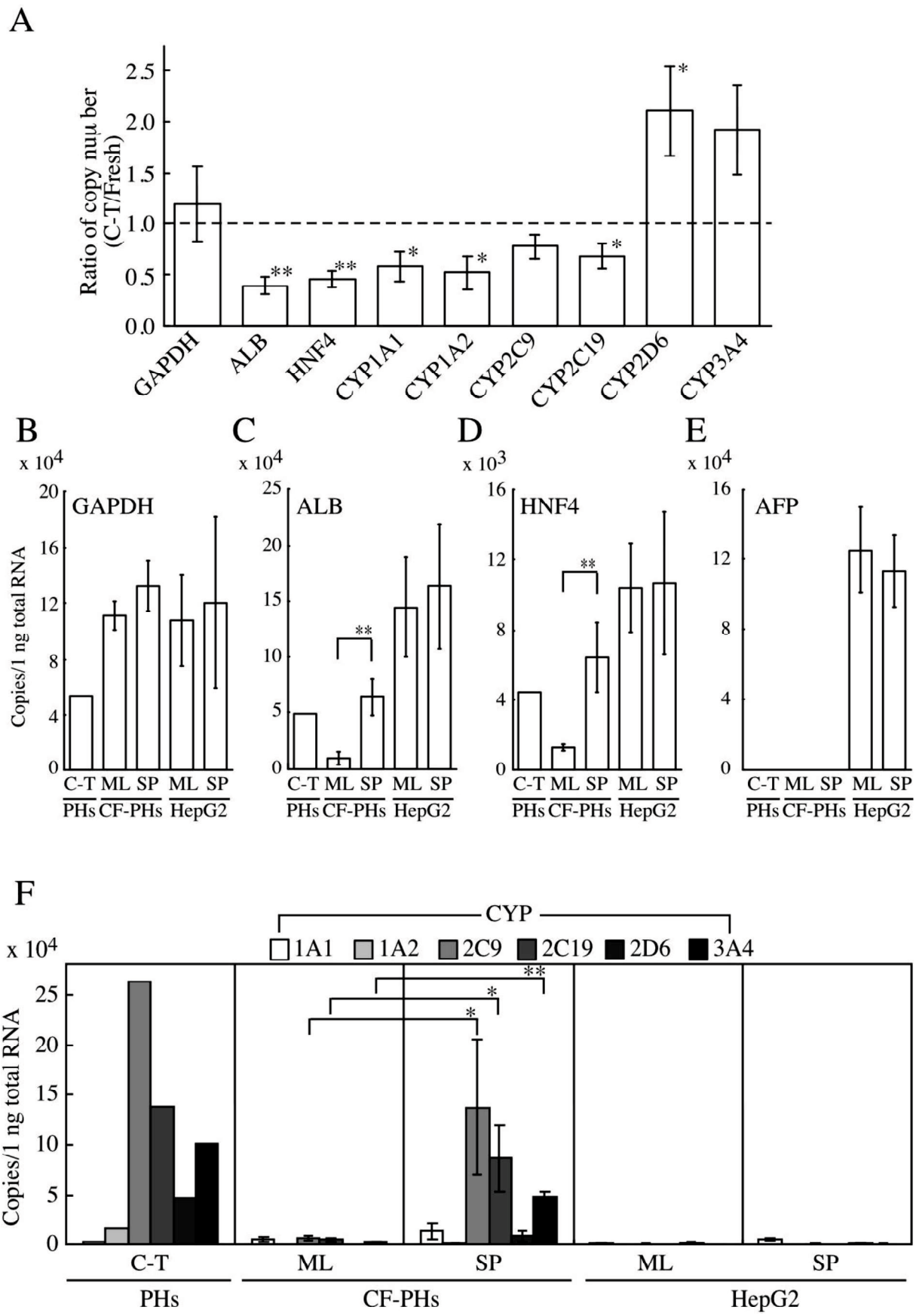
A
Ratio of copy nuu ber (C-T/Fresh)
2.5
2.0
1.5
1.0
0.5
0.0
GAPDH
ALB
HNF4
CYP1A1
CYP1A2
CYP2C9
CYP2C19
CYP2D6
CYP3A4
B
C
D
E
x 10^4
x 10^3
Copies/1 ng total RNA
GAPDH
ALB
HNF4
AFP
C-T ML SP ML SP
PHs CF-PHs HepG2
F
CYP
1A1 1A2 2C9 2C19 2D6 3A4
x 10^4
Copies/1 ng total RNA
C-T ML SP ML SP
PHs CF-PHs HepG2

Fig. 6. Expression of mRNAs of ALB, HNF4, AFP, and CYPs in monolayer- and spheroid-culture of CF-PHs. **A**. Comparison of gene expression between fresh and C-T PHs. PHs were prepared from 3 different donors (51M, 53M2, and 68F), and their aliquots were subjected to C-T. Fresh and C-T cells were used to quantify mRNAs of GAPDH, ALB, HNF4, AFP, and CYPs by real-time RT-PCR. We calculated the mean ratio of copy number of these mRNAs of C-T PHs to that of fresh ones. Each value represents the mean ± S.D. (n=3). **B** through **F**. mRNA expression in CF-PHs in monolayer- and spheroid-culture. Fresh 12M-PHs were subjected to C-T. Aliquots of C-T PHs were used for RNA extraction and the remaining was subcultured up to 3 passages. CF-PHs at 3 passages and HepG2 cells were cultured in monolayer (ML) and spheroid (SP) for 7 days and were determined for mRNA expression by RT-PCR. **B**. GAPDH mRNA. **C**. ALB mRNA. **D**. HNF4 mRNA. **E**. AFP mRNA. **F**. CYPs mRNA. Values represent the mean ± S.D. (n=3). * and ** indicate statistical significance of difference by Student's *t*-test at $P<0.05$ and $P<0.01$, respectively.

III-(1). *In vitro* Evaluation of Cytochrome P450 and Glucuronidation Activities in Hepatocytes Isolated from Liver-Humanized Mice

Abstract

Cryopreserved human (h-) hepatocytes are currently regarded as the best *in vitro* model for predicting human intrinsic clearance of xenobiotics. Although fresh h-hepatocytes have greater plating efficiency on dishes and greater metabolic activities than cryopreserved cells, performing reproducible studies using fresh hepatocytes from the same donor and having an “on demand” supply of fresh hepatocytes are not possible. In this study, cryopreserved h-hepatocytes were transplanted into albumin enhancer/promoter-driven, urokinase-type plasminogen activator, transgenic/severe combined immunodeficient (uPA/SCID) mice to produce chimeric mice, the livers of which were largely replaced with h-hepatocytes. We determined whether the chimeric mouse could serve as a novel source of fresh h-hepatocytes for *in vitro* studies. h-Hepatocytes were isolated from chimeric mice (chimeric hepatocytes), and cytochrome P450 (P450) activities were determined. Compared with cryopreserved cells, the P450 (1A2, 2C9, 2C19, 2D6, 2E1, 3A) activities of fresh chimeric hepatocytes were similar or greater. Moreover, ketoprofen was more actively metabolized through glucuronide conjugates by fresh chimeric hepatocytes than by cryopreserved cells. We conclude that chimeric mice may be a useful tool for supplying fresh h-hepatocytes on demand that provide high and stable phase I enzyme and glucuronidation activities.

Introduction

"Chimeric mice" with livers repopulated with human hepatocytes (h-hepatocytes), created using urokinase-type plasminogen activator (uPA)/severe combined immunodeficient (SCID) mice (1), were previously established previously, and the expression of both cytochrome P450 enzymes (P450s, CYPs) and phase II enzymes in the liver of these chimeric mice, as well as *in vivo* induction of P450, were examined (1-4).

P450 has been found to play an important role in the metabolism of xenobiotics, including drugs. Indeed, approximately 80% of oxidative metabolism is catalyzed by P450s (5), and to predict pharmacokinetics and drug interactions precisely, investigation of the pharmacokinetics of a P450 substrate using chimeric mice would be of considerable value.

Species differences are known to exist in the metabolism of ketoprofen (6). Ketoprofen is a propionic acid-class nonsteroidal anti-inflammatory drug with analgesic and antipyretic effects. Rat and mouse P450s primarily metabolize ketoprofen to hydroxyketoprofen (6,7). In humans, ketoprofen is primarily metabolized by UDP-glucuronosyltransferase (UGT) and is converted to ketoprofen glucuronides (8). Recently, it was demonstrated that when chimeric mice were administered ketoprofen, glucuronide conjugates were detected in their sera and bile. However, these conjugates are minor products; ketoprofen was primarily hydrolyzed in mice and the main metabolites were hydrolyzed ketoprofen and glucuronide-conjugated ketoprofen (7).

The metabolism of chemical entities has been examined using animals in the laboratory, but this approach fails to address differences in drug metabolism that exist between animal species. Because of the species differences in metabolic abilities, fresh h-hepatocytes are a better model for predicting the

metabolism of drugs in the human body. For technical reasons, preparing fresh h-hepatocytes ahead of time and performing reproducible studies using the same donor are not possible. Thus, cryopreserved h-hepatocytes have been used, but they are compromised on thawing, resulting in decline and alteration of their normal function. Additionally, h-hepatocytes exhibit large individual differences in P450 activities. The differences might be due to real individual differences and/or the cryopreserving and thawing conditions.

We hypothesized that these practical problems in using h-hepatocytes for *in vitro* drug testing could be addressed if h-hepatocytes isolated from chimeric mouse livers exhibited human-type drug metabolism capacities *in vitro*. In the present study, we first determined the yield, viability, and purity of isolated h-hepatocytes from chimeric mice (chimeric hepatocytes). We compared the P450 activities of fresh and cryopreserved chimeric hepatocytes and assessed glucuronide activities toward ketoprofen using fresh and cryopreserved chimeric hepatocytes and cryopreserved donor hepatocytes.

We demonstrate that the chimeric mouse liver is a useful tool that can supply fresh hepatocytes retaining high P450 and UGT activities and allowing reproducible assays using hepatocytes derived from the same donor.

Materials and methods

Materials: Phenacetin, tolbutamide, *S*-mephenytoin, dextromethorphan, chlorzoxazone, testosterone, ketoprofen, and Krebs-Henseleit buffer (KHB) were purchased from Sigma-Aldrich (St. Louis, MO). Coumarin and midazolam were obtained from Wako Pure Chemical Industries (Osaka, Japan). All other chemicals and solvents were of the highest or analytical grade commercially available.

Generation of Mice with Humanized Livers: The present study was approved by the ethics committee of PhoenixBio Co., Ltd. and the Hiroshima Prefectural Institute of Industrial Science and Technology Ethics Board.

Cryopreserved h-hepatocytes from three donors (4YF, a 4-year-old Caucasian girl; 6YF, a 6-year-old African-American girl; and 2YM, a 2-year-old Caucasian boy) were purchased from BD Biosciences (San Jose, CA). Three (donor 4YF), 17 (donor 6YF), and 4 (donor 2YM) chimeric mice with humanized livers, generated by a method described previously, were used (1). The concentration of human albumin (hAlb) in the blood of the chimeric mice and the replacement index (RI, the rate of hepatocyte replacement from mouse to humans) were well correlated (1). In the current study, we used 11–15-week-old male and female chimeric mice with approximately 11–14 mg/mL hAlb in mouse blood (RI >70%); uPA/SCID mice were used as controls.

Isolation of Hepatocytes from Chimeric Mouse Liver, SCID Mouse Liver, and Human Liver Tissue: Hepatocytes were isolated from the 4YF-, 6YF-, and 2YM-chimeric mice using a two-step collagenase perfusion method. The liver was perfused at 38°C for 10 min at 1.5 mL/min with Ca^{2+}-free and Mg^{2+}-free Hanks' balanced salt solution (CMF-HBSS) containing 200 μg/mL ethylene glycol tetraacetic acid (EGTA), 1 mg/mL glucose, 10 mM *N*-2-hydroxyethylpiperazine-*N'*-2-ethanesulfonic acid (HEPES),

and 10 μg/mL gentamycin. The perfusion solution was then changed to CMF-HBSS containing 0.05% collagenase (Wako Pure chemical Industries), 0.6 mg/mL $CaCl_2$, 10 mM HEPES, and 10 μg/mL gentamycin, and perfusion was continued for 17-23 min at 1.5 mL/min. The liver was dissected and transferred to a dish; liver cells were gently disaggregated in the dish with CMF-HBSS containing 1% bovine Alb, 10 mM HEPES, and 10 μg/mL gentamycin. The disaggregated cells were centrifuged three times (50×*g*, 2 min). The pellet was suspended in medium consisting of Dulbecco's modified Eagle's medium (DMEM), 10% fetal bovine serum (FBS), 20 mM HEPES, 44 mM $NaHCO_3$, and antibiotics (100 IU/mL penicillin G and 100 μg/mL streptomycin). Cell number and viability were assessed using the trypan blue exclusion test.

Normal liver tissues were obtained from the resected liver of nine patients (51-, 53-, and 64-year-old men and a 68-year-old woman for plating efficiency; 54-, 57-, and 75-year-old men for P450 activity; and 55- and 69-yearold women for screening of monoclonal antibodies) after receiving consent prior to surgery, in accordance with the 1975 Declaration of Helsinki. Hepatocytes were isolated via two-step collagenase perfusion and low-speed centrifugation(1). Aliquots of freshly isolated hepatocytes from four individuals, used for determining plating efficiency, were suspended at 1–2× 10^7 cells/mL/vial in cryopreservation solution (Cellbanker; Juji Field, Inc., Tokyo, Japan), cryopreserved using a program freezer (Kryo-10 Series III; Planer Products Ltd., Sunbury-on Thames, Middlesex, UK), and kept in liquid nitrogen. To measure the plating efficiency of the hepatocytes, 4YFchimeric hepatocytes and hepatocytes from human livers were inoculated onto 13.5-mm Celldesks (Sumitomo Bakelite, Tokyo, Japan) in 24-well plates (BD Biosciences) for 24 h, followed by fixation with ethanol and staining with hematoxylin and eosin. Adhered hepatocytes were counted under the microscope and plating efficiency was calculated by dividing number

of adhered cells by the cell number inoculated in a well.

Hepatocytes were isolated from three male uPA (wt/wt)/SCID mice by collagenase perfusion methods (9). They were used for *in vitro* glucuronidation activity studies

Purification of h-hepatocytes from total hepatocytes of the chimeric mouse livers: A Fischer 344 rat was immunized intraperitoneally three times (once a week) with 10^7 mouse hepatocytes (m-hepatocytes) of SCID mice as an antigen, and injected with a booster of 2.5×10^7 m-hepatocytes at 3 weeks after the last immunization. Hybridomas were obtained by conventional methods and screened on immunohistochemical sections using m- and h- (from a 55-year-old woman) liver tissues. Frozen h- and m- liver sections were incubated with hybridoma supernatants and fluorescein-labeled anti-rat IgG antibodies (Alexa Fluor 594; Molecular Probes, Eugene, OR). Supernatants from 10 hybridoma clones were reacted with the plasma membrane of m-hepatocytes, but not with h-hepatocytes on the sections. The reactivity of each of the supernatants to the cell surface was determined with a fluorescence-activated cell sorter (FACS) as follows. Isolated m- and h- (69-year-old woman) hepatocytes were incubated with the supernatants and fluorescein isothiocyanate (FITC)-conjugated second antibodies (Alexa Fluor 488; Molecular Probes) and analyzed with a FACS Vantage SE (BD Biosciences) using a 100-µm nozzle. Fluorescence excited at 488 nm was measured through a 530-nm filter (FL1) with 4-decade logarithmic amplification. A hybridoma clone was selected as the clone that produced antibodies reactive to the cell surface of m-hepatocytes, but not h-hepatocytes. The antibody was purified from the culture medium of the hybridoma cells by protein G affinity column or ion exchange chromatography; the antibody was named 66Z. Isolated h-hepatocytes from chimeric mice were contaminated with m-hepatocytes. To remove the m-hepatocytes, 6YF-hepatocytes isolated from the chimeric mice were incubated with the 66Z antibody, washed with

DMEM containing 10% FBS, and incubated with Dynabeads M450-conjugated sheep anti-rat IgG (Dynal Biotech, Milwaukee, WI) in a tube for 30 min on ice. The tube was placed in Dynal MPC-1 (Dynal Biotech) for 1–2 min to remove 66Z-positive ($66Z^+$) m-hepatocytes. Enriched h-hepatocytes were collected as 66Z-negative ($66Z^-$) cells. Aliquots of chimeric hepatocytes from before and after enrichment were incubated with FITC conjugated 66Z antibodies, and the proportion of $66Z^+$ cells in the h-hepatocytes was determined by FACS.

***In vitro* metabolic study using hepatocytes and microsomes**: For the measurement of the P450 activities of four fresh and five cryopreserved 6YF-chimeric mice, cryopreserved donor cells (6YF), and fresh hhepatocytes from three individuals, suspended hepatocytes (6× 104 cells) were incubated in KHB with each of eight substrates specific for seven P450 subtypes (phenacetin for CYP1A2, coumarin for CYP2A6, tolbutamide for CYP2C9, S-mephenytoin for CYP2C19, dextromethorphan for CYP2D6, chlorzoxazone for CYP2E1, and midazolam and testosterone for CYP3A) in 96-well plates (BD Biosciences) for 1 or 2 h (Table 1). The incubated solution was collected and an equivalent volume of methanol containing 1 mM niflumic acid (internal standard) was added. After centrifugation (10,000 rpm), the supernatant was subjected to liquid chromatography-tandem mass spectrometry (LC-MS/MS)(MDS SCIEX; Applied Biosystems, Foster City, CA). The LC system consisted of an HP 1100 system including a binary pump, an automatic sampler, and a column oven (Agilent Technologies, Waldbronn, Germany), equipped with a Symmetry Shield C18 column (Waters, Tokyo, Japan). The column temperature was 359C. The mobile phase was 40% acetonitrile/0.1% formic acid (v/v). The flow rate was 0.3 mL/min. The LC was connected to a PE Sciex API2000 tandem mass spectrometer (Applied Biosystems), operated in positive electrospray ionization mode. The turbo gas was maintained at 5509C. Nitrogen was used as the nebulizing

gas, turbo gas, and curtain gas at 65, 85, and 30 psi, respectively. Parent and/or fragment ions were filtered in the first quadrupole and dissociated in the collision cell using nitrogen as the collision gas. The analytical conditions for each substrate are shown in Table 2. The experiments were performed in triplicate per mouse, and the results are expressed as the average value of three mice or humans.

To assess changes in the P450 activities of fresh and cryopreserved 2YM-chimeric hepatocytes during storage at 49C for 3 and 6 h, fresh and cryopreserved chimeric hepatocytes were prepared from two 2YM chimeric mice. The isolated hepatocytes from the chimeric mice were purified by isodensity centrifugation (27% Percoll, 7 min, 4ºC) to remove dead hepatocytes. Cells (4× 10^5 cells) were incubated in KHB with four different substrates specific for four P450s (phenacetin for CYP1A2, diclofenac for CYP2C9, S-mephenytoin for CYP2C19, and midazolam for CYP3A) in 24-well plates (BD Biosciences) for 2 h (Table 1). The incubated solution was collected and the concentration of the metabolites was measured by high-performance liquid chromatography (HPLC; Lachome Elite; Hitachi High Technology Co., Tokyo, Japan). HPLC was performed at a flow rate of 1.0 mL/min using the CAPCELL PAK C18, UG120 (4.6× 250 mm, 5 µm; Shiseido, Tokyo, Japan) for CYP1A2 and CYP2C19, Inertsil ODS-3 (4.6× 250 mm, 5 µm; GL Sciences Inc., Tokyo, Japan) for CYP2C9, and Xterra RP18 (4.6× 150 mm, 5 µm; Waters) for CYP3A. Other analytical conditions are shown in Table 3. The measurements were performed in duplicate.

Liver microsomes were prepared from a 6YF-chimeric mouse and control uPA/SCID mice as described previously(10). They were stored at -80ºC until analysis. The protein concentration was determined using a Bradford protein assay kit (Bio-Rad, Hercules, CA), using bovine serum albumin as the standard. Microsomes from a chimeric mouse liver, pooled microsomes of six uPA/SCID mice, and pooled microsomes of 20 human livers (BD Gentest; BD Biosciences) were incubated with the substrates at 37ºC

for 5 min following incubation with the reduced form of nicotinamide adenine dinucleotide phosphate (NADPH) cofactor solution (3.8 mM bNADP$^+$, 9.7 mM glucose-6-phosphate, 9.7 mM $MgCl_2$, 1.2 U/mL glucose-6-phosphate dehydrogenase) at 37ºC for 10 or 20 min (Table 1). The incubated solution was collected and the concentration of the metabolites was measured by LC-MS/MS. The experiments were performed in triplicate per microsome preparation, and the results are expressed as the average value.

Detection of CYP2A6 gene mutations by the Invader assay: CYP2A6 polymorphism was determined by BML, Inc. (Tokyo, Japan). Genomic DNA was isolated from thawed human hepatocytes and the DNA was used for determining CYP2A6 polymorphism by the Invader assay (11).

***In vitro* glucuronidation activity study using hepatocytes**: Ketoprofen metabolism was examined using three types of hepatocytes: fresh and cryopreserved 6YF-chimeric hepatocytes, cryopreserved donor cells (6YF), and fresh uPA(wt/wt)/SCID mouse hepatocytes. Hepatocytes (4×10^5 cells) suspended in KHB were plated in 24-well, non-treated plates (BD Biosciences) and incubated at 37ºC for 15 min. The cells were treated with 1 μM ketoprofen at 37ºC for 3 h. The medium was harvested and aliquots of the medium were incubated at 37ºC for 4 h with 0.25 M acetic acid buffer as a solvent control (A) and with 2500 units/mL b-glucuronidase (B). Equivalent 1 N KOH was added into (B) and incubated at 80ºC for 3 h (C). After incubation, an equivalent of methanol containing 1 μM niflumic acid (as an internal standard) was added. After centrifugation (10,000 rpm), the supernatant was subjected to LC-MS/MS.

The relevant concentrations can then be obtained:

[Concentration of ketoprofen in (B)]-[Concentration of ketoprofen in (A)] gives [Concentration of ketoprofen-glucuronide].

[Concentration of ketoprofen in (C)]-[Concentration of ketoprofen in (B)] gives [Concentration

of transferred ketoprofen-glucuronide].

The transferred ketoprofen is the acyl glucuronide positional isomer, formed by acyl migration, which may be the glucuronide form transferred from ketoprofen glucuronide during incubation. The experiments were performed in triplicate for a given mouse, and the results are expressed as the average value of three chimeric mice for fresh chimeric hepatocytes, the average of five chimeric mice for cryopreserved hepatocytes, and the average of three uPA(wt/wt)/SCID mice for fresh control mouse hepatocytes.

Statistics: The data were analyzed using Statcel2 (OMS Publishing Inc., Tokorozawa, Japan). Results are expressed as the mean± SD, and the significance of the difference between two groups was analyzed by Student's t-test when data were normally distributed, and by Welch's t-test otherwise. $P<0.05$ was deemed to indicate statistical significance.

Results

Yield, viability, and plating efficiency of isolated h-hepatocytes: Hepatocytes from the 4YF-, 6YF-, and 2YM-donors were transplanted into uPA/SCID mice, and chimeric mice were obtained bearing the respective donor hepatocytes (Table 4). The chimeric mice (4YF, 3 mice; 6YF, 17 mice; 2YM, 4 mice) were sacrificed at 54–83 days post-transplantation (Table 4). On the day they were sacrificed, blood was collected for the determination of hAlb concentrations (Table 4). Hepatocytes were then isolated by the collagenase perfusion method. Numbers (yield) of isolated viable hepatocytes were approximately 2–3× 10^7 cells/mouse (Table 4). The viabilities were approximately 60–70% and 50–60% for fresh and cryopreserved chimeric hepatocytes, respectively, without Percoll purification.

The plating efficiency of hepatocytes from the chimeric mice was about 66.6± 3.4% (mean± SD), while those of fresh hepatocytes and cryopreserved hepatocytes from human livers were 34.0± 19.3% and 9.3± 8.3%, respectively.

Purification of h-hepatocytes isolated from chimeric mice: Chimeric hepatocyte preparations consisted of h- and m-hepatocytes. It was found that 17.3± 6.7% of the fresh hepatocytes from 6YF-chimeric mice were $66Z^+$ (n=4; Table 4) by FACS analysis. The enriched chimeric hepatocytes were found to be 3.3±1.0% $66Z^+$ (m-hepatocytes; n= 4; Table 4).

P450 activities of hepatocytes from the chimeric mice: The P450 activities of hepatocytes from 6YF-chi meric mice were determined using eight substrates (Table 1). The reactions of P450 activities with all substrates shown in Table 1 were linear with incubation time. The activities of fresh chimeric hepatocytes were compared with cryopreserved chimeric hepatocytes and cryopreserved donor cells. Three experiments were performed and the means± SD are given in Figure 1. CYP1A2, 2C19, and 2D6

activities in fresh chimeric hepatocytes were approximately twice those in cryopreserved cells (Fig. 1). CYP2A6, 2C9, 2E1, and 3A activities in fresh chimeric hepatocytes were similar to those of cryopreserved hepatocytes (Fig. 1). The activities of cryopreserved donor cells (6YF) were lower than those of cryopreserved 6YF-chimeric hepatocytes in CYP1A2, 2C19, and 3A (midazolam); higher in CYP2A6 and 2E1; and similar in CYP2C9, 2D6, 3A (testosterone; Fig. 1). Compared with CYP2A6 activities of two of the three fresh hepatocytes, CYP2A6 activity was extremely low in the chimeric hepatocytes (Fig. 1). Interestingly, the Invader assay revealed that donor 6YF had the *1/*4 CYP2A6 polymorphism; livers with the *1/*4 polymorphism in CYP2A6 are known to show low CYP2A6 activity (12). We concluded that the low CYP2A6 activity was due to the *1/*4 polymorphism of donor 6YF. Three kinds of fresh h-hepatocytes were also examined for P450 activity. One of the three samples did not show CYP1A2 or 2C19 activity. Large individual differences were observed among the three in CYP2A6, 2C9, and 2E1 activities. The activities of CYP1A2, 2C19, 2D6, and 3A in fresh h-hepatocytes were lower than those in fresh chimeric hepatocytes.

We determined changes in the P450 activities of fresh and cryopreserved 2YM-chimeric hepatocytes after Percoll purification during storage at 49C after isolation and thawing, respectively. CYP1A2, 2C9, 2C19, and 3A activities did not change for up to 6 h after isolation or thawing (Fig. 2). CYP1A2, 2C19, and 3A activities were lower in cryopreserved chimeric hepatocytes, and CYP2C9 activity was similar compared to fresh chimeric hepatocytes at 0 h after isolation or thawing (Fig. 2). The results were reproducible and are similar to those in Figure 1.

Contribution of m-hepatocyte contamination in chimeric hepatocytes to P450 activity: The

proportions of m-hepatocytes in the fresh chimeric hepatocytes were approximately 17% and 3% before and after purification with 66Z antibodies, respectively, as described above. To determine how the contaminating m-hepatocytes affected P450 activities, we measured P450 activities using liver microsomes from a 6YF-chimeric mouse, pooled host uPA/SCID mice, and pooled human liver microsomes. Except for CYP2D6 and 2E1, P450 activities were similar or lower in uPA/SCID mouse liver microsomes than in human pooled microsomes (Fig. 3). Because the activities of CYP2D6 and 2E1 in uPA/SCID mouse liver microsomes were 50–100% higher than in pooled human microsomes (Fig. 3), we considered that m-hepatocytes contaminating the chimeric hepatocytes at around 17% might not significantly affect the activities of chimeric hepatocytes. We measured the P450 activity of pre- and post-purified chimeric hepatocytes (6YF) using 66Z antibodies. The purified hepatocytes from the chimeric mice showed similar P450 activities to unpurified ones, supporting this suggestion (Fig. 1).

Glucuronide conjugation of ketoprofen in chimeric m-hepatocytes: Glucuronide conjugates were detected by *in vitro* metabolic assay for ketoprofen using fresh and cryopreserved hepatocytes from the 6YF-chimeric mouse and cryopreserved donor cells (6YF); however, uPA(wt/wt)/SCID mouse hepatocytes did not show products of UGT activity. The proportion of nonmetabolized ketoprofen in fresh chimeric hepatocytes was similar to that in donor cells and lower than that in cryopreserved chimeric hepatocytes (Fig. 4). The proportion of ketoprofen-glucuronide in fresh chimeric hepatocytes was significantly higher than that of both cryopreserved chimeric hepatocytes ($P<0.05$). The transferred ketoprofen-glucuronide levels in fresh chimeric hepatocytes were also higher than those of both cells, but not significantly so (Fig. 4). From these results, we suggest that the freeze-thaw procedure decreased cellular glucuronide conjugation activities on drugs such as ketoprofen.

Discussion

Recent studies have revealed that chimeric mice may be a useful model for the examination of drug absorption, distribution, metabolism, and excretion (ADME) and drug interactions via enzyme induction and inhibition *in vivo* (1,3,4,7,12–14). S-Warfarin has been shown to be metabolized to S-7-hydroxywarfarin, catalyzed by CYP2C9, and is primarily recovered in urine in humans.15) The mass balance and metabolic disposition of Swarfarin in chimeric mice were found to be similar to reported human data (14,16). In humans, ketoprofen is primarily metabolized by UGT and converted to ketoprofen glucuronides (8). When chimeric mice were administered ketoprofen, glucuronide conjugates were detected in their sera and bile (7). By treatment with typical inducers of P450 (3-methylcholanthrene and rifampicin), human CYP1A and CYP3A4, respectively, were induced in the chimeric mouse liver (1,3). After treatment with quinidine, a specific inhibitor of human CYP2D6, the area under the curve (AUC) of CYP2D6 metabolites was significantly decreased in the chimeric mice, but not in control mice (13). These findings demonstrate that hhepatocytes in the chimeric mouse liver had normal human phase I and II enzyme activity, and that the chimeric mice may have advantages in studies of ADME and drug interactions. However, no study had examined the metabolic activity of fresh h-hepatocytes isolated from chimeric mice. In the present study, we determined whether the chimeric mouse could be a useful source of fresh hhepatocytes for *in vitro* metabolic studies.

The metabolic capacities of fresh and corresponding cryopreserved hepatocytes from several donors have been compared by testosterone hydroxylation, 7-ethoxyresorufin-O-deethylase (EROD), and 7-ethoxycoumarinO-deethylase (ECOD). These activities were found to be lower in cryopreserved hepatocytes than in fresh ones (17,18). Phase II enzyme activities, GST, UGT toward

4-methylumbelliferone (MUF), and sulfotransferase (SULT) were also significantly reduced after cryopreservation of h-hepatocytes, whereas the activity of UGT toward 4-hydroxybiphenyl (HOBI) and that of SULT were similar to those measured in fresh h-hepatocytes.17) Despite the observed reductions of these enzyme activities, cryopreserved h-hepatocytes are regarded as the best *in vitro* model for use in predicting human intrinsic clearance of xenobiotics (19). This is because ahead-of-time experimental planning using fresh h-hepatocytes and attaining reproducible studies using the same donor of fresh h-hepatocytes is not feasible. Additionally, because large individual variations are known to exist among h-hepatocytes, pooled hepatocytes derived from several donors could help eliminate such individual variation, but such pooling of fresh h-hepatocytes is not possible. Here, we compared the P450 activities of fresh and cryopreserved chimeric hepatocytes originating from the same donor, and fresh h-hepatocytes from human livers. Results indicated that CYP1A2, 2C19, and 2D6 activities declined, while CYP2A6, 2C9, 2E1, and 3A activities were not affected by the freeze-thaw procedure. Fresh and cryopreserved chimeric h-hepatocytes were used for the determination of ketoprofen glucuronidation. Concentrations of ketoprofen-glucuronide and transferred ketoprofen-glucuronide were higher in fresh chimeric hepatocytes than in their cryopreserved counterparts. Chimeric hepatocytes from the same donor showed smaller variations in P450 activities than fresh h-hepatocytes from different individuals (Fig. 1). These results indicated that fresh chimeric hepatocytes may address the problem of individual differences in fresh h-hepatocytes. Additionally, the fresh and cryopreserved chimeric hepatocytes tested retained P450 (CYP1A2, 2C9, 2C19, and 3A) activities for at least 6 h. These studies demonstrated that chimeric mice can provide fresh h-hepatocytes ahead of time, making reproducible studies using the same donor possible.

The decreased metabolism in cryopreserved hepatocytes could be attributable to two mechanisms: inactivation of P450 enzymes and loss of the cofactor NADPH due to cell membrane damage (20). The addition of a NADPH-generating system to the incubation mixture has been shown to increase benzo[a]pyrene metabolite formation by cryopreserved rat hepatocytes to approximately the level of freshly isolated rat hepatocytes (21). When cryopreserved rat hepatocytes were purified by Percoll centrifugation after thawing, to remove dead and membrane-damaged cells, benzo[a]pyrene metabolism recovered to equal that of fresh rat hepatocytes (21). The decline in phase II enzyme activities has also been shown to be overcome by Percoll centrifugation, but not completely to the level of freshly isolated cells (21). Addition of endogenous cofactors uridine 5'-diphosphoglucuronic acid (UDPGA) and adenosine 3'-phosphate 5'-phosphosulfate (PAPS) to cryopreserved rat hepatocytes improved 7-hydroxycoumarin-glucuronide and 7-hydroxycoumarin-sulfate formation to levels observed in fresh hepatocytes (22). The UDPGA and PAPS synthesis machineries may be damaged during freezing and thawing. Fresh or cryopreserved chimeric hepatocytes would be useful in clarifying the mechanisms underlying the decline in metabolic activities after freezing and thawing. The results of this study also suggest that fresh chimeric hepatocytes are useful for testing phase I and II reactions, including glucuronidation, without the need for Percoll purification or the addition of cofactors.

Chimeric hepatocytes contain about 17% of m-hepatocytes, and 66Z antibodies react specifically with mhepatocytes. We purified h-hepatocytes from the chimeric hepatocytes by 66Z rat IgG and magnetic bead-conjugated anti-rat IgG antibodies. After the magnetic removal of m-hepatocytes, the proportion of m-hepatocytes decreased to approximately 3%. We measured the P450 activities of microsomes isolated from the chimeric mouse and pooled microsomes from uPA/SCID mice and human

livers using the same substrates as those used in the cell suspension study. Because we were not able to obtain microsomes from the donor of the chimeric mice (6YF), pooled human microsomes were used for this study. Except for CYP2D6 and 2E1, the activities of uPA/SCID mouse liver microsomes were similar to, or lower than, those of pooled human liver microsomes. The activities of CYP2D6 and 2E1 in uPA/SCID mouse liver microsomes were 50–100% higher than those of pooled human liver microsomes, respectively. We also found that P450 activities were similar between pre- and postpurified chimeric hepatocytes. From these results, we deduced that m-hepatocytes contaminating the chimeric hepatocytes might not significantly affect the activities of chimeric hepatocytes.

Gender differences in CYP3A4 activities have been reported when using cryopreserved human hepatocytes (23). We assumed that P450 activities were independent of the gender in recipient uPA/SCID mice, because we recently showed that there was no significant difference in P450 activity (CYP1A2, 2C9. 2C19, 2D6, and 3A) between microsomes from male and female chimeric mice (24). In the present study, hepatocytes isolated from both male and female chimeric mice were used, and there was no difference in P450 or UGT activity between them (data not shown); however, the number of animals was limited.

Non-platable 4YF- and 6YF-donor cells were engrafted and grown in the uPA/SCID mice and hepatocytes were isolated from the livers using the collagenase perfusion method. Fresh chimeric hepatocytes adhered well onto the culture dishes, compared with fresh and cryopreserved h-hepatocytes. This suggests that fresh chimeric hepatocytes would be suitable for P450 induction and toxicity studies that are usually performed with plated cells.

Cryopreserved h-hepatocytes isolated from the chimeric mice were demonstrated to be useful for evaluating the induction of CYP1A2 and 3A4 (25); in addition, CYP1A2 and 3A4 mRNA induction and expression from three different donor hepatocytes were reproduced in cryopreserved chimeric hepatocytes (26). Due to the higher plating efficiency of fresh hepatocytes compared to cryopreserved cells, fresh chimeric hepatocytes would be useful for evaluating the human P450 induction abilities of xenobiotics.

We conclude that fresh and reproducible h-hepatocytes isolated from chimeric mice could be a useful tool in predicting the pharmacokinetics of chemical entities in addition to *in vivo* chimeric mouse studies. Comparative *in vitro* and *in vivo* studies using chimeric mice with the same donor could generate abundant data for resolving poorly understood phenomena and mechanisms.

Acknowledgements

We thank Mss. Y. Yoshizane, S. Nagai, and H. Kohno for providing excellent technical assistance.

References

1) Tateno, C., Yoshizane, Y., Saito, N., Kataoka, M., Utoh, R., Yamasaki, C., Tachibana, A., Soeno, Y., Asahina, K., Hino, H., Asahara, T., Yokoi, T., Furukawa, T., and Yoshizato, K.: Near completely humanized liver in mice shows human-type metabolic responses to drugs. *Am. J. Pathol.*, **165**: 901–912 (2004).

2) Katoh, M., Matsui, T., Nakajima, M., Tateno, C., Kataoka, M., Soeno, Y., Horie, T., Iwasaki, K., Yoshizato, K., and Yokoi, T.: Expression of human cytochrome P450 in chimeric mice with humanized liver. *Drug Metab. Dispos.*, **32**: 1402–1410 (2004).

3) Katoh, M., Matsui, T., Nakajima, M., Tateno, C., Soeno, Y., Horie, T., Iwasaki, K., Yoshizato, K., and Yokoi, T.: *In vivo* induction of human cytochrome P450 enzymes expressed in chimeric mice with humanized liver. *Drug Metab. Dispos.*, **33**: 754–763 (2005).

4) Katoh, M., Matsui, T., Okumura, H., Nakajima, M., Nishimura, M., Naito, S., Tateno, C., Yoshizato, K., and Yokoi, T.: Expression of human phase II enzymes in chimeric mice with humanized liver. *Drug Metab. Dispos.*, **33**: 1333–1340 (2005).

5) Wilkinson, G.R.: Drug metabolism and variability among patients in drug response. *N. Engl. J. Med.*, **352**: 2211–2221 (2005).

6) Populaire, P., Terlain, B., Pascal, S., Decouvelaere, B., Renard, A., and Thomas, JP.: Biological behavior: serum levels, excretion and biotransformation of (3-benzoylphenyl)-2-propionic acid, or ketoprofen, in animals and men. *Ann. Pharm. Fr.*, **12**: 735–749 (1973).

7) Hashizume, K., Ohzone, Y., Adachi, Y., Ninomiya, A., Inoue, T., and Horie, T.: Characterization of chimeric mouse on *in vivo* metabolism of ketoprofen. *The Cell*, **40**: 26–29 (2008) in Japanese.

8) Ishizaki, T., Sasaki, T., Suganuma, T., Horai, Y., Chiba, K., Watanabe, M., Asuke, W., and Hoshi, H.: Pharmacokinetics of ketoprofen following single oral, intramuscular and rectal doses and after repeated oral administration. *Eur. J. Clin. Pharmacol.*, **18**: 407–414 (1980).

9) Ohashi, K., Tatsumi, K., Utoh, R., Takagi, S., Shima, M., Okano, T.: Engineering liver tissues under the kidney capsule site provides therapeutic effects to hemophilia B mice. Cell Transplant., in press

10) Sugihara, K., Kitamura, S., Yamada, T., Ohta, S., Yamashita, K., Yasuda, M., and Fujii-Kuriyama, Y.: Aryl hydrocarbon receptor (Ah)-mediated induction of xanthine oxidase/xanthine dehydrogenase activity by 2,3,7,8-tetrachlorodibenzo-p-dioxin. *Biochem. Biophys. Res. Commun.*,. **281**: 1093–1099 (2001).

11) Nagano, M., Yamashita, S., Hirano, K., Ito, M., Maruyama, T., Ishihara, M., Sagehashi, Y., Oka, T., Kujiraoka, T., Hattori, H., Nakajima, N., Egashira, T., Kondo, M., Sakai, N., and Matsuzawa, Y.:Two novel missense mutations in the CETP gene in Japanese hyperalphalipoproteinemic subjects: high-throughput assay by Invader assay. *J. Lipid Res.*, **43**: 1011–1018 (2002).

12) Kiyotani, K., Yamazaki, H., Fujieda, M., Iwano, S., Matsumura, K., Satarug, S., Ujjin, P., Shimada, T., Guengerich, F.P., Parkinson, A., Honda, G. Nakagawa, K., Ishizaki, T., and Kamataki, T.: Decreased coumarin 7-hydroxylase activities and CYP2A6 expression levels in humans caused by genetic polymorphism in CYP2A6 promoter region (CYP2A6*9). *Pharmacogenetics* **13**: 689–695 (2003).

13) Katoh, M., Sawada, T., Soeno, Y., Nakajima, M., Tateno, C., Yoshizato, K., and Yokoi, T.: *In vivo* drug metabolism model for human cytochrome P450 enzyme using chimeric mice with humanized liver. *J. Pharm. Sci.*, **96**: 428–437 (2007).

14) Inoue, T., Nitta, K., Sugihara, K., Horie, T., Kitamura, S., and Ohta, S.: CYP2C9-catalyzed

metabolism of S-warfarin to 7-hydroxywarfarin *in vivo* and *in vitro* in chimeric mice with humanized liver. *Drug Metab. Dispos.*, **36**: 2429–2433 (2008).

15) Rettie, A.E., Korzekwa, K.R/, Kunze, K.L., Lawrence, R.F., Eddy, A.C., Aoyama, T., Gelboin, H.V., Gonzalez, F.J., and Trager, W.F.: Hydroxylation of warfarin by human cDNA-expressed cytochrome P-450: a role for P-4502C9 in the etiology of (S)-warfarin-drug interactions. *Chem. Res. Toxicol.*, **5**: 54–59 (1992).

16) Inoue, T., Sugihara, K., Ohshita, H., Horie, T., Kitamura, S., and Ohta, S.: Prediction of human disposition toward S-3H-warfarin using chimeric mice with humanized liver. *Drug Metab. Pharmacokinet.*, **24**: 153–160 (2009).

17) Steinberg, P., Fischer, T., Kiulies, S., Biefang, K., Platt, K.L., Oesch, F., Böttger, T., Bulitta, C., Kempf, P., and Hengstler, J.: Drug metabolizing capacity of cryopreserved human, rat, and mouse liver parenchymal cells in suspension. *Drug Metab. Dispos.*, **27**: 1415–1422 (1999).

18) Gebhardt, R., Hengstler, J.G., Müller, D., Glöckner, R., Buenning, P., Laube, B., Schmelzer, E., Ullrich, M., Utesch, D. Hewitt, N., Ringel, M., Hilz, B.R., Bader, A., Langsch, A., Koose, T., Burger, H.J,, Maas, J., and Oesch, F.: New hepatocyte *in vitro* systems for drug metabolism: metabolic capacity and recommendations for application in basic research and drug development, standard operation procedures. *Drug Metab. Rev.*, **35**: 145–213 (2003).

19) Lau, Y.Y., Sapidou, E., Cui, X., White, R.E., and Cheng, K.C.: Development of a novel *in vitro* model to predict hepatic clearance using fresh, cryopreserved, and sandwich-cultured hepatocytes. *Drug Metab. Dispos.*, **30**: 1446–1454 (2002).

20) Hengstler, J.G., Utesch, D., Steinberg, P., Platt, K.L., Diener, B., Ringel, M., Swales, N., Fischer, T.,

Biefang, K., Gerl, M., Böttger, T., and Oesch, F.: Cryopreserved primary hepatocytes as a constantly available *in vitro* model for the evaluation of human and animal drug metabolism and enzyme induction. *Drug Metab. Rev.*, **32**: 81–118 (2000).

21) Diener, B., Utesch, D., Beer, N., Dürk, H., and Oesch, F.: A method for the cryopreservation of liver parenchymal cells for studies of xenobiotics. *Cryobiology*, **30**: 116–127 (1993).

22) Wang, Q., Jia, R., Ye, C., Garcia, M., Li, J., and Hidalgo, I.J.: Glucuronidation and sulfation of 7-hydroxycoumarin in liver matrices from human, dog, monkey, rat, and mouse. *In vitro Cell Dev. Biol. Anim.*, **41**: 97–103 (2005).

23) Parkinson A., Mudra D.R., Johnson, C., Dwyer A., and Carroll, K.M.: The effects of gender, age, ethnicity, and liver cirrhosis on cytochrome p450 enzyme activity in human liver microsomes and inducibility in cultured human hepatocytes. *Toxicol Appl. Pharmacol.* **199**:193-209 (2004).

24) Nishimura, M., Yokoi, T., Tateno, C., Kataoka, M., Takahashi, E., Horie, T., Yoshizato, K., and Naito, S.: Induction of human CYP1A2 and CYP3A4 in primary culture of hepatocytes from chimeric mice with humanized liver. *Drug Metab. Pharmacokinet.*, **20**: 121–126 (2005).

25) Yoshitsugu, H., Nishimura, M., Tateno, C., Kataoka, M., Takahashi, E., Soeno, Y., Yoshizato, K., Yokoi, T., and Naito, S.: Evaluation of human CYP1A2 and CYP3A4 mRNA expression in hepatocytes from chimeric mice with humanized liver. *Drug Metab. Pharmacokinet.*, **21**: 465–474 (2006).

Tables and figures

Table 1.

Reaction conditions for determination of CYP activities using cells and microsomes for LC-MS/MS and HPLC analysis

Enzymes measured	Enzyme activity	Substrate (concentration, μM)	Metabolite	Cells (LC-MS/MS)	Cells (HPLC)	Microsomes (LC-MS/MS)	
				Incubation time (h)	Incubation time (h)	Buffer*	Incubation time (min)
CYP1A2	Phenacetin *O*-deethylase	Phenacetin (15)	Acetaminophen	2	2	PB	20
CYP2A6	Coumarin 7-hydroxylase	Coumarin (8)	7-Hydroxycoumarin	2	-	TB	20
CYP2C9	Tolbutamide 4-hydroxylase	Tolbutamide (150)	Hydroxytolbutamide	2	-	TB	10
	Diclofenac 4'-hydroxylase	Diclofenac (100)	4-Hydroxydiclofenac	-	2	-	-
CYP2C19	*S*-Mephenytoin 4'-hydroxylase	*S*-Mephenytoin (20)	(±)-4'-Hydroxymephenytoin	2	2	PB	20
CYP2D6	Dextromethorphan *O*-demethylase	Dextromethorphan (8)	Dextrorphan	2	-	PB	20
CYP2E1	Chlorzoxazone 6-hydroxylase	Chlorzoxazone (100)	6-Hydroxychlorzoxazone	2	-	PB	20
CYP3A	Midazolam 1'-hydroxylase	Midazolam (10)	1'-Hydroxymidazolam	1	2	PB	10
	Testosterone 6β-hydroxylase	Testosterone (50)	6β-Hydroxytestosterone	2	-	PB	10

*TB, Tris-HCl buffer (pH 7.5); PB, potassium phosphate buffer (pH 7.4).

Table 2.

Analytical parameters of LC-MS/MS for CYP1A2, 2A6, 2C9, 2C19, 2D6, 2E1, and 3A assays

Enzymes measured	Analyte	Mass spectrometer conditions						
		Mode	Declustering potential (eV)	Collision energy (eV)	Entrance potential (eV)	Collision cell exit potential (eV)	Ionspray voltage (V)	Analyte *m/z* transition
CYP1A2	Acetaminophen	Positive	40	25	7	10	5000	152.2→110.3
CYP2A6	7-Hydroxycoumarin	Positive	80	30	7	10	4200	162.8→107.2
CYP2C9	Hydroxytolbutamide	Positive	40	25	7	10	5000	286.9→171.3
CYP2C19	(±)-4'-Hydroxymephenytoin	Positive	80	25	7	10	4200	234.9→150.1
CYP2D6	Dextrorphan	Positive	120	40	7	10	4200	259.0→200.2
CYP2E1	6-Hydroxychlorzoxazone	Negative	–80	–25	–7	–10	–4200	184.1→120.0
CYP3A	6β-Hydroxytestosterone	Positive	60	25	7	10	4200	305.9→270.3
	1'-Hydroxymidazolam	Positive	100	40	7	10	5000	341.6→203.3
Ketoprofen	Ketoprofen	Positive	80	35	7	10	5000	255.5→104.9

Table 3.

Analytical conditions of HPLC for CYP1A2, 2C9, 2C19, and 3A assays

Enzymes measured	Analyte	Internal standard	Injection volume (μL)	Mobile phase				
				Solvent A*	Solvent B	Gradient program, %B (min)	Column temperature (°C)	UV detection (nm)
CYP1A2	Acetaminophen	0.1 μg Caffeine monohydrate	95	50 mM PB (pH 4.0)	Acetonitrile	Isocratic mode (A/B=91/9)	35	245
CYP2C9	4'-Hydroxydiclofenac	0.4 μg Phenacetin	50	0.5% (v/v) AAAS	Methanol containing 0.5% (v/v) acetic acid	40 (0)→90 (30) →90 (35)→40 (36)	50	280
CYP2C19	(±)-4'-Hydroxymephenytoin	0.1 μg Phenobarbital sodium	95	50 mM PB	Acetonitrile	Isocratic mode (A/B=80/20)	35	240
CYP3A	1'-Hydroxymidazolam	0.01 μg Phenacetin	50	10 mM PB (pH 7.4)	Acetonitrile/methanol mixture (7/5, v/v)	30 (0)→30 (5)→60 (17) →60 (25)→30 (26)	40	263

* PB, potassium phosphate buffer; AAAS, acetic acid aqueous solution.

Table 4.

Hepatocytes used for the experiments

Purpose	Origin	Fresh or cryopreserved	n (sex of host animals or patients)	hAl in mouse blood (mg/mL)	Yield of hepatocytes ($\times 10^7$ cells)	Viability (%)	Ratio of mouse hepatocytes (%)	
							Before purification	After purification
Plating efficiency	Chimeric mouse (4YF)	Fresh	3 (M: 1, F: 2)	11.5±3.6	2.90±2.7/mouse	63.9±6.5	N.D.*4)	N.D.
	Human liver (51–68-year-old)	Fresh	4 (M: 3, F: 1)	-	0.98±0.4/g liver	87.9±8.2	-	-
		Cryopreserved	4 (M: 3, F: 1)	-	-	56.2±7.5*5)	-	-
CYP activities	Chimeric mouse (6YF)	Fresh	4*1) (F)	11.8±0.6	1.78±0.9/mouse	61.8±6.9	17.3±6.7	3.3±1.0
		Cryopreserved	5*2) (M: 2, F: 3)	12.6±2.1	-	60.5±10.6*5)	5.8±4.7*5)	2.1±1.0*5)
	Human liver (54–75-year-old)	Fresh	3 (M: 3)	-	0.43±0.4/g liver	96.1±2.4	-	-
	Donor cell (6YF)	Cryopreserved	1 (F)	-	-	71.1	-	-
CYP activities at different time points after perfusion or thawing	Chimeric mouse (2YM)	Fresh	2*3) (F)	11.8	3.05*5), 6)/mouse	84.8*5), 6)	N.D.	N.D.
		Cryopreserved	2*3) (F)	11.8	-	86.4*5), 6)	N.D.	N.D.
Glucronide activities	Chimeric mouse (6YF)	Fresh	3 (F)	13.5±2.9	3.24±1.0/mouse	69.8±11.2	9.8±2.0	-
		Cryopreserved	5 (M: 3, F: 2)	13.4±2.4	-	50.7±5.1*5)	12.5±7.2	-
	Donor cell (6YF)	Cryopreserved	1 (F)	-	-	86.7	-	-
	uPA (wt/wt)/SCID mouse	Fresh	3	-	1.51±0.3/mouse	73.2±4.7	-	-

*1) Hepatocytes from one of four mice were used for CYP1A2, 2C9, and 3A (testosterone), and those from another were used for CYP2A6, 2C19, 2D6, 2E1, and 3A (midazolam). Hepatocytes from two mice were used for all tested P450s.

*2) Hepatocytes from one of five mice were used for CYP1A2, 2C9, and 3A (testosterone); those from a second mouse were used for CYP2A6, 2C19, and 2E1; those from a third mouse were used for CYP2C19, 2D6, 3A (midazolam); and those from a fourth mouse were used for tested P450s except for CYP2C19.
Those from a fifth mouse were used for all tested P450s.
*3) Hepatocytes from one of two mice were used for CYP1A2 and 3A, and those from the second mouse were used for CYP2C9 and 2C19.
* 4) Not determined.
*5) Data after thaw.
*6) Data after purification with Percoll.

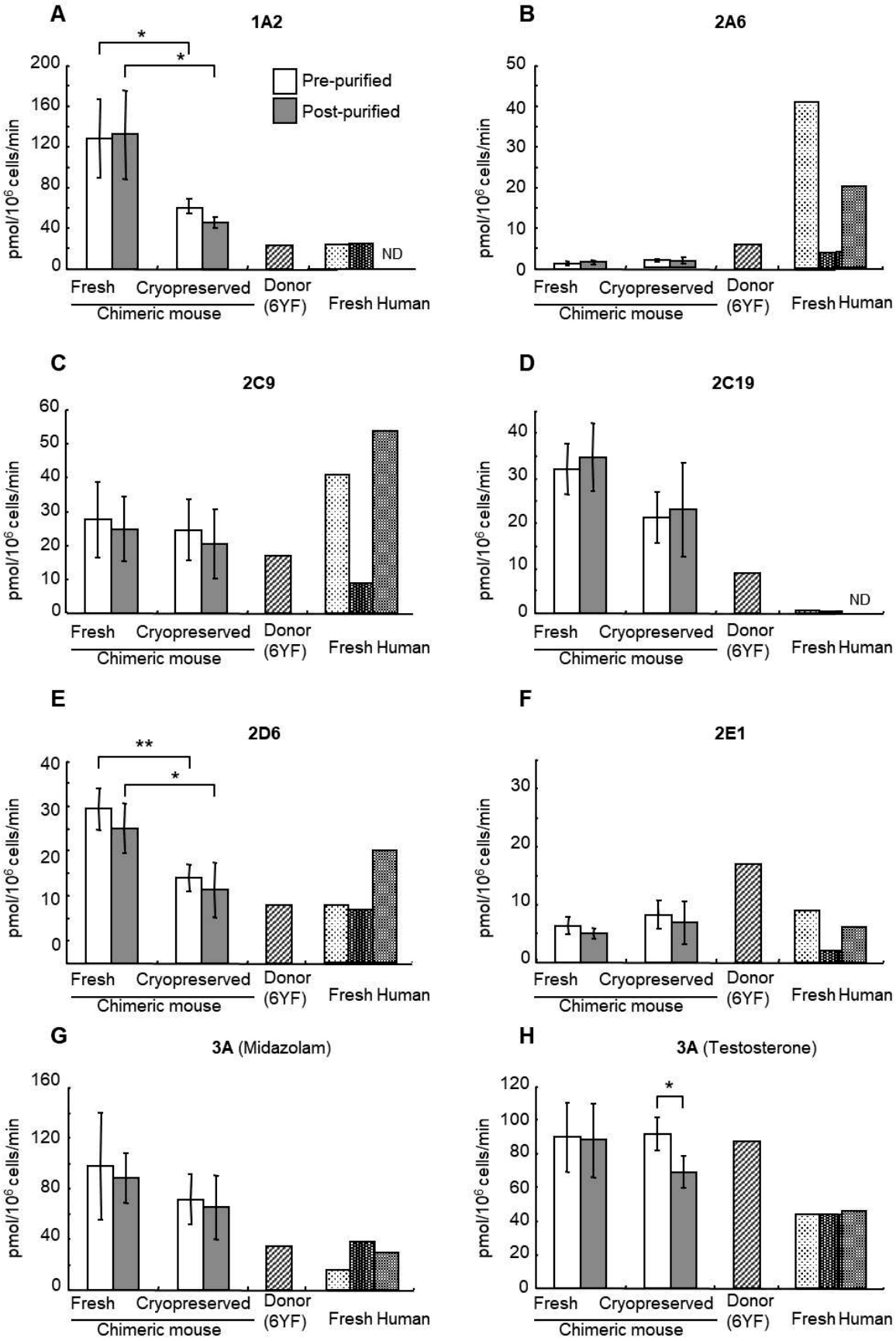
A
1A2
*
*
Pre-purified
Post-purified
pmol/10^6 cells/min
200
160
120
80
40
0
ND
Fresh
Cryopreserved
Donor (6YF)
Fresh Human
Chimeric mouse
B
2A6
50
40
30
20
10
0
C
2C9
60
50
40
30
20
10
0
D
2C19
40
30
20
10
0
ND
E
2D6
**
*
F
2E1
G
3A (Midazolam)
H
3A (Testosterone)
*
120
100
80
60
40
20

Fig. 1. P450 activities of fresh and cryopreserved chimeric hepatocytes, cryopreserved donor hepatocytes, and fresh h-hepatocytes, determined by LC-MS/MS

Hepatocytes were isolated from 6YF-chimeric mice. Aliquots of the isolated hepatocytes were frozen with a programmed freezer. Aliquots of fresh and thawed cryopreserved chimeric hepatocytes were purified with 66Z antibodies by magnetic sorting. Cryopreserved donor hepatocytes (6YF) for the chimeric mice were thawed. Fresh h-hepatocytes were isolated from resected livers after surgery from three patients. Eight kinds of suspended hepatocytes were incubated with eight substrates specific for seven P450s (Table 1): (A) 1A2, (B) 2A6, (C) 2C9, (D) 2C19, (E) 2D6, (F) 2E1, (G) 3A, midazolam, and (H) 3A, testosterone. The incubated medium was analyzed for each metabolite by LC-MS/MS (Table 2) and the metabolic activity of each P450 is shown as pmol/106 cells/min. Data in fresh and cryopreserved chimeric hepatocytes are shown as means± SD of metabolite concentrations of three different chimeric mice. *$p<0.05$, **$p<0.01$. ND, not detected.

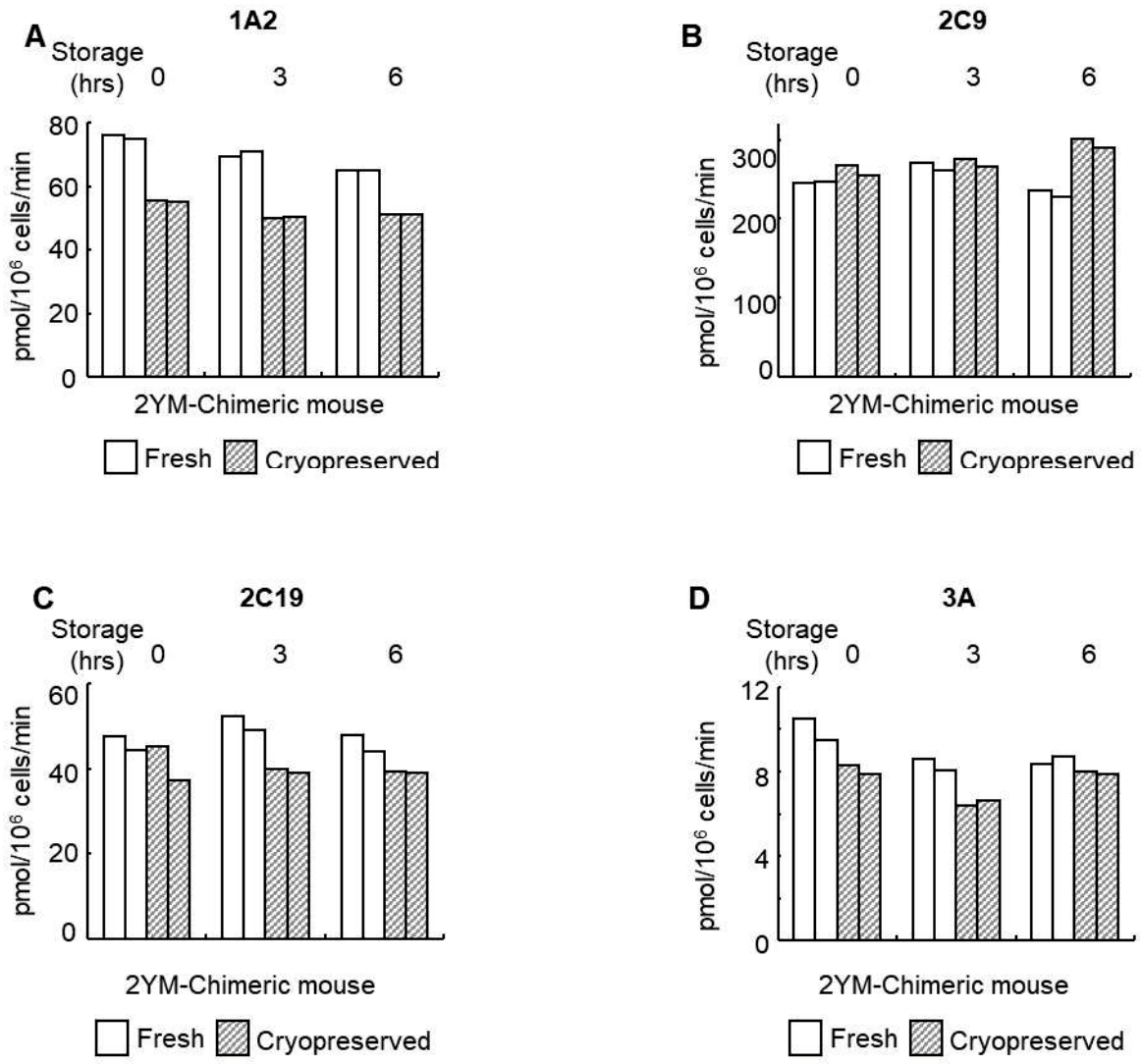

Fig. 2. Time course of P450 activities in fresh and cryopreserved chimeric hepatocytes after isolation or thawing, respectively, as assessed by HPLC

Fresh and cryopreserved 2YM-chimeric hepatocytes were stored after isolation and thawing, respectively, at 49C for 3 and 6 h. The fresh and cryopreserved chimeric hepatocytes were purified by Percoll isodensity centrifugation after isolation or thawing. Fresh and cryopreserved chimeric hepatocytes, just after purification (0 h) and after storage for 3 h and 6 h, were treated with four substrates specific for four P450s (Table 1): (A) 1A2, (B) 2C9, (C) 2C19, and (D) 3A. The incubated medium was used to analyze each metabolite by HPLC; the metabolic activity of each P450 is shown as pmol/10^6 cells/min (Table 3).

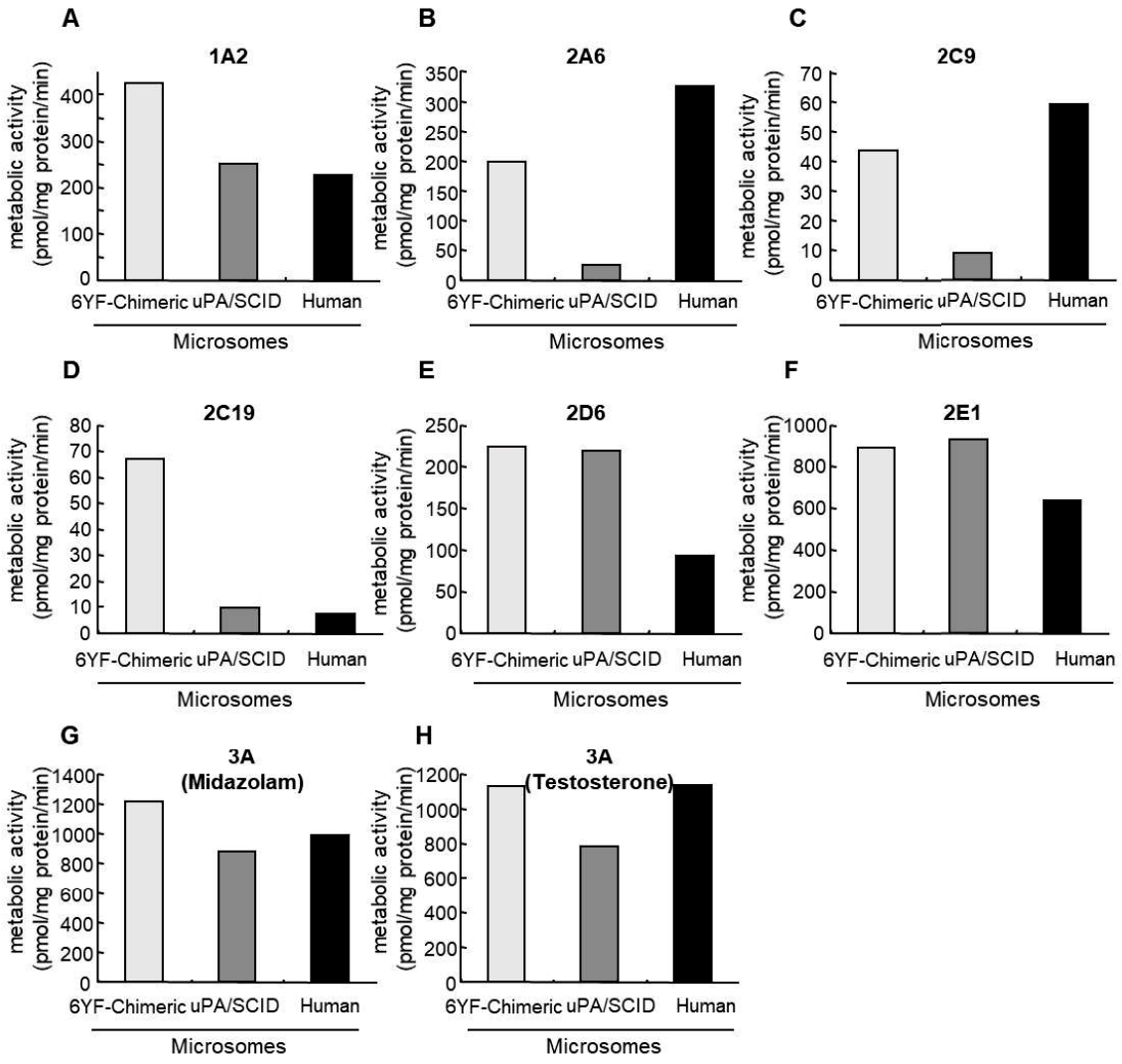

Fig. 3. P450 activities of liver microsomes from chimeric mice, uPA/SCID mice, and human livers as determined by LC-MS/MS

Microsomes from a 6YF-chimeric mouse and pooled microsomes of uPA/SCID mice and human livers were treated with eight substrates specific for seven P450s (Table 1), and the metabolite concentrations were measured by LC-MS/MS; the metabolic activity of each P450 is shown as pmol/mg protein/min (Table 2): (A) 1A2, (B) 2A6, (C) 2C9, (D) 2C19, (E) 2D6, (F) 2E1, (G) 3A, midazolam, and (H) 3A, testosterone.

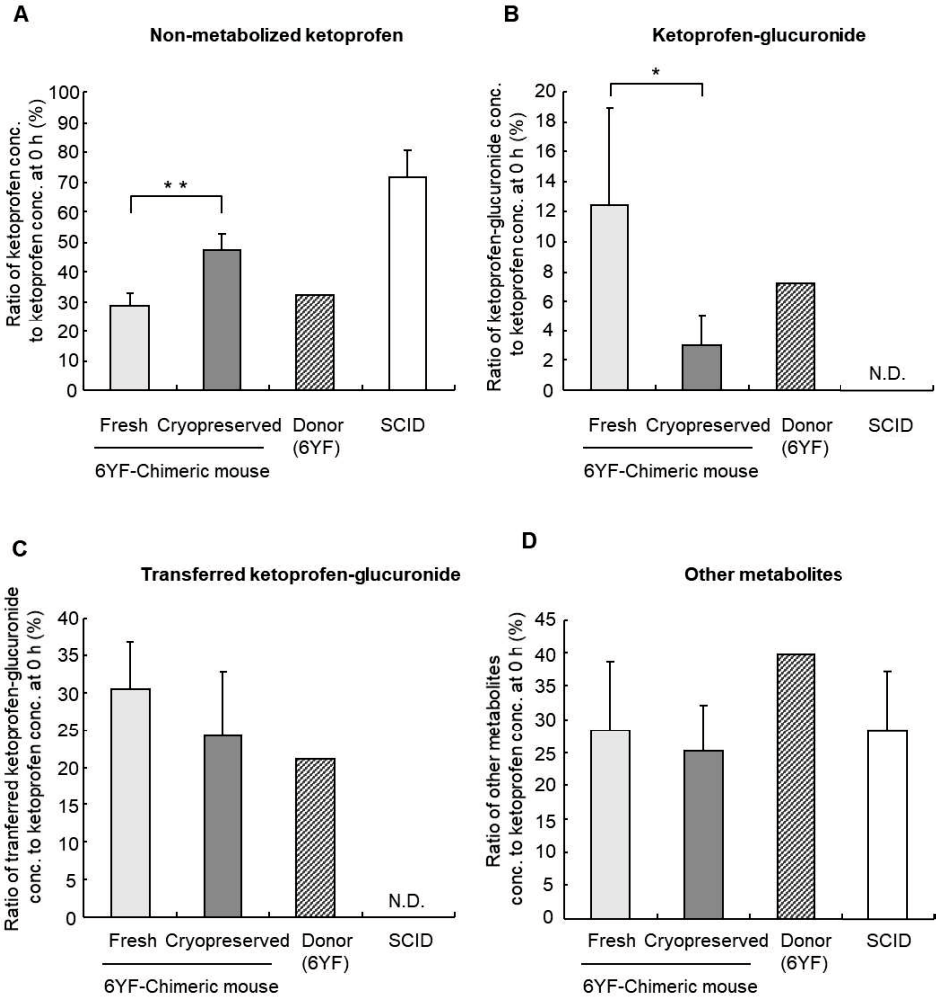

Fig. 4. Glucuronidation of ketoprofen in fresh and cryopreserved chimeric hepatocytes, uPA(wt/wt)/SCID mouse hepatocytes, and cryopreserved donor hepatocytes, as determined by LC-MS/MS

Fresh and cryopreserved chimeric hepatocytes, uPA(wt/wt)/SCID mouse hepatocytes, and cryopreserved donor hepatocytes (6YF) were incubated with ketoprofen for 3 h. The conditioned medium was treated with b-glucuronidase and 1 N KOH, and the concentration of ketoprofen was measured by LC-MS/MS (Table 2): (A) Non-metabolized ketoprofen, (B) Ketoprofen-glucuronide, (C) Transferred ketoprofenglucuronide, and (D) other metabolites. The concentrations of ketoprofen-glucuronide and transferred ketoprofen-glucuronide were calculated by the formulas indicated in Materials and Methods, and the activities were expressed as the ratio of the concentration of ketoprofen or its glucuronide conjugate to the ketoprofen concentration at 0 h. The values shown are the means± SD of three or five different chimeric mice. *$p<0.05$, **$p<0.01$. ND, not detected.

III-(2). Culture density contributes to hepatic functions of fresh human hepatocytes isolated from chimeric mice with humanized livers: Novel, long-term, functional two-dimensional *in vitro* tool for developing new drugs

Abstract

Chimeric mice with humanized livers are considered a useful animal model for predicting human (h-) drug metabolism and toxicity. In this study, the characteristics of fresh h-hepatocytes (cFHHs, PXB-cells®) isolated from chimeric mice (PXB-mice®) were evaluated *in vitro* to confirm their utility for drug development. cFHHs cultured at high density (2.13×10^5 cells/cm^2) displayed stable production of h-albumin and cytochrome P450 (CYP) 3A activities for at least 21 days. The mRNA expression levels of 10 of 13 CYP, UDP-glucuronosyltransferase (UGT), and transporters were maintained at >10% of the levels of freshly isolated cFHHs after 21 days. From 1 week, many bile canaliculi were observed between cFHHs, and the accumulation of the multidrug resistance-associated protein and bile salt export pump substrates in these bile canaliculi was clearly inhibited by cyclosporin A. Microarray analysis of cFHHs cultured at high density and at low density (0.53×10^5 cells/cm^2) revealed that high density culture maintained high expressions of some transcription factors (HNF4α, PXR, and FXR) perhaps involved in the high CYP, UGT and transporter gene expressions of cFHHs. These results strongly suggest that cFHHs could be a novel *in vitro* tool for drug development studies.

Introduction

Drug metabolism, transporter, and hepatotoxicity tests for new chemical entities have been performed using cryopreserved human (ch-) hepatocytes as the gold standard. Although fresh human (h-) hepatocytes retain higher metabolic activities to some extent than ch-hepatocytes [1, 2], an on-demand supply and reproducible experiments using fresh h-hepatocytes from the same donor are impossible.

Generally, when rat hepatocytes are inoculated at high density on dishes (>2×10^5 cells/cm^2), attachment efficiency decreases due to overlaying [3]. In our experience, when rat or mouse (m-) hepatocytes were inoculated at high density on collagen-coated dishes (>2×10^5 cells/cm^2), hepatocytes detached from the dishes because cell-cell adhesion was stronger than cell dish adhesion. Therefore, in general, fresh hepatocytes have been preconfluently inoculated for metabolism or toxicology studies. However, cytochrome P450 enzyme (CYP) mRNA expression and activity in preconfluently cultured hepatocytes promptly decline [4, 5]. Therefore, studies of drug metabolism have been performed using h-hepatocytes suspended for 1 or 2 hours. In addition, because fresh m-hepatocytes and thawed ch-hepatocytes do not remain viable for longer than 1 week in traditional two-dimensional (2D) cultures, novel 2D culture system [6], sandwich 2D cultures [7], or three-dimensional cultures are needed for long-term experiments.

In the last decade, chimeric mice with humanized livers have been developed using several host mice, including urokinase-type plasminogen activator/severe combined immunodeficiency (uPA/SCID) mice [8, 9], Fah(-/-)Rag2(-/-)Il2rg (-/-) mice [10], and NOG-Tg (Alb-UL23) 7-2/ShiJic (TK-NOG) mice [11]. We succeeded in the stable and mass production of chimeric mice with humanized livers using uPA/SCID mice (PXB-mice®) [8]. The mRNA expression levels of approximately 82% of h-hepatocyte

genes from chimeric mice were similar to or within 2-fold of the levels in human liver [12]. Protein expression levels of phase I CYPs and transporters in chimeric mouse livers were similar to or within 4-fold of the levels in human liver [13]. In addition, we recently developed a new type of host mouse, the cDNA-uPA/SCID mouse [14]. Chimeric mice generated from cDNA-uPA/SCID mice exhibited improved characteristics over those of chimeric mice generated from uPA/SCID mice. The improvements included increased body weight and higher stable repopulation rates of h-hepatocytes [14]. Our chimeric mice have been utilized for *in vivo* drug metabolism and pharmacokinetics (DMPK) [15, 16, 17], drug-drug interaction [5, 18], and toxicology studies [19, 20, 21]. The chimeric mice also have been used for efficacy studies of chemical entities against hepatitis B virus and hepatitis C virus, because the chimeric mice are susceptible to these hepatitis viruses [22, 23, 24].

We obtained fresh h-hepatocytes (cFHHs, PXB-cells®) from our chimeric mice obtained by a collagenase perfusion method [1] and reported that CYP activities of suspended fresh h-hepatocytes and ch-hepatocytes from cFHHs were similar [1]. We also reported *in vitro* and *in vivo* CYP mRNA induction studies using chimeric mice and cFHHs with the same donor hepatocytes [5].

Recently, we demonstrated that cultured cFHHs were susceptible to HBV infection and that HBV-infected cFHHs can be maintained for more than 3 weeks when the cFHHs were cultured on collagen-coated dishes at a high density (2.13×10^5 cells/cm^2) [25]. Therefore, cFHHs have been used for *in vitro* efficacy studies of anti-HBV agents [25]. In those studies, we found that cFHHs can attach to collagen-coated dishes in high density cultures without the detachment seen in rodent hepatocytes and can be maintained for more than 3 weeks [25].

In the present study, high density 2D-cultures of cFHHs enabled long-term culture of h-hepatocytes maintaining CYP, UDP-glucuronosyltransferase (UGT), transporter mRNA expression and the activities of CYP3A and multidrug resistance-associated protein (MRP2) transporter and bile salt export pump (BSEP). We also evaluated differences in donors and individual chimeric mice using ch-hepatocytes isolated from three different donors. Finally, the role of the high density culture condition was determined by microarray analysis of cFHHs cultured at high and low density.

Materials and methods

Chemicals

Krebs–Henseleit buffer was purchased from Sigma-Aldrich (St. Louis, MO). Midazolam, and cyclosporin A (CsA) were obtained from Wako Pure Chemical Industries (Osaka, Japan). 5(6)-Carboxy-2',7'-dichlorofluorescein diacetate (CDFDA) was purchased from Thermo Fisher Scientific (Waltham, MA). N-(24-[7-(4-N,N-dimethylaminosulfonyl-2,1,3-benzoxadiazole)]amino-3α,7α,12α-trihydroxy-27-nor-5β-cholestan-26-oyl)-2'-aminoethanesulfonate (Tauro-nor-THCA-24-DBD, DBD) was purchased from GenoMembrane (Kanagawa, Japan). All other chemicals and solvents were of the highest grade commercially available.

Generation of chimeric mice (PXB-mice®)

ch-Hepatocytes, BD195 (donor A, platable, inducible, and transporter activity qualified, 2-year-old Hispanic girl), BD342 (donor B, platable, 2-year-old white girl), and BD85 (donor C, non-platable, 5-year-old African American girl) were purchased from BD Biosciences (Woburn, MA). cH-hepatocytes, IVT-JFC (donor D, platable, 1-year-old white boy) was purchased from BioIVT (Westbury, NY). These samples were obtained after written informed consent and this study was approved by Utilization of Human Tissue Ethical Committee of PhoenixBio Co., Ltd. (0028). ch-hepatocytes were thawed and transplanted into 2 to 4-week-old cDNA-uPA/SCID mice (PhoenixBio Co., Ltd., Higashihiroshima, Japan) via the spleen after butorphanol (Meiji Seika Pharma Co. Ltd., Tokyo, Japan) injection as previously described [14]. Three weeks after transplantation, 2 μL of blood was collected periodically from the tail vein to measure human albumin (h-Alb) concentration. Blood h-Alb levels in

chimeric mice were measured by immunonephelometry in a model BM6050 autoanalyzer (JEOL, Tokyo, Japan) using LX Reagent Eiken Alb II (Eiken Chemical, Tokyo, Japan). All experimental animals reported in this article were housed with environmental enrichments under pathogen-free conditions and maintained in a 12-h light/dark cycle with sterilized ad libitum water and regular diet CRF-1 (Oriental Yeast, Tokyo, Japan). All experimental procedures were conducted in accordance with the guidelines provided by Proper Conduct of Animal Experiments (June 1, 2006; Science Council of Japan) and approved by the Animal Care and Use Committee of PhoenixBio Co., Ltd. (2287).

Isolation and culture of cFHHs (PXB-cells®)

To isolate cFHHs, 14 to 17-week-old chimeric mice with blood h-Alb levels >12 mg/mL (estimated replacement indexes >85% [donor A through C; Table 1]) were used. cFHHs were isolated from 62 chimeric mice (9 mice for real-time quantitative reverse transcription polymerase chain reaction [qPCR] analysis, measurement of albumin secretion and CYP3A activity [Table 1], 6 mice for measurement of urea synthesis, 3 mice for CYP activity assay using a cocktail mixture of probe substrates, 6 mice for transporter immunohistochemistry and function assay, 24 mice for measurement of purity of h-hepatocytes, and 14 mice for culture under several cell density conditions and microarray analysis) which were euthanized by exsanguination from the inferior vena cava under anesthesia using isofluorane (Mylan Pharmaceuticals Inc., Canonsburg, PA) in a two-step collagenase perfusion method as described below.

The liver was perfused at 38ºC for 10 min at 1.5 mL/min with Ca^{2+}-free and Mg^{2+}-free Hanks' balanced salt solution (CMF-HBSS) containing 200 µg/mL ethylene glycol tetraacetic acid (EGTA), 1 mg/mL glucose, 10 mM N-2 hydroxyethylpiperazine-N'-2- ethanesulfonic acid (HEPES), and 10 µg/mL gentamicin. The perfusion solution was then changed to CMF-HBSS containing 0.05% type IV collagenase

(Sigma-Aldrich Japan, Tokyo, Japan), 0.6 mg/mL $CaCl_2$, 10 mM HEPES, and 10 μg/mL gentamicin, and perfusion was continued for 9–12 min at 1.5 mL/min. The liver was dissected and transferred to a dish; liver cells were gently disaggregated in the dish with CMF-HBSS containing 1% bovine serum Alb, 10 mM HEPES, and 10 μg/mL gentamicin. The disaggregated cells were centrifuged three times (50× g, 2 min). The pellet was suspended in medium consisting of Dulbecco's modified Eagle's medium (DMEM), 10% fetal bovine serum (FBS), 20 mM HEPES, 44 mM $NaHCO_3$, and antibiotics (100 IU/mL penicillin G and 100 μg/mL streptomycin). Cell number and viability were assessed using the trypan blue exclusion test.

For each assay, cFHHs isolated from a chimeric mouse or pooled cFHHs isolated from three or four chimeric mice were used. The cFHHs were inoculated in wells of type I collagen-coated 24-well or 96-well plates at 0.53, 1.06, 1.60, or 2.13×10^5 cells/cm^2, and cultured with dHCGM (DMEM containing 10% FBS, 2% dimethylsulfoxide [DMSO], 20 mM HEPES, 44 mM $NaHCO_3$, 15 μg/mL L-proline, 0.25 μg/mL insulin, 5×10^{-8} M dexamethasone, 5 ng/mL epidermal growth factor, 0.1 mM L-ascorbic acid 2-phosphate, 100 IU/mL penicillin G, and 100 μg/mL streptomycin) as we previously reported [25, 26]. The medium was replaced every 3 to 4 days. Portions of cells from day 0 samples were used for CYP3A activity measurements (in suspension) and total RNA isolation. ch-hepatocytes of donor A were thawed and cultured as cFHHs.

Measurement of purity of h-hepatocytes in cFHHs

Contamination by mouse cells in isolated cFHHs (donor A) was confirmed using 66Z rat IgG antibody specific for mouse cells [1]. The isolated cFHHs were incubated for 30 min with antibody conjugated to Dynabeads (Thermo Fisher Scientific, Waltham, MA) to recognize the surface of mouse cells, but not human cells. The ratio of bead-negative and -positive hepatocytes in the suspension of cFHHs was

determined by microscopy. The cFHHs were inoculated on type I collagen-coated wells of 24-well plates (2.13×10^5 cells/cm^2) and cultured using dHCGM. The cells were fixed with 10% formaldehyde for 10 min and stained with 4 μg/mL Hoechst33258 (#S-23387; Sigma) for 10 min at 2, 13, 23, and 33 days at room temperature. The h-hepatocytes and m-cells were counted on the culture plates under a microscope. The h-hepatocytes were distinguished from mouse cells based on different patterns resulting from the Hoechst staining of the nuclei [27]. Two independent experiments were performed.

Measurement of h-Alb concentration in culture supernatant and CYP3A activity

cFHHs (donor A, B, C, Table 1) were inoculated in wells of type I collagen-coated 24-well plates (2.13×10^5 cells/cm^2) and cultured with dHCGM for 21 days. Three wells were used for each condition. The culture supernatant was collected at 2, 7, 14, and 21 days, and h-Alb levels were measured by latex agglutination immunonephelometry as described above. Three independent experiments were performed using cFHHs isolated from three different mice (Table 1). The data are presented as mean ± SD.

Sample preparation for evaluation of the CYP3A activities of cFHHs was conducted as previously reported [1]. The isolated (day 0) or cultured hepatocytes at 2, 7, 14, and 21 days were incubated in Krebs–Henseleit buffer with 10 μM midazolam as substrate specific for the CYP3A subtype at 37°C for 2 h. The incubated solution was collected, and the concentration of the 1'-hydroxymidazolam metabolite was measured by high-performance liquid chromatography (HPLC) using a Lachome Elite device (Hitachi High-Technology Co., Tokyo, Japan). HPLC was performed at a flow rate of 1.0 mL/min using an Xterra RP18 column (4.6 × 150 mm, 5 μm; Waters). The measurements were performed in duplicate. Lower limit quantification of 1'-hydroxymidazolam was 0.1 μmol/L. Three independent experiments using cFHHs isolated from three different mice were performed (Table 1). The data are presented as mean ± SD.

Measurement of mRNA expression levels by real-time qPCR

The cFHHs (donor A, B, C; Table 1) were inoculated in wells of type I collagen-coated 24-well plates (2.13×10^5 cells/cm^2) and cultured with dHCGM for 2, 7, 14, and 21 days. The mRNA expression levels of human and mouse genes were quantified by qPCR. Total RNA was isolated from each hepatocyte sample of three wells at the defined times using TRIzol (*In vitro*gen Corporation, Carlsbad, CA) and treated with DNase (*In vitro*gen). cDNA was synthesized using 1 μg of RNA, SuperScript III reverse transcriptase (*In vitro*gen), and random primers (*In vitro*gen) according to the manufacturer's instructions, then subjected to qPCR. Genes were amplified with a set of gene-specific primers (S1 Table) and SYBR Green PCR mix (Applied Biosystems, Tokyo, Japan) using a 7500 Real-Time PCR System (Applied Biosystems). Cycling conditions were described previously [12]. Three independent experiments were performed using cFHHs isolated from three different mice (Table 1). The data are presented as mean ± SD. The species specificities of the human and mouse primers were confirmed using h- and m-hepatocyte cDNA, and non-specific amplification was not observed (data not shown).

Immunostaining for MRP2

The cFHHs (donor A) were inoculated in wells of type I collagen-coated 96-well plates (2.13×10^5 cells/cm^2) and cultured with dHCGM for 2, 7, and 14 days. For indirect immunofluorescence analysis, the primary antibody was anti-MRP2 antibody (GeneTex, Inc. Irvine, CA). cFHHs were fixed with formalin for 10 min and permeabilized with 0.25% Triton X-100 in 10 mM PBS (pH 7.5) for 10 min at room temperature. After incubation in PBS containing 10% donkey serum for 30 min, cells were incubated with primary antibodies and diluted in PBS overnight at 4°C. After washing with PBS containing Tween, cells were incubated with Alexa 488-conjugated anti-mouse IgG donkey serum as the secondary antibody

(Life Technologies Corporation, Carlsbad, CA) for 1 h at room temperature. Nuclei were stained with Hoechst 33258.

Measurement of MRP2, sodium-taurocholate cotransporting polypeptide (NTCP), and BSEP activities

The cFHHs (donor A, pooled cFHHs from three or four animals) were inoculated in wells of type I collagen-coated 24-well plates (2.13×10^5 cells/cm^2) and cultured with dHCGM for 7 and 16 days (for the assay using CDFDA) or for 9 days (DBD). Sixteen days after plating, the cFHHs were incubated with 1.25 μM CDFDA, a substrate for MRP2, in Hanks' Balanced Salt Solution (HBSS) for 5 min. The cells were washed twice followed by incubation with HBSS or Ca^{2+}- and Mg^{2+}-free HBSS. Cell morphology, bile canaliculi formation, and accumulation of 5-(and-6)-carboxy-2',7'-dichlorofluorescein (CDF) in bile canaliculi were analyzed with phase contrast and fluorescence microscopy (Bz-X, KEYENCE CORPORATION, Osaka, Japan), respectively. Seven days after plating, the cFHHs were preincubated in Ca^{2+}- and Mg^{2+}-free HBSS with or without cyclosporin A (CsA; 10 or 100 μM) for 30 min, followed by incubation with 1.25 μM CDFDA, with or without CsA (10 or 100 μM), for a further 20 min. Fluorescence of CDF was observed using fluorescence microscope (KEYENCE CORPORATION). Two independent experiments using cFHHs isolated from two different mice were performed to ensure reproducibility.

Nine days after plating, the cFHHs (donor A) were preincubated in HBSS with or without 10 μM CsA at 37°C for 30 min. This was followed by incubation with 10 μM DBD in the presence or absence of 10 μM CsA at 37°C for 10 min. The cFHHs were washed three times with HBSS at 4°C.The cells were incubated in HBSS at 37°C for 5 to 210 min. To inhibit substrate uptake by NTCP, cells were treated with CsA from the preincubation process onwards. To inhibit excretion of the substrate by the BSEP, cells were

treated with CsA with the DBD treatment during the washing process. The fluorescence of DBD that had accumulated in bile canaliculi was analyzed using fluorescence microscope (KEYENCE CORPORATION). Two independent experiments using cFHHs isolated from two different mice were performed to ensure reproducibility.

Microarray analysis

For microarray analysis, cFHHs (donor A, pooled cFHHs from 3-4 animals) were plated at high density (2.13×10^5 cells/cm^2) or low density (0.53×10^5 cells/cm^2) in wells of type I collagen-coated 24-well plates and cultured for 7 days. Total RNA was isolated from pooled cells of three wells of each fresh and cultured cFHH at high density or low density. RNA extraction was conducted as described above. RNA integrity was assessed using a Bioanalyzer (Agilent Technologies, Santa Clara, CA). After total RNA was deemed to be of sufficient quality (A260/A280 >1.9 and 28S/18S ratios approaching 2), the samples were stored at -80°C until further analysis. Three individual experiments using cFHHs isolated from three different mice were performed and these RNA samples were used for microarray analysis. For this analysis, RNA samples were applied to the GeneChip® Human Genome U-133 Plus 2.0 Array (Affymetrix, Santa Clara, CA) containing 54,675 probe sets according to the manufacturer's instructions. Gene expression array data were normalized using the MAS5 algorithm (Affymetrix). The signal reliability of each probe was determined based on the MAS5 Call algorithm (Affymetrix), and each probe was assigned to one of three flags (P: present, M: marginal, and A: absent). To correct for bias between chips, GeneChip CEL files were imported into GeneSpring14.8 (Agilent Technologies). Correlation analyses for the RMA-normalized logarithmic expression levels of all probe sets were performed using GeneSpring14.8. We deposited our array data to NCBI GEO (Gene Expression Omnibus https://www.ncbi.nlm.nih.gov/geo/) (accession no.

GSE153298).

Statistical analysis

The data were analyzed with Statcel 4 (OMS Publishing Inc., Tokorozawa, Japan). Log_{10}-transformed data obtained in qPCR analysis were used for statistical analysis. Results are expressed as mean ± SD, and the significance of the difference between two groups was analyzed by Student's *t*-test when data were normally distributed, and otherwise by Welch's *t*-test. Multiple-sample comparisons were made by one-way analysis of variance followed by post hoc analysis. Statistical significance was considered at p-values <0.05.

Urea synthesis assay

cFHHs (donor A) were cultured from day 1 in dHCGM. For the urea synthesis measurement at days 8, the medium was changed at days 6 and 7 in dHCGM containing GlutaMax™ (Thermo Fisher Scientific, Waltham, MA) instead of L-glutamine and removed FBS (GlutaMax medium). The culture medium at days 8 was collected and the concentration of urea was measured using QuantiChrom Urea Assay Kit (BioAssay systems, Hayward, CA). For the measurement at days 15, the medium was changed at days 13 and 14 in the GlutaMax medium. The culture medium at days 15 was collected and the concentration of urea was measured.

Measurement of CYP activities using a cocktail mixture of probe substrates

Sample preparation for the evaluation of the CYP1A2, CYP2C19, and CYP3A activities of cFHHs (Donor D) were conducted. The isolated (day 0) cFHHs were incubated in Williams'E medium containing Primary Hepatocyte Maintenance Supplements (Thermo Fisher Scientific, Waltham, MA) with a probe substrate at 37°C for 2 h, namely 50 μM phenacetin, 50 μM S-mephenytoin, and 5 μM midazolam

for the assessment of the CYP1A2, CYP2C19, and CYP3A activities, respectively. The incubated solution was collected and the concentration of the metabolites (acetaminophen, 4'-hydroxy S-mephenytoin, and 1'-hydroxymidazolam) was measured by liquid chromatography-tandem mass spectrometry (LC-MS/MS). LC-MS/MS analysis was performed on HPLC LC20A system (Shimadzu Corporation Kyoto, Japan) and API 4000™ (AB Sciex Pte. Ltd., Framingham, MA) by Sumika Chemical Analysis Service, Ltd. (Osaka, Japan).

Preparation of samples for mRNA expression analysis in fresh h-hepatocytes from human normal tissues

Fresh h-hepatocytes isolated at Hiroshima University Hospital were provided. Normal liver tissues were obtained from the resected liver of four patients (39- and 61-year-old men and 25- and 57-year-old women) after written receiving consent prior to surgery, in accordance with the 1975 Declaration of Helsinki. The hepatocytes were isolated via two-step collagenase perfusion and low-speed centrifugation [9]. They were then incubated in lysed in lysis buffer and stored in freezer until further use. Total RNA was isolated from each sample using RNeasy Micro Kit (Qiagen, Hilden, Germany). DNase treatment, cDNA synthesis, and qPCR analysis were conducted using the same procedure in the Materials and Methods. This study was approved by Utilization of Human Tissue Ethical Committee of PhoenixBio Co., Ltd. (0051).

Results

Morphology of cFHHs and contamination of mouse cells in cFHHs

To verify the lot-to-lot variations, cFHHs were isolated from chimeric mice transplanted with cells from the three different donors and cultured at high density. Animal information, yield, and viability of the cFHHs from each chimeric mouse are summarized in Table 1. At least 10^8 cells were collected from each chimeric mouse. Regardless of the original characteristics of ch-hepatocytes (donor A and B: platable, donor C: non-platable) before transplantation into host mice, all cFHHs were highly platable. The cultured cFHHs showed matured hepatocyte morphology for at least 3 weeks and many bile canaliculi had formed between cells at 7 days (Fig 1A and S3 Fig.). There were no clear differences in cFHH morphologies among the donors (Fig 1A).

To analyze the presence of contaminating mouse cells, freshly isolated cFHHs were treated with 66Z-conjugated magnetic beads. In this culture condition, hepatocytes do not proliferate. Microscopic observation revealed that the average ratio of h-hepatocytes to total cells in the freshly isolated cFHHs was 90.3 ± 2.9% (22 animals). We also counted the number of h-hepatocytes and contaminating mouse cells at 2, 13, 23, and 33 days after plating. Two days after plating, the cultured cell density (h-hepatocytes and mouse cells) was approximately 1.5×10^5 cells/cm^2. At day 13, cell density decreased to approximately 80% of the day 2 density, and then remained stable for at least 33 days. The m-hepatocytes decreased in this condition, and the ratio of h-hepatocytes to total cells was 93% at 2 days, and then gradually increased to 98% at 33 days (Fig 1B). These results suggested that the present culture conditions were more suitable for h-hepatocytes than for mouse cells.

The expression profiles of mouse cyp (m-cyp) 1a2 and 3a11 mRNAs were analyzed by qPCR using mouse-specific primer sets. Expression of both m-cyp mRNAs drastically decreased and the lowest level was <1% (cyp1a2) and 0.1% (cyp3a11) of basal expression level (day 0) at 7 days (Fig 1C).

Evaluation of h-Alb secretion, urea synthesis, CYP activities, and CYP, UGT, and transporter mRNA expressions in cFHHs

All cFHHs showed similar h-Alb secretion ability at 2 days (approximately 0.7 μg/10^5 cells/day) and 7 days (approximately 1.4 μg/10^5 cells/day). After day 7, the secretion of albumin was maintained until day 21 (Donor A and C) or gradually reduced to day 2 levels (Donor B) (Fig 2A).

The synthesis of urea by cFHHs (donor A) was measured at days 8 and 15. Stable urea synthesis levels were observed in cFHHs at days 8 (1.47 mM/day, 110.42 μg/10^6 cells/day) and 15 (1.42 mM/day, 106.44 μg/10^6 cells/day). These data were similar to those in the previous report (0.42 mM/day, approximately 113.28 μg/10^6 cells/day) [28].

The CYP3A activity of cFHHs was measured using midazolam as a substrate (Fig 2B). The activities in suspension (day 0) were different among the donors, but all activities decreased at 2 days and then recovered to or increased over basal levels after 7 days. The CYP3A activity in donor A was lower than in those in donors B and C. The recovered activity levels were maintained during the culture period. According to the mouse hepatocyte contamination rate and m-cyp3a11 mRNA expression levels (Fig 1B and 1C), CYP3A activities in cFHHs might be derived from human hepatocytes.

Expression patterns of several human hepatic genes were analyzed by qPCR using cultured cFHHs from three donors (Fig 2C-2O). Two genes, CYP1A2 and UGT2B7, showed donor differences in

these expression levels at day 0. In the case of cFHHs, the expression level of CYP1A2 in donor B was 10 times lower than in donors A or C (Fig 2D). The expression level of UGT2B7 in donor A was also 10 times lower than those in donors B and C in the case of cFHHs (Fig 2K). Except for CYP1A2 and UGT2B7, the other hepatic genes showed similar basal expression levels at day 0. Through the culture period, the h-hepatocytes from the three donors showed similar expression profiles. Two expression patterns were evident during culture. In the first pattern, expression levels decreased at day 2 and then remained stable between 2% and 120% of the initial levels (day 0, isolated hepatocytes; CYP1A1, CYP1A2, CYP2B6, CYP2C9, CYP2D6, CYP2E1, UGT2B7, BSEP, organic anion transporting polypeptide [OATP] 1B1, and OATP1B3). In the second pattern, expression levels decreased at 2 days, but increased to higher than the initial levels, which were maintained until 21 days (CYP3A4, UGT1A1, and MRP2). The expression pattern of CYP3A4 mRNA was very similar to CYP3A activity (Fig 2B and 2I). Although CYP3A activities of donor A was a little lower than those of donor B and C, mRNA expressions of CYP3A4 were similar among the three donors. The mRNA expression levels of 10 of 13 CYP and UGT enzymes and transporters were maintained at >10% of the levels of freshly isolated cFHHs after 21 days. Those of hUGT2B7 (7.1%), hBSEP (2.3%), and hOATP1B1 (7.7%) were decreased by <10% of the initial levels (Table 2).

Expression levels of the genes in PXB-cells cultured for 2, 7, 14, and 21 days were compared to those in freshly isolated PXB-cells (day 0). The results represent mean (ratio (%) of the day 0 level) ± SD of three independent experiments.

Comparison of Characteristics between cFHHs and ch-hepatocytes from same donor or fresh adult h-hepatocytes.

The ch-hepatocytes from donor A were specified by the provider as platable hepatocytes with CYP induction and transporter abilities. The ch-hepatocytes were thawed and cultured in the same conditions as cFHHs for 14 days to compare their morphologies, h-Alb secretion, and CYP and UGT mRNA expression levels. In the present culture conditions, the ch-hepatocytes also maintained matured hepatocyte morphology. The results of h-Alb quantification indicated that there was no significant difference in the h-Alb production abilities of the cultured ch-hepatocytes and the cFHHs after at least 14 days (S1 Fig.). qPCR analysis revealed that there was a difference of over two log in the CYP3A4 mRNA expression levels between the ch-hepatocytes and cFHHs at day 0. However, after day 2, the CYP3A4 mRNA expression levels in the cultured ch-hepatocytes were comparable or slightly lower than those in the cultured cFHHs at the same time points. The mRNA expression patterns of the CYPs and UGTs were similar to those in cFHHs (S1 Fig.). The ch-hepatocytes of donor C did not attach to the dishes as observed in donor A.

The cryopreserved hepatocytes used for transplantation in chimeric mice were derived from very young donors (2-5 years old). To confirm the phenotype of hepatic expression in the chimeric mouse liver, we compared hepatic gene expression (CYPs and UGTs) in cFHHs (from donor A, B, and C) and fresh h-hepatocytes from 4 adult donors (25-, 39-, 57-, and 61-year-old). The expression levels of CYP1A2 and UGT1A1 among the measured 6 genes (CYP1A2, CYP2C9, CYP2D6, CYP3A4, UGT1A1, and UGT2B7) in cFHHs were similar to those in h-hepatocytes from adult donors. Although the expression levels of

CYP2D6 and CYP3A4 were higher and those of UGT2B7 were lower in fresh h-hepatocytes than in cFHHs, there were no statistical differences between them (S2 Fig.).

Localization and function of MRP2, NTCP, and BSEP in cFHHs

Localization of the efflux transporter MRP2 in the cFHHs of donor A was confirmed by immunocytochemistry. There were no obvious signals in the cFHHs at day 0 and 2 (Fig 3A). However, MRP2 was localized to bile canalicular membranes at 7 days and the positive spots were enlarged at 14 days (Fig 3A). To analyze the transporter activity of MRP2, the cultured cFHHs (donor A) were treated with CDFDA at 16 days. Sustained accumulation of CDF, a fluorescent metabolite of CDFDA, was observed in the bile canaliculi in the presence of Ca^{2+} (S3 Fig). On the other hand, the CDF signals rapidly disappeared from the bile canaliculi in the absence of Ca^{2+}. This observation indicated that in the presence of Ca^{2+} the integrity of the bile canalicular networks remains intact, while in the absence of $Ca2^{+}$ the integrity of the canalicular space is disrupted, causing leakage of the canalicular contents, as reported previously [29]. Treatment with the potent MRP2 inhibitor CsA at 10 and 100 μM significantly inhibited the accumulation of CDF in the bile canaliculi, and intense fluorescence signals were observed in the cytoplasm (Fig 3B). To analyze the transporter activity of NTCP and BSEP, the cultured cFHHs (donor A) were treated with DBD at 9 days. DBD was incorporated into the cFHHs and accumulated in bile canaliculi (Fig 3C). To inhibit uptake of the substrate by NTCP, cells were treated with CsA from the preincubation process onwards, before treatment with DBD at 37℃. To inhibit excretion of the substrate by BSEP, cells were treated with CsA from the washing process onwards, following DBD treatment at 37℃. Treatment with CsA before or after DBD addition decreased the accumulation of DBD in the bile canaliculi (Fig 3C

and D). cFHHs retained MRP2 and BSEP activities, although mRNA expression level of BSEP were 2% to 3% at 7, 14, and 21 days compared with day 0 (Table 2).

Effects of cell density on morphologies and liver-specific functions of the cultured cFHHs

We predicted that the high density culture might induce the maintenance of high gene expression levels of phase I and II enzymes and transporters. To test this hypothesis, cFHHs were inoculated on type I collagen-coated plates at densities of 0.53, 1.06, 1.60, and 2.13×10^5 cells/cm^2. The freshly isolated cFHHs were highly platable, and firmly attached to type I collagen-coated plates 15 to 30 min after plating. Seven days after plating, cells inoculated at 0.53 and 1.06×10^5 cells/cm^2 were pre-confluent, and cells and nuclei were flattened at these plating densities (Fig 4A). When hepatocytes were plated at 1.60 and 2.13×10^5 cells/cm^2, they became confluent. Cells cultured at 2.13×10^5 cells/cm^2 were densely packed and bile canalicular structures were clearly observed between hepatocytes. However, cells plated at 1.60×10^5 cells/cm^2 were somewhat flat and bile canalicular structures were fewer than those between cells plated at 2.13×10^5 cells/cm^2 (Fig 4A). Microscopic observation revealed that approximately 60% to 73% of cells were attached to the plate surface in the various density conditions at 7 days (Table 3). To evaluate the effect of cell density on hepatocyte functions, h-Alb levels in the culture media were examined at 7 days. The h-Alb levels per 10^5 attached cells at 7 days are shown in Fig 4B. Compared with those cultured at lower cell densities, cFHHs cultured at higher densities displayed significantly higher albumin secretion (Fig 4B). The qPCR results clearly indicated that the mRNA expression levels of CYP1A1, CYP1A2, CYP2B6, CYP3A4, MRP2, OATP 1B1, and BSEP decreased in the PXB-cells cultured at the lowest

density, although the difference in MRP2 expression was not statistically significant (Fig. 4C). However, UGT1A1 expression was stable at all examined densities

From these results, gene expression profiles of isolated cFHHs and cultured cFHHs from donor A at high density (2.13×10^5 cells/cm^2) or low density (0.53×10^5 cells/cm^2) were compared by microarray analysis. The gene expression profile of cFHHs cultured at 7 days at high density was close to that of isolated cFHHs (correlation efficiency: 0.911). In contrast, correlation efficiency between isolated cFHHs and cFHHs cultured at low density at 7 days was very low (0.736).

The mRNA expression profiles of cFHHs cultured at high density and low density were compared. Gene profiles were compiled using microarrays representing 54675 human transcripts. Among these, 22893 transcripts (42% of total probes) were assigned as present (P flag) for all cFHHs at either high density or low density. Moreover, of those 22893 transcripts, 1247 (5.4%) were expressed at levels two-fold lower in the cFHHs at low density than at high density ($p<0.05$, two-sided Student's *t*-test).

Pathway analysis was then performed on the 1247 transcripts down-regulated in cFHHs at low density on day 7. As a result, 32 pathways were detected ($p>0.001$ minimum number of matches > 10), of which five were nuclear receptor (NR)-related pathways (Table 4). The 1247 transcripts down-regulated in low density cultured cFHHs included seven transcription factors (TFs), 27 phase I metabolic enzymes, 11 phase II metabolic enzymes, and 53 transporters. Down-regulated TF, phase I and II enzymes, and transporter genes are shown in S2 Table.

mRNA expression of HNF4α and other TFs in cFHHs

In NR-related pathways detected by pathway analysis, the gene expression levels of significantly down-regulated TFs including NRs (HNF4α, CAR, and PXR) and an unchanged NR (FXR) were determined from the cFHHs of three donors (Table 1) cultured for 21 days. The mRNA expression of HNF4α, PXR, and FXR were quantified using qPCR. Levels were maintained at day 0 levels for at least 21 days. In contrast, CAR expression decreased to approximately 10% at day 2 and this level was maintained for 21 days (Fig 5). From these results, we concluded that CYP and UGT genes and transporter genes might be regulated by the expression of these TFs in high density cultured cFHHs.

Discussion

It is recognized that ch-hepatocytes are the gold standard for *in vitro* studies of DMPK and toxicology [30-33]. However, the use of ch-hepatocytes is limited by lot size (at most several hundred vials from one donor), and there are individual differences among donors. Because of these limitations, researchers have been using immortalized liver-derived cell lines, such as HepG2, HepaRG, and induced pluripotent stem cell-derived hepatocytes for their *in vitro* studies [34]. Although some liver-specific functions are confirmed in these cells, many other liver functions were still significantly lower than those in primary h-hepatocytes [34-36]

In the case of humanized-liver mice, the transplanted ch-hepatocytes dramatically proliferate more than 1000-fold in the host mouse liver. Therefore, more than 10^8 hepatocytes can be isolated from a chimeric mouse. Our previous results revealed that most genes showed comparable expression levels in the human hepatocytes of both human and chimeric mouse livers [12]. The humanized-liver mouse has been used in many studies of DMPK, safety, and hepatitis B virus and hepatitis C virus infections. These facts indicate that chimeric mice transplanted with ch-hepatocytes derived from one donor could stably and repeatedly supply a large amount of fresh h-hepatocytes.

In general, h-hepatocytes undergo changes in cell morphology and rapidly lose their hepatic functions, such as CYP expression and albumin secretion, in tradittional 2D culture model [37, 38]. To overcome this problem, several different types of culture methods have been established [6, 39]. In this study, we developed a novel culture system in which human hepatocytes maintain high hepatic function for at least 21 days. In this culture system, cFHHs isolated from PXB-mice were plated on type I collagen-coated plates at high density (2.13×10^5 cells/cm^2) in the dHCGM medium we previously

developed [25]. h-Alb secretion, CYP3A activity, and mRNA expression levels were compared among three types of cFHHs isolated from three PXB-mice transplanted using different donors. Individual differences between mice were small in all data tested. There were no significant differences between the hepatic function of donors, except for CYP3A activity and the mRNA expressions of hCYP1A2 and hUGT2B7.

We previously compared the activities of cFHHs and the corresponding cryopreserved ch-hepatocytes [1]. As a result, the CYP1A2, 2C19, 2D6, and 3A activities in cFHHs were more than twice those in the cryopreserved ch-hepatocytes. We also compared the activities in cFHHs and cryopreserved cFHHs by a programmed freezer. Freezing decreased the CYP1A2 and 2D6 activities significantly. The decreased metabolism in cryopreserved hepatocytes may be attributable to two mechanisms: inactivation of P450 enzymes and loss of the cofactor NADPH due to cell membrane damage [40]. In addition, the CYP activities of cFHHs and thawed ch-hepatocytes (manufacture's data, donor D) were compared. The activity of CYP1A2 using phenacetin in cFHHs and thawed ch-hepatocytes was 75.9 ± 1.8 and 3.9 pmol/10^6 cells/min, respectively. The activity of CYP2C19 using S-mephenytoin in cFHHs and thawed ch-hepatocytes was 35.5 ± 0.9 and 3.1 pmol/10^6 cells/min, respectively. The activity of CYP3A using midazolam in cFHHs and thawed ch-hepatocytes was 18.4 ± 1.2 and 5.0 pmol/10^6 cells/min, respectively. These results of the CYP activities of cFHHs were similar or higher than those in ch-hepatocytes. We measured the major CYPs and UGTs mRNA expression levels in the ch-hepatocytes of donor A, resulting in extremely low levels (1/5-1/1000 compared to cFHHs), most likely due to the degradation of RNAs as a result of freeze and thaw. Interestingly, after 2 days, the mRNA expression levels of ch-hepatocytes recovered to levels of cFHHs (S1 Fig).

Several previous studies have reported that cultured cell density could affect hepatocyte-specific functions in h-hepatocytes [41], rat hepatocytes [42], and HepaRG [43]. Regardless of the culture models and hepatocyte sources, the cell density of cultured hepatocytes might be one of the most essential factors for the maintenance of liver-specific functions *in vitro*. We predicted that the high density culture of cFHHs should generate long-term high liver function levels. To test this hypothesis, cFHHs were cultured at both high density and low density, and the gene expression levels were compared using microarray analysis. The mRNA expressions of 1247 genes, including phase I and II metabolic enzymes and transporter genes, were significantly up-regulated in the high density culture conditions compared to low density conditions. NR pathways were significantly overrepresented following pathway analysis of the 1247 genes. The mRNA expression levels of HNF4α and six TFs were up-regulated in high density culture. The mRNA expression of HNF4α, PXR, and FXR in high density culture at 21 days were maintained at similar levels to the freshly isolated cFHHs, while the level of CAR mRNA decreased to approximately 10% of the level in freshly isolated cFHHs.

HNF4α and the CAR, PXR, and FXR control hepatic genes including CYP, UGT, and transporters. CYP2B6, 2C9, 2D6, and 3A4 are regulated by HNF4α [44-52]. The expression of CYP2B6 and CYP2C9 mRNA are also affected by CAR and PXR [53-55]. Although, the expression of PXR and HNF4 in cultured cFHHs were maintained at day 0 levels for 21 days, a CAR expression decreased to approximately 10% of day 0 level during the culture period. We suggest that the decreased expressions of CYP2B6 and CYP2C9 in cultured cFHHs might be due to decreased CAR expression. OATP1B1 is regulated by PXR, FXR, and CAR [56-59], suggesting that its gene expression in cultured cFHHs might be affected by the decrease in CAR expression.

CAR may also regulate expressions of CYP3A4, MRP2, and UGT1A1 [60-65]. However, their gene expressions were maintained in cFHHs in the present study, suggesting that other regulatory mechanisms might be involved in their gene expressions. In addition to HNF4α, PXR, CAR and FXR, CYP1A1 and UGT1A1 are affected by AhR. It was reported that C/EPBa and VDR affect CYP2D6 and MRP2, respectively. These data highlight the need for further explorations of the changes in the expression of these genes.

In this study, we provide the first evidence that the mRNA expressions of HNF4α, PXR, and FXR are maintained in high density culture conditions. These results suggest that the expression levels of some TFs might affect the maintenance of hepatic genes, such as CYP UGT, and transporters of cFHHs in high density culture conditions. Better understanding of the cross-talk mechanisms of TFs and their target genes, such as CYPs and UGTs, and transporters *in vitro* and *in vivo* by optimization of culture conditions are important. Further experiments involving siRNAs or gene transfer-mediated overexpression of these TFs into cFHHs are needed.

In this paper, we mainly measured the mRNA expression levels of metabolic enzymes, and the CYP3A activity, albumin secretion, and urea synthesis were determined during culture. Recently, we published the CYP activities of cFHHs of donor A after 21 days in the same culture condition [66]. CYP mRNA expression in the present study was compared with the corresponding activities in this paper during culture. The mRNA expression levels and the activities of CYP1A2 and CYP2D6 were decreased at day 7 and remained at similarly low levels until day 21. On the other hand, the CYP2C9 mRNA decreased gradually and reached 0.3 at day 21 compared to that at day 0; however, the activity was around 1.0 during culture. The CYP3A4 mRNA levels increased gradually and reached 4.0 at day 21 compared to that at day

0; however, the activity of CYP3A was around 1.0 during culture. Thus, the relation of the mRNA expression levels and activities were different among CYPs.

We already compared the CYP activities of cFHHs derived from young donors and adult PHHs (54-, 57-, and 75-year-old) in our previous paper [1]. The resulting CYP activities were similar between the cFHHS from young donors and adult PHHs. We have newly determined the level of mRNA CYP expression between cFHHs from young donors and adult PHHs , resulting there were no statistical differences between them (S2 Fig.)

A disadvantage to the use of humanized-liver mice as a source of h-hepatocytes is contamination by mouse parenchymal and non-parenchymal cells. In this study, h-hepatocytes isolated from chimeric mice showed a high replacement index (>90%). In a previous study, we demonstrated that contamination with m-hepatocytes did not show any effects on the results of a drug metabolizing assay using cFHHs in suspension cultures [1]. In this study, we investigated the viability of the mouse cells and several liver-specific gene expressions of m-hepatocytes in the culture conditions. The ratio of mouse cells to total cultured cells was approximately 6% to 7% at 2 days after seeding and decreased to 2% to 3% at 32 days. In addition, m-cyp1a2 and cyp3a11 mRNAs drastically and quickly decreased to 0.1% to 1% of the basal expression levels during the culture period. These results suggest that the m-cyps, at least cyp1a2 and 3a11, only marginally, if at all, affect the results of the metabolic study using the present *in vitro* model.

We compared the hepatic functions of cFHHs and original ch-hepatocytes in the present culture conditions. The original ch-hepatocytes (donor A) are commercially as Transporter-Qualified Plateable Cryopreserved Human Hepatocytes. The original hepatocytes also attached on collagen-coated plates at high cell densities, as did the cFHHs, and the expression levels of CYP3A4 mRNA in the original

ch-hepatocytes were comparable or lower than those in the cFHHs at 7 days and 14 days. On the other hand, the original ch-hepatocytes derived from donor C showed poor platability, and it was impossible for them to attach in the culture conditions even at high density (data not shown). These results suggest that, regardless of the characteristics of the original ch-hepatocytes, the liver-specific functions of cFHHs were comparable or higher than those of ch-hepatocytes classified as the highest grade.

Here, we demonstrated that cFHHs cultured at a high density could stably maintain several hepatic functions for long periods, using a conventional culture method with collagen-coated plates. In conclusion, cFHHs are a valuable tool for *in vitro* metabolic and pharmaco-toxicological studies.

References

1) Yamasaki C, Kataoka M, Kakuni M, Usuda S, Ohzone Y, Matsuda S, et al. *In vitro* evaluation of cytochrome P450 and glucuronidation activities in hepatocytes isolated from liver-humanized mice. Drug Metab Pharmacokinet. 2010;25(6):539-50. Epub 2010/10/12. doi: 10.2133/dmpk.dmpk-10-rg-047. PubMed PMID: 20930422.

2) Steinberg P, Fischer T, Kiulies S, Biefang K, Platt KL, Oesch F, et al. Drug metabolizing capacity of cryopreserved human, rat, and mouse liver parenchymal cells in suspension. Drug Metab Dispos. 1999;27(12):1415-22. Epub 1999/11/26. PubMed PMID: 10570022.

3) Tanaka K, Sato M, Tomita Y, Ichihara A. Biochemical studies on liver functions in primary cultured hepatocytes of adult rats. J Biochem. 1978;84(4):937-46. Epub 1978/10/01. doi: 10.1093/oxfordjournals.jbchem.a132207. PubMed PMID: 711706.

4) Grant MH, Burke MD, Hawksworth GM, Duthie SJ, Engeset J, Petrie JC. Human adult hepatocytes in primary monolayer culture. Maintenance of mixed function oxidase and conjugation pathways of drug metabolism. Biochem Pharmacol. 1987;36(14):2311-6. Epub 1987/07/15. doi: 10.1016/0006-2952(87)90596-x. PubMed PMID: 3111481.

5) Kakuni M, Yamasaki C, Tachibana A, Yoshizane Y, Ishida Y, Tateno C. Chimeric mice with humanized livers: a unique tool for *in vivo* and *in vitro* enzyme induction studies. Int J Mol Sci. 2013;15(1):58-74. doi: 10.3390/ijms15010058. PubMed PMID: 24362577; PubMed Central PMCID: PMCPmc3907798.

6) Chan TS, Yu H, Moore A, Khetani SR, Tweedie D. Meeting the challenge of predicting hepatic clearance of compounds slowly metabolized by cytochrome P450 using a novel hepatocyte model,

HepatoPac. Drug Metab Dispos. 2013;41(12):2024-32. doi: 10.1124/dmd.113.053397. PubMed PMID: 23959596.

7) Dunn JC, Yarmush ML, Koebe HG, Tompkins RG. Hepatocyte function and extracellular matrix geometry: long-term culture in a sandwich configuration. FASEB J. 1989;3(2):174-7. Epub 1989/02/01. doi: 10.1096/fasebj.3.2.2914628. PubMed PMID: 2914628.

8) Mercer DF, Schiller DE, Elliott JF, Douglas DN, Hao C, Rinfret A, et al. Hepatitis C virus replication in mice with chimeric human livers. Nat Med. 2001;7(8):927-33. Epub 2001/08/02. doi: 10.1038/90968. PubMed PMID: 11479625.

9) Tateno C, Yoshizane Y, Saito N, Kataoka M, Utoh R, Yamasaki C, et al. Near completely humanized liver in mice shows human-type metabolic responses to drugs. Am J Pathol. 2004;165(3):901-12. Epub 2004/08/28. doi: 10.1016/s0002-9440(10)63352-4. PubMed PMID: 15331414; PubMed Central PMCID: PMCPmc1618591.

10) Azuma H, Paulk N, Ranade A, Dorrell C, Al-Dhalimy M, Ellis E, et al. Robust expansion of human hepatocytes in Fah-/-/Rag2-/-/Il2rg-/- mice. Nat Biotechnol. 2007;25(8):903-10. Epub 2007/08/01. doi: 10.1038/nbt1326. PubMed PMID: 17664939; PubMed Central PMCID: PMCPmc3404624.

11) Hasegawa M, Kawai K, Mitsui T, Taniguchi K, Monnai M, Wakui M. et al. The reconstituted 'humanized liver' in TK-NOG mice is mature and functional. Biochem Biophys Res Commun. 2011;405(3):405-10. Epub 2011/01/18. doi: 10.1016/j.bbrc.2011.01.042. PubMed PMID: 21238430; PubMed Central PMCID: PMCPmc3648850.

12) Tateno C, Miya F, Wake K, Kataoka M, Ishida Y, Yamasaki C, et al. Morphological and microarray analyses of human hepatocytes from xenogeneic host livers. Lab Invest. 2013;93(1):54-71. Epub 2012/11/14. doi: 10.1038/labinvest.2012.158. PubMed PMID: 23147226.

13) Ohtsuki S, Kawakami H, Inoue T, Nakamura K. Tateno C, Katsukura Y, et al. Validation of uPA/SCID mouse with humanized liver as a human liver model: protein quantification of transporters, cytochromes P450, and UDP-glucuronosyltransferases by LC-MS/MS. Drug Metab Dispos. 2014;42(6):1039-43. Epub 2014/04/09. doi: 10.1124/dmd.114.057646. PubMed PMID: 24711249.

14) Tateno C, Kawase Y, Tobita Y. Hamamura S, Ohshita H, Yokomichi H, et al. Generation of novel chimeric mice with humanized livers by using hemizygous cDNA-uPA/SCID mice. PLoS One. 2015;10(11): e0142145. doi: 10.1371/journal.pone.0142145. PubMed PMID: 26536627.

15) Sanoh S, Horiguchi A, Sugihara K, Kotake Y. Tayama Y. Ohshita H, et al. Prediction of *in vivo* hepatic clearance and half-life of drug candidates in human using chimeric mice with humanized liver. Drug Metab Dispos. 2012;40(2):322-8. doi: 10.1124/dmd.111.040923. PubMed PMID: 22048522.

16) Sanoh S, Naritomi Y, Fujimoto M, Sato K, Kawamura A, Horiguchi A, et al. Predictability of plasma concentration-time curves in humans using single-species allometric scaling of chimeric mice with humanized liver. Xenobiotica. 2015;45(7):605-14. doi: 10.3109/00498254.2015.1007112. PubMed PMID: 25733030.

17) Miyamoto M, Iwasaki S, Chisaki I, Nakagawa S, Amano N, Kosugi Y, et al. Prediction of human pharmacokinetics of long half-life compounds using chimeric mice with humanised liver. Xenobiotica. 2019;49(12):1379-87. Epub 2019/02/13. doi: 10.1080/00498254.2019.1579394. PubMed PMID: 30744481.

18) Hasegawa M, Tahara H. Inoue R, Kakuni M, Tateno C, Ushiki J. Investigation of drug-drug interactions caused by human pregnane X receptor-mediated induction of CYP3A4 and CYP2C subfamilies in chimeric mice with a humanized liver. Drug Metab Dispos. 2012;40(3):474-80. doi: 10.1124/dmd.111.042754. PubMed PMID: 22126990.

19) Foster JR, Jacobsen M, Kenna G, Schulz-Utermoehl T, Morikawa Y, Salmu J, et al. Differential effect of troglitazone on the human bile acid transporters, MRP2 and BSEP, in the PXB hepatic chimeric mouse. Toxicol Pathol. 2012; 40(8):1106-16. Epub 2012/06/08. doi: 10.1177/0192623312447542. PubMed PMID: 22673116.

20) Kakuni M, Morita M, Matsuo K, Katoh Y, Nakajima M, Tateno C, et al. Chimeric mice with a humanized liver as an animal model of troglitazone-induced liver injury. Toxicol Lett. 2012;214(1):9-18. Epub 2012/08/21. doi: 10.1016/j.toxlet.2012.08.001. PubMed PMID: 22902350.

21) Yamada T, Okuda Y, Kushida M, Sumida K, Takeuchi H, Nagahori H, et al. Human hepatocytes support the hypertrophic but not the hyperplastic response to the murine nongenotoxic hepatocarcinogen sodium phenobarbital in an *in vivo* study using a chimeric mouse with humanized liver. Toxicol Sci. 2014;142(1):137-57. Epub 2014/08/26. doi: 10.1093/toxsci/kfu173. PubMed PMID: 25145657.

22) Tsuge M, Hiraga N, Takaishi H, Noguchi C, Oga H, Imamura M, et al. Infection of human hepatocyte chimeric mouse with genetically engineered hepatitis B virus. Hepatology (Baltimore, Md). 2005;42(5):1046-54. doi: 10.1002/hep.20892. PubMed PMID: 16250045.

23) Hiraga N, Imamura M, Tsuge M, Noguchi C, Takahashi S, Iwao E, et al. Infection of human hepatocyte chimeric mouse with genetically engineered hepatitis C virus and its susceptibility to

interferon. FEBS Lett. 2007;581(10):1983-7. doi: 10.1016/j.febslet.2007.04.021. PubMed PMID: 17466983.

24) Kimura T, Imamura M, Hiraga N, Hatakeyama T, Miki D, Noguchi C, et al. Establishment of an infectious genotype 1b hepatitis C virus clone in human hepatocyte chimeric mice. J Gen Virol. 2008;89(Pt 9):2108-13. doi: 10.1099/vir.0.83658-0. PubMed PMID: 18753219.

25) Ishida Y, Yamasaki C, Yanagi A, Yoshizane Y, Fujikawa K, Watashi K, et al. Novel robust *in vitro* hepatitis B virus infection model using fresh human hepatocytes isolated from humanized mice. Am J Pathol. 2015;185(5):1275-85. doi: 10.1016/j.ajpath.2015.01.028. PubMed PMID: 25791527.

26) Yamasaki C, Tateno C, Aratani A, Ohnishi C, Katayama S, Kohashi T, et al. Growth and differentiation of colony-forming human hepatocytes *in vitro*. J Hepatol. 2006;44(4):749-57. Epub 2006/02/14. doi: 10.1016/j.jhep.2005.10.028. PubMed PMID: 16469405.

27) Cunha GR, Vanderslice KD. Identification in histological sections of species origin of cells from mouse, rat and human. Stain Technol. 1984;59(1):7-12. Epub 1984/01/01. doi: 10.3109/10520298409113823. PubMed PMID: 6206625.

28) Laemmle A, Gallagher RC, Keogh A, Stricker A, Gautschi M, Nuoffer JM, et al. Frequency and Pathophysiology of Acute Liver Failure in Ornithine Transcarbamylase Deficiency (OTCD). PLoS ONE. 2016; 11(4): e0153358. doi:10.1371/journal.pone.0153358

29) Liu X, LeCluyse EL, Brouwer KR, Gan LS, Lemasters JJ, Stieger B, et al. Biliary excretion in primary rat hepatocytes cultured in a collagen-sandwich configuration. Am J Physiol. 1999;277(1 Pt 1): G12-21. doi: 10.1152/ajpgi.1999.277.1.G12. PubMed PMID: 10409146

30) Hewitt NJ, Lechon MJ, Houston JB, Hallifax D, Brown HS, Maurel P, et al. Primary hepatocytes: current understanding of the regulation of metabolic enzymes and transporter proteins, and pharmaceutical practice for the use of hepatocytes in metabolism, enzyme induction, transporter, clearance, and hepatotoxicity studies. Drug Metab Rev. 2007;39(1):159-234. Epub 2007/03/17. doi: 10.1080/03602530601093489. PubMed PMID: 17364884.

31) Soars MG, McGinnity DF, Grime K, Riley RJ. The pivotal role of hepatocytes in drug discovery. Chem Biol Interact. 2007;168(1):2-15. Epub 2007/01/09. doi: 10.1016/j.cbi.2006.11.002. PubMed PMID: 17208208.

32) Gomez-Lechon MJ, Lahoz A, Gombau L, Castell JV, Donato MT. *In vitro* evaluation of potential hepatotoxicity induced by drugs. Curr Pharm Des. 2010;16(17):1963-77. Epub 2010/03/20. doi: 10.2174/138161210791208910. PubMed PMID: 20236064.

33) Gomez-Lechon MJ, Castel JV, Donato MT. The use of hepatocytes to investigate drug toxicity. Methods Mol Biol. 2010; 640:389-415. Epub 2010/07/21. doi: 10.1007/978-1-60761-688-7_21. PubMed PMID: 20645064.

34) Godoy P, Hewitt NJ, Albrecht U, Andersen ME, Ansari N, Bhattacharya S, et al. Recent advances in 2D and 3D *in vitro* systems using primary hepatocytes, alternative hepatocyte sources and non-parenchymal liver cells and their use in investigating mechanisms of hepatotoxicity, cell signaling and ADME. Arch Toxicol. 2013;87(8):1315-530. Epub 2013/08/27. doi: 10.1007/s00204-013-1078-5. PubMed PMID: 23974980; PubMed Central PMCID: PMCPMC3753504.

35) Wilkening S, Stahl F, Bader A. Comparison of primary human hepatocytes and hepatoma cell line Hepg2 with regard to their biotransformation properties. Drug Metab Dispos. 2003;31(8):1035-42. Epub 2003/07/18. doi: 10.1124/dmd.31.8.1035. PubMed PMID: 12867492.

36) Sauer V, Roy-Chowdhury N, Guha C, Roy-Chowdhury J. Induced pluripotent stem cells as a source of hepatocytes. Curr Pathobiol Rep. 2014;2(1):11-20. doi: 10.1007/s40139-013-0039-2. PubMed PMID: 25650171; PubMed Central PMCID: PMCPMC4312414.

37) Nishimura M, Ueda N, Naito S. Effects of dimethyl sulfoxide on the gene induction of cytochrome P450 isoforms, UGT-dependent glucuronosyl transferase isoforms, and ABCB1 in primary culture of human hepatocytes. Biol Pharm Bull. 2003;26(7):1052-6. Epub 2003/07/05. doi: 10.1248/bpb.26.1052. PubMed PMID: 12843640.

38) Soldatow VY, Lecluyse EL, Griffith LG, Rusyn I. *In vitro* models for liver toxicity testing. Toxicol Res (Camb). 2013;2(1):23-39. doi: 10.1039/C2TX20051A. PubMed PMID: 23495363; PubMed Central PMCID: PMCPMC3593300.

39) Bell CC, Hendriks DF, Moro SM, Ellis E, Walsh J, Renblom A, et al. Characterization of primary human hepatocyte spheroids as a model system for drug-induced liver injury, liver function and disease. Sci Rep. 2016;6:25187. doi: 10.1038/srep25187. PubMed PMID: 27143246; PubMed Central PMCID: PMCPMC4855186.

40) Hengstler JG, Utesch D, Steinberg P, Platt K.L, Diener B, Ringel, M, et al. Cryopreserved primary hepatocytes as a constantly available *in vitro* model for the evaluation of human and animal drug metabolism and enzyme induction. Drug Metab. Rev. 2000; 32(1):81-118. doi: 10.1081/dmr-100100564. PubMed PMID: 10711408

41) Greuet J, Pichard L, Ourlin JC, Bonfils C, Domergue J, Le Treut P, et al. Effect of cell density and epidermal growth factor on the inducible expression of CYP3A and CYP1A genes in human hepatocytes in primary culture. Hepatology (Baltimore, Md). 1997;25(5):1166-75. Epub 1997/05/01. doi: 10.1002/hep.510250520. PubMed PMID: 9141435.

42) Nakazawa K, Shinmura Y, Yoshiura Y, Sakai Y. Effect of cell spot sizes on micropatterned cultures of rat hepatocytes. Biochem Eng J. 2010;53(1):85-91. doi: 10.1016/j.bej.2010.09.013.

43) Le Vee M, Jigorel E, Glaise D, Gripon P, Guguen-Guillouzo C, Fardel O. Functional expression of sinusoidal and canalicular hepatic drug transporters in the differentiated human hepatoma HepaRG cell line. Eur J Pharm Sci. 2006;28(1-2):109-17. Epub 2006/02/21. doi: 10.1016/j.ejps.2006.01.004. PubMed PMID: 16488578.

44) Ding X, Lichti K, Kim I, Gonzalez FJ, Staudinger JL. Regulation of constitutive androstane receptor and its target genes by fasting, cAMP, hepatocyte nuclear factor alpha, and the coactivator peroxisome proliferator-activated receptor gamma coactivator-1alpha. J Biol Chem. 2006;281(36):26540-51. Epub 2006/07/11. doi: 10.1074/jbc.M600931200. PubMed PMID: 16825189; PubMed Central PMCID: PMCPMC2991045.

45) Benet M, Lahoz A, Guzman C, Castell JV, Jover R. CCAAT/enhancer-binding protein alpha (C/EBPalpha) and hepatocyte nuclear factor 4alpha (HNF4alpha) synergistically cooperate with constitutive androstane receptor to transactivate the human cytochrome P450 2B6 (CYP2B6) gene: application to the development of a metabolically competent human hepatic cell model. J Biol Chem. 2010;285(37):28457-71. Epub 2010/07/14. doi: 10.1074/jbc.M110.118364. PubMed PMID: 20622021; PubMed Central PMCID: PMCPMC2937871.

46) Ibeanu GC, Goldstein JA. Transcriptional regulation of human CYP2C genes: functional comparison of CYP2C9 and CYP2C18 promoter regions. Biochemistry. 1995;34(25):8028-36. Epub 1995/06/27. doi: 10.1021/bi00025a008. PubMed PMID: 7794915.

47) Chen Y, Kissling G, Negishi M, Goldstein JA. The nuclear receptors constitutive androstane receptor and pregnane X receptor cross-talk with hepatic nuclear factor 4alpha to synergistically activate the human CYP2C9 promoter. J Pharmacol Exp Ther. 2005;314(3):1125-33. Epub 2005/05/28. doi: 10.1124/jpet.105.087072. PubMed PMID: 15919766.

48) Yang X, Zhang B, Molony C, Chudin E, Hao K, Zhu J, et al. Systematic genetic and genomic analysis of cytochrome P450 enzyme activities in human liver. Genome Res. 2010;20(8):1020-36. Epub 2010/06/12. doi: 10.1101/gr.103341.109. PubMed PMID: 20538623; PubMed Central PMCID: PMCPMC2909567.

49) Cairns W, Smith CA, McLaren AW, Wolf CR. Characterization of the human cytochrome P4502D6 promoter. A potential role for antagonistic interactions between members of the nuclear receptor family. J Biol Chem. 1996;271(41):25269-76. doi: 10.1074/jbc.271.41.25269. PubMed PMID: 8810289.

50) Jover R, Bort R, Gomez-Lechon MJ, Castell JV. Cytochrome P450 regulation by hepatocyte nuclear factor 4 in human hepatocytes: a study using adenovirus-mediated antisense targeting. Hepatology (Baltimore, Md). 2001;33(3):668-75. Epub 2001/03/07. doi: 10.1053/jhep.2001.22176. PubMed PMID: 11230748.

51) Corchero J, Granvil CP, Akiyama TE, Hayhurst GP, Pimprale S, Feigenbaum L, et al. The CYP2D6 humanized mouse: effect of the human CYP2D6 transgene and HNF4alpha on the disposition of

debrisoquine in the mouse. Mol Pharmacol. 2001;60(6):1260-7. Epub 2001/11/28. doi: 10.1124/mol.60.6.1260. PubMed PMID: 11723233.

52) Tirona RG, Lee W, Leake BF, Lan LB, Cline CB, Lamba V, et al. The orphan nuclear receptor HNF4alpha determines PXR- and CAR-mediated xenobiotic induction of CYP3A4. Nat Med. 2003;9(2):220-4. Epub 2003/01/07. doi: 10.1038/nm815. PubMed PMID: 12514743.

53) Sueyoshi T, Kawamoto T, Zelko I, Honkakoski P, Negishi M. The repressed nuclear receptor CAR responds to phenobarbital in activating the human CYP2B6 gene. J Biol Chem. 1999;274(10):6043-6. Epub 1999/02/26. doi: 10.1074/jbc.274.10.6043. PubMed PMID: 10037683.

54) Goodwin B, Moore LB, Stoltz CM, McKee DD, Kliewer SA. Regulation of the human CYP2B6 gene by the nuclear pregnane X receptor. Mol Pharmacol. 2001;60(3):427-31. Epub 2001/08/15. PubMed PMID: 11502872.

55) Wang H, Faucette S, Sueyoshi T, Moore R, Ferguson S, Negishi M, et al. A novel distal enhancer module regulated by pregnane X receptor/constitutive androstane receptor is essential for the maximal induction of CYP2B6 gene expression. J Biol Chem. 2003;278(16):14146-52. Epub 2003/02/07. doi: 10.1074/jbc.M212482200. PubMed PMID: 12571232.

56) Jigorel E, Le Vee M, Boursier-Neyret C, Parmentier Y, Fardel O. Differential regulation of sinusoidal and canalicular hepatic drug transporter expression by xenobiotics activating drug-sensing receptors in primary human hepatocytes. Drug Metab Dispos. 2006;34(10):1756-63. Epub 2006/07/14. doi: 10.1124/dmd.106.010033. PubMed PMID: 16837569.

57) Oscarson M, Zanger UM, Rifki OF, Klein K, Eichelbaum M, Meyer UA. Transcriptional profiling of genes induced in the livers of patients treated with carbamazepine. Clin Pharmacol Ther. 2006;80(5):440-56. Epub 2006/11/23. doi: 10.1016/j.clpt.2006.08.013. PubMed PMID: 17112801.

58) Meyer Z, Schwabedissen HE, Bottcher K, Chaudhry A, Kroemer HK, Schuetz EG, et al. Liver X receptor alpha and farnesoid X receptor are major transcriptional regulators of OATP1B1. Hepatology. 2010;52(5):1797-807. Epub 2010/09/10. doi: 10.1002/hep.23876. PubMed PMID: 20827719.

59) Meyer zu Schwabedissen HE, Kim RB. Hepatic OATP1B transporters and nuclear receptors PXR and CAR: interplay, regulation of drug disposition genes, and single nucleotide polymorphisms. Mol Pharm. 2009;6(6):1644-61. Epub 2009/06/30. doi: 10.1021/mp9000298. PubMed PMID: 19558188.

60) Burk O, Koch I, Raucy J, Hustert E, Eichelbaum M, Brockmoller J, et al. The induction of cytochrome P450 3A5 (CYP3A5) in the human liver and intestine is mediated by the xenobiotic sensors pregnane X receptor (PXR) and constitutively activated receptor (CAR). J Biol Chem. 2004;279(37):38379-85. doi: 10.1074/jbc.M404949200. PubMed PMID: 15252010.

61) Faucette SR, Sueyoshi T, Smith CM, Negishi M, Lecluyse EL, Wang H. Differential regulation of hepatic CYP2B6 and CYP3A4 genes by constitutive androstane receptor but not pregnane X receptor. J Pharmacol Exp Ther. 2006;317(3):1200-9. Epub 2006/03/04. doi: 10.1124/jpet.105.098160. PubMed PMID: 16513849.

62) Kast HR, Goodwin B, Tarr PT, Jones SA, Anisfeld AM, Stoltz CM, et al. Regulation of multidrug resistance-associated protein 2 (ABCC2) by the nuclear receptors pregnane X receptor, farnesoid X-activated receptor, and constitutive androstane receptor. J Biol Chem. 2002;277(4):2908-15. Epub 2001/11/14. doi: 10.1074/jbc.M109326200. PubMed PMID: 11706036.

63) Smetanina MA, Pakharukova MY, Kurinna SM, Dong B, Hernandez JP, Moore DD, et al. Ortho-aminoazotoluene activates mouse constitutive androstane receptor (mCAR) and increases expression of mCAR target genes. Toxicol Appl Pharmacol. 2011;255(1):76-85. Epub 2011/06/16. doi: 10.1016/j.taap.2011.05.019. PubMed PMID: 21672546; PubMed Central PMCID: PMCPMC3148291.

64) Sugatani J, Kojima H, Ueda A, Kakizaki S, Yoshinari K, Gong QH, et al. The phenobarbital response enhancer module in the human bilirubin UDP-glucuronosyltransferase UGT1A1 gene and regulation by the nuclear receptor CAR. Hepatology (Baltimore, Md). 2001;33(5):1232-8. Epub 2001/05/09. doi: 10.1053/jhep.2001.24172. PubMed PMID: 11343253.

65) Saini SP, Mu Y, Gong H, Toma D, Uppal H, Ren S, et al. Dual role of orphan nuclear receptor pregnane X receptor in bilirubin detoxification in mice. Hepatology (Baltimore, Md). 2005;41(3):497-505. Epub 2005/02/24. doi: 10.1002/hep.20570. PubMed PMID: 15726644.

66) Watari R, Kakiki M, Oshikata A, Takezawa T, Yamasaki C, Ishida Y, et al. A Long-Term Culture System Based on a Collagen Vitrigel Membrane Chamber That Supports Liver-Specific Functions of Hepatocytes Isolated From Mice With Humanized Livers. J Toxicol Sci. 2018;43(8):521-529. doi: 10.2131/jts.43.521. PubMed PMID: 30078838.

Tables and figures

Table 1. Data of isolated hepatocytes for evaluation of drug metabolizing enzymes (phase I and II) and transporters gene expression

Donor	Animal No.	Sex	Age (weeks)	Body weight (g)	h-Alb concentration (mg/mL)	Yield of cells (cells/mouse)	Viability (%)
A BD195	A-1	male	15	18.79	17.2	2.24×10^8	91.7
	A-2	male	15	17.42	16.4	1.69×10^8	92.6
	A-3	male	15	19.06	17.1	1.52×10^8	83.9
B BD342	B-1	male	16	17.45	12.6	1.31×10^8	87.5
	B-2	male	16	17.54	15.2	1.53×10^8	93.8
	B-3	male	17	17.19	12.6	1.42×10^8	87.3
C BD85	C-1	female	14	15.3	13.0	1.42×10^8	89.5
	C-2	male	15	14.4	14.0	1.27×10^8	86.7
	C-3	male	15	20.6	14.3	1.04×10^8	79.5

Table 2. Relative gene expression levels of human drug metabolizing enzymes (phase I and II) and transporters

	Days in culture											
	2			7			14			21		
Phase I enzymes												
hCYP1A1	2.4	±	1.2	12.2	±	5.5	25.9	±	8.2	38.9	±	7.0
hCYP1A2	6.3	±	7.6	9.0	±	14.1	20.7	±	33.1	21.0	±	32.8
hCYP2B6	29.7	±	21.5	40.3	±	16.9	25.1	±	9.2	31.1	±	11.0
hCYP2C9	16.6	±	8.2	25.0	±	14.3	15.6	±	9.8	23.8	±	10.0
hCYP2E1	9.7	±	5.2	8.4	±	4.1	21.4	±	17.1	23.2	±	12.1
hCYP2D6	13.0	±	5.2	8.8	±	6.7	8.2	±	5.1	11.8	±	4.9
hCYP3A4	7.8	±	2.5	127.8	±	70.6	178.7	±	122.1	238.3	±	155.1
Phase II enzymes												
hUGT1A1	52.4	±	17.9	269.2	±	143.2	214.2	±	105.4	292.9	±	118.2
hUGT2B7	26.3	±	8.4	9.4	±	7.2	6.1	±	3.7	7.1	±	2.1
Transporters												
hBSEP	5.7	±	2.5	3.0	±	1.2	2.1	±	1.0	2.3	±	0.7
hMRP2	53.5	±	22.0	167.4	±	72.5	206.1	±	125.3	256.8	±	114.8
hOATP1B1	3.9	±	1.8	2.9	±	1.3	5.9	±	2.3	7.7	±	1.3
hOATP1B3	4.5	±	1.6	12.6	±	4.8	13.3	±	4.9	14.7	±	0.3

Table 3. Attached cell number and ratio of the number of attached cells to seeded cell number

Seeding cell number ($\times 10^5$ cells/cm^2)	Attached cell number on day 7 ($\times 10^5$ cells/cm^2)			Cell adhesion ratio on day 7 (%)		
2.13	1.27	±	0.22	59.75	±	10.27
1.60	1.00	±	0.18	62.36	±	11.30
1.06	0.74	±	0.08	69.42	±	7.91
0.53	0.39	±	0.02	72.51	±	3.53

Table 4. Top 20 pathways in descending order in pathway analysis (p>0.001 Minimal number of matches>10) on day 7

Pathway	p-value
Hs_Constitutive_Androstane_Receptor_Pathway_WP2875_94791	0
Hs_Statin_Pathway_WP430_90508	0
Hs_Blood_Clotting_Cascade_WP272_93044	0
Hs_Nuclear_Receptors_in_Lipid_Metabolism_and_Toxicity_WP299_89331	0
Hs_Pregnane_X_Receptor_pathway_WP2876_94792	0
Hs_Tamoxifen_metabolism_WP691_92400	6.34E-19
Hs_Fatty_Acid_Omega_Oxidation_WP206_94194	1.76E-15
Hs_PPAR_Alpha_Pathway_WP2878_94794	6.16E-15
Hs_Drug_Induction_of_Bile_Acid_Pathway_WP2289_88593	1.53E-14
Hs_Fatty_Acid_Biosynthesis_WP357_94197	1.73E-14
Hs_Fatty_Acid_Beta_Oxidation_WP143_94768	2.96E-11
Hs_Tryptophan_metabolism_WP465_94086	3.22E-11
Hs_Amino_Acid_metabolism_WP3925_90737	4.11E-11
Hs_Complement_and_Coagulation_Cascades_WP558_90196	4.64E-11
Hs_One_carbon_metabolism_and_related_pathways_WP3940_94312	6.82E-11
Hs_PPAR_signaling_pathway_WP3942_94205	9.45E-11
Hs_Oxidation_by_Cytochrome_P450_WP43_94176	9.88E-11
Hs_Vitamin_B12_Metabolism_WP1533_85340	1.03E-10
Hs_Selenium_Micronutrient_Network_WP15_94185	1.19E-10
Hs_Metapathway_biotransformation_WP702_73516	4.19E-10

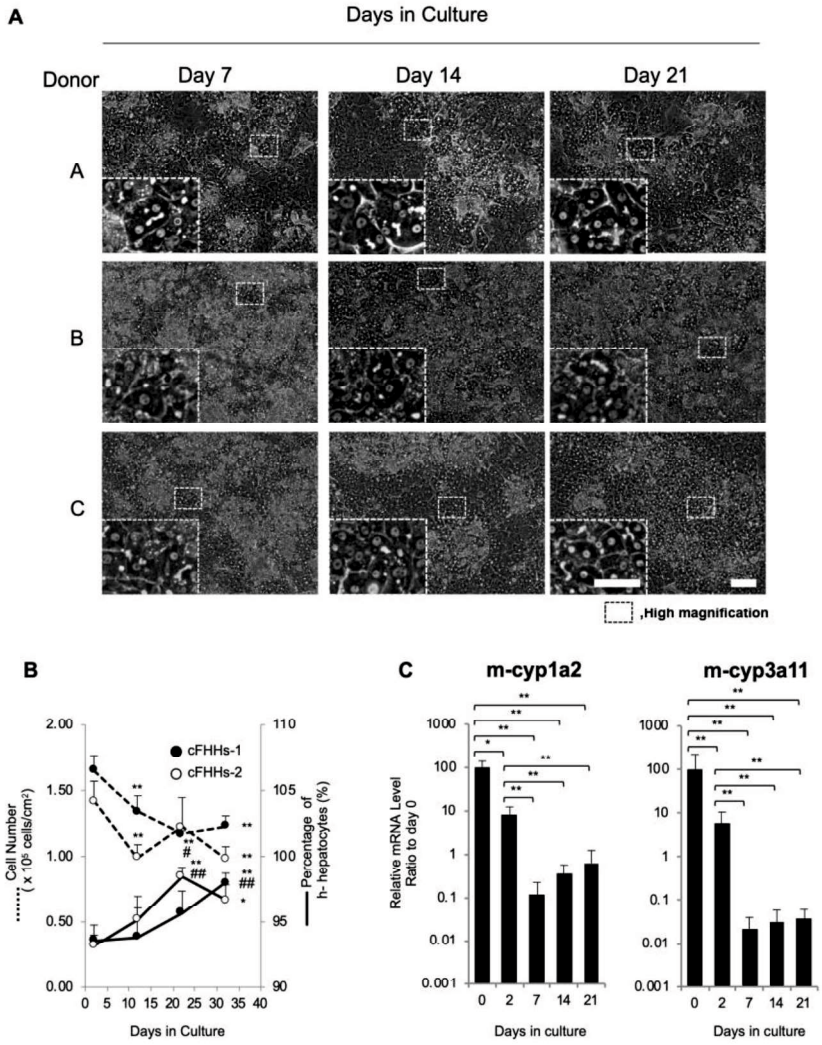

Fig 1. Morphology, viability, and purity of cFHHs during culture.

A: Phase contrast microphotographs of cFHHs during culture at day 7, 14 and 21. cFHHs isolated from chimeric mice transplanted with three different donor cells (Donor A, B, and C) were plated at 2.13 x 10^5 cells/cm^2 and cultured. The inserts are high magnification images. Scale bars denote 100 μm in the low magnification images and 50 μm in the high magnification images. **B:** Cell numbers and ratio of h-hepatocytes during culture. cFHHs isolated from two different chimeric mice transplanted with donor A cells were plated (2.13×10^5 cells/cm^2) and fixed at days 2, 13, 23, and 33. After Hoechst staining, h-hepatocytes and mouse cells were counted by microscopic observation of three to five fields. Total cell numbers and percentages of h-hepatocytes are denoted by dotted and normal lines, respectively. **C:** Mouse gene expression levels during culture. Expression levels of m-cyp1a2 and 3a11 mRNA were measured by qPCR on days 0, 2, 7, 14, and 21. Data are expressed as mean ± SD. *$p<0.05$ versus at day 2; **$p<0.01$ versus at day 2; $^{\#}p<0.05$ versus at day 12; $^{\#\#}p<0.01$ versus at day 12.

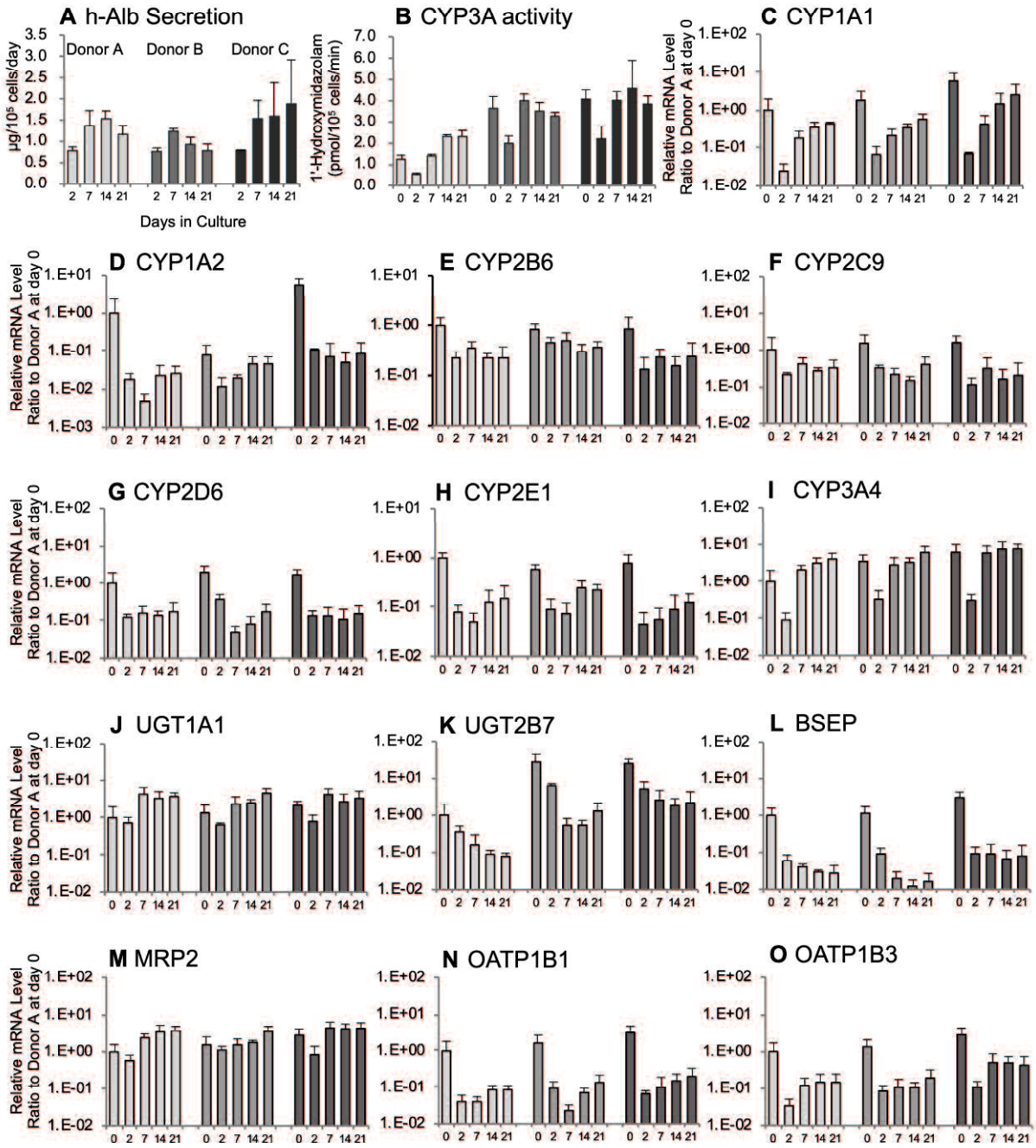

Fig 2. Hepatic function and gene expression in cFHHs during culture.

A: h-Alb production, **B:** CYP3A activities, **C-O:** Human gene expression levels (C: CYP1A1, D: CYP1A2, E: CYP2B6, F: CYP2C9, G: CYP2D6, H: CYP2E1, I: CYP3A4, J: UGT1A1, K: UGT2B7, L: BSEP, M: MRP2, N: OATP1B1, O: OATP1B3). cFHHs collected from chimeric mice transplanted with cells of three different donors (A, B, and C) were plated at 2.13×10^5 cells/cm^2 and cultured for up to 21 days. Results represent means ± SD of three independent experiments. The Y-axis of C to O represents the relative expression level of each gene to that in freshly isolated cFHHs originating from donor A. Day 0 shows the values of isolated cFHHs.

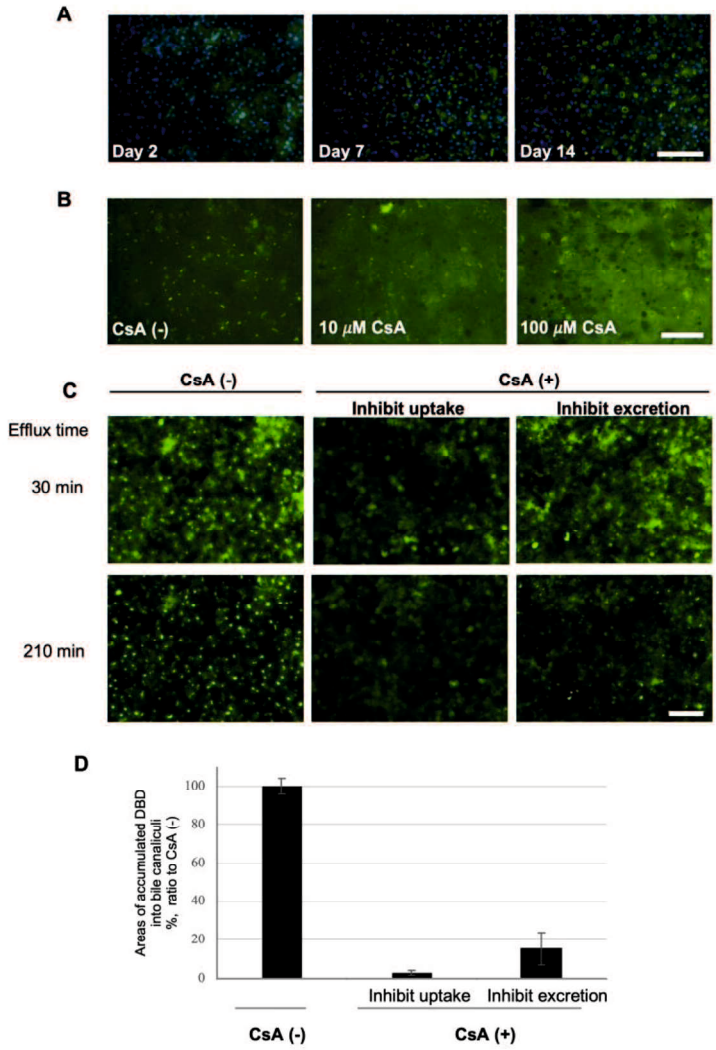

Fig 3. Expression and function of transporters in cFHHs during culture.

A: Transporter protein localization and activity in cultured cFHHs. cFHHs (donor A) were plated at 2.13 × 10^5 cells/cm^2. cFHHs were cultured for 7 and 14 days and fixed, and MRP2 protein expression was determined by immunostaining. Images of cFHHs after double staining with MRP2 (green) and Hoechst (blue) are presented. Scale bar denotes 100 μm. **B**: MRP2 transporter activity was determined in cultured cFHHs using CDFDA. cFHHs were incubated with CDFDA and CsA (10 or 100 μM) at day 7. CsA treatment inhibited the accumulation of CDF in the bile canaliculi, and intense fluorescence signals were observed in the cytoplasm at 10 and 100 μM CsA. Scale bar denotes 100 μm. **C**: NTCP and BSEP transporter activities were determined in cultured cFHHs using DBD and CsA. DBD was incorporated into cFHHs and accumulated in bile canaliculi between cFHHs at day 9, as shown in green. To inhibit uptake of the substrate by NTCP, cells were treated with CsA from the preincubation process onwards, before DBD treatment. To inhibit excretion of the substrate by BSEP, cells were treated with CsA from the washing process onwards, after DBD treatment. Scale bar denotes 100 μm. Effect of CsA treatment on DBD-uptake in cells via NTCP, and DBD-excretion in bile canaliculi via BSEP. **D**: Photographs of microscopy images were taken at 210 min and areas of DBD accumulation in bile canaliculi were measured using a Bz-X analyzer. DBD that had accumulated in bile canaliculi was expressed as a ratio with the control (CsA [-]).

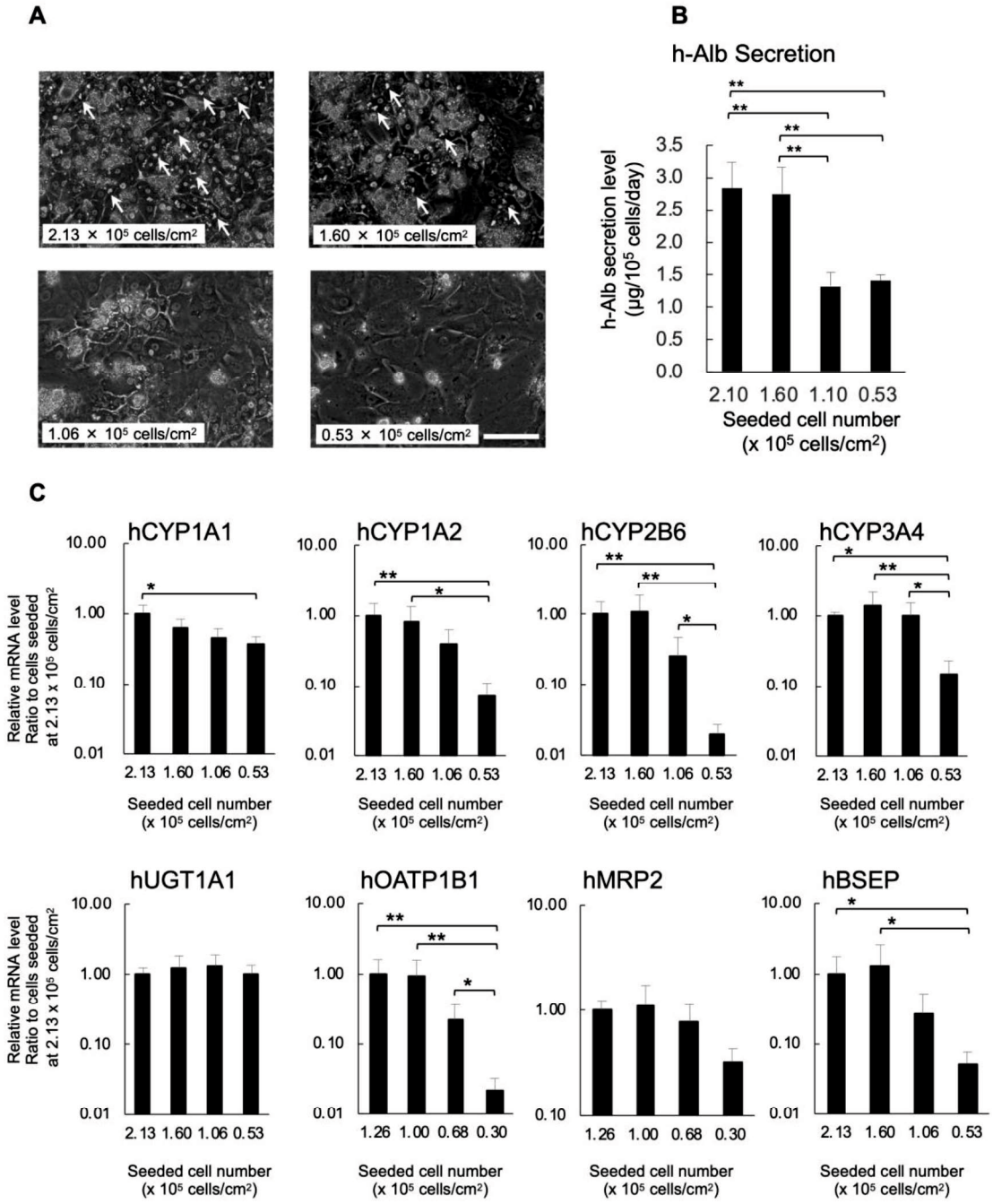

Fig 4. **cFHHs cultured at different cell densities.**

A: Phase contrast microphotographs of cFHHs plated at 0.53, 1.06, 1.60, and 2.13×10^5 cells/cm^2 and cultured for 7 days. Arrows show bile canalicular structures. Scale bar denotes 100 μm. **B:** h-Alb levels in culture supernatant of cFHHs cultured at different cell densities. These results represent the mean ± SD of three independent experiments. **p<0.01 C: Gene expression levels of human phase I and II enzymes in cFHHs plated at 0.53, 1.06, 1.60, and 2.13×10^5 cells/cm^2 and cultured for 7 days. Each gene expression level was measured by qPCR. These results represent the mean ± SD of three independent experiments. *p < 0.05, **p < 0.01

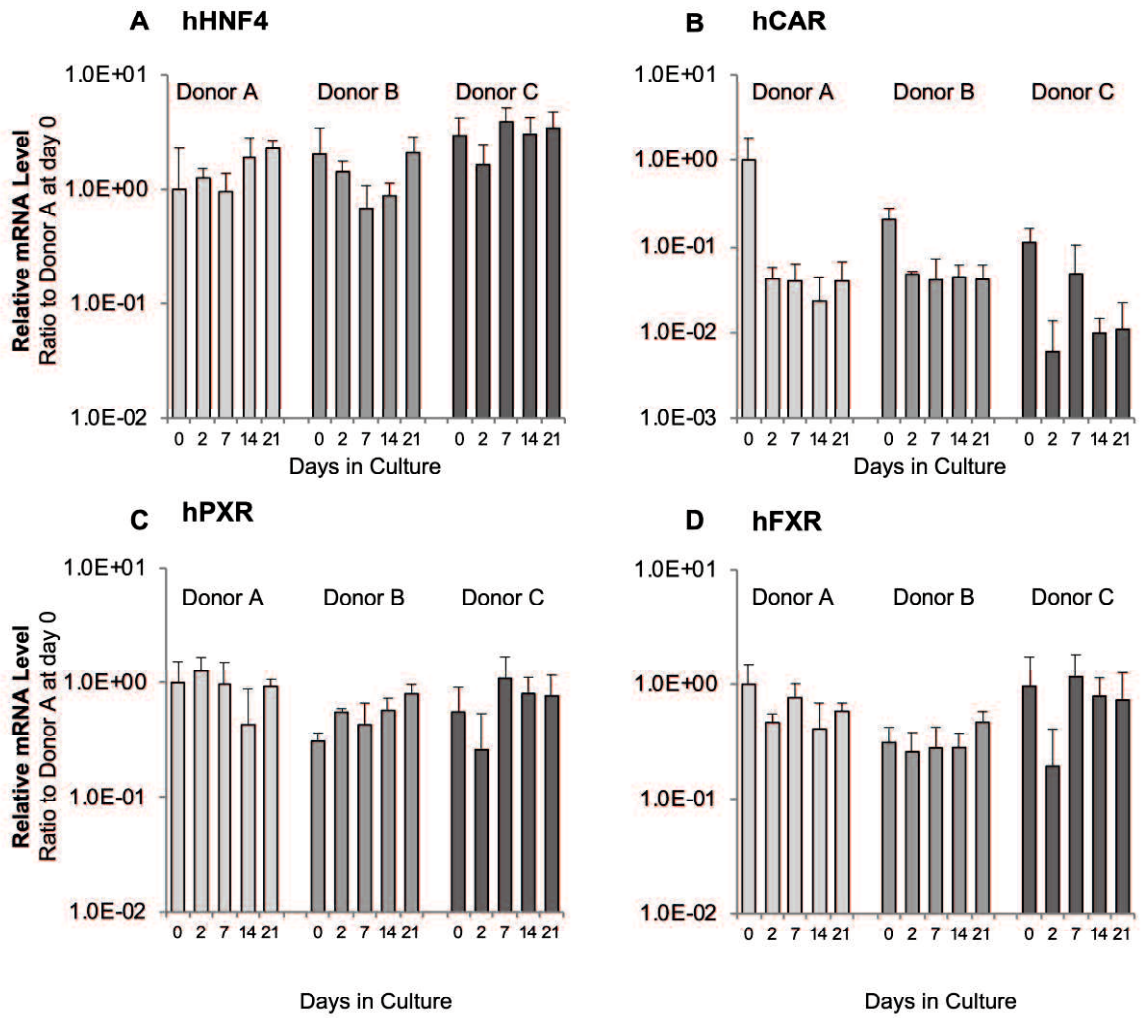

Fig 5. Human TF gene expression levels in cultured cFHHs.

A: hHNF4α, **B:** hCAR, **C:** hPXR, **D:** hFXR. cFHHs from three different donors were plated at 2.13×10^5 cells/cm^2 and cultured for up to 21 days. The gene expression levels were measured by qPCR. Results indicate the mean ± SD of three independent experiments. The y-axis represents the relative expression level of each gene to the level in freshly isolated cFHHs originating from donor A. Day 0 shows the mRNA levels of isolated cFHHs.

S1 Table. Primer sets

Gene name	F-primer	R-primer
hCYP1A1	TCAACCATGACCAGAAGCTA	AAGATAATCACCTTCTCACTTAACAC
hCYP1A2	GCTTCTACATCCCCAAGAAAT	ACCACTTGGCCAGGACT
hCYP2B6	ACCCAACACACCAGCTTCCG	CAGGATTGAAGGCGTCTGGTTTTTC
hCYP2C9	CCAGATCTGCAATAATTTTTCTC	CAAGCTTTCAATAGTAAATTCAGATG
hCYP2D6	CTTGGACAAAGCCGTGA	GACAGCATTCAGCACCTC
hCYP2E1	GGCTGAAGTAAAAGAGTATGTGTC	TTTCCTTCTCCATTTCCAC
hCYP3A4	ACTGCCTTTTTTGGGAAATA	GGCTGTTGACCATCATAAAAG
hUGT1A1	TTGATCCCAGTGGATGGC	ATGCTCCGTCTCTGATGTACAAC
hUGT2B7	TGACATGAAGAAGTGGGATCAG	CAACATTTGGTAAGAGTGGATATGG
hOATP1B1	TCATACTCTGTGAAAACAAATCAG	CAGACTGGTTCCCATTGAC
hOATP1B3	CTCTGTTTGCTAAAATGTACGTG	GAAGAAATAATGGAAAATAGTCCAG
hBSEP	AAATATGCTTTTGGGTCATTG	GTCAGCTATGGCATCATTG
hMRP2	TCCAACTGTGCTTCAAGC	GGCATCCACAGACATCAG
hHNF4α	GACCGCCAGTATGACTCG	CGTTGGTTCCCATATGTTCC
hCAR	ATTGAAGATGGAGCCCG	GAGCTGCAGTTTTCGTAGTG
hPXR	AGCTACTCCTTGATCGATCC	AAAGTCAGCATGGTTCCAG
hFXR	ATGGATTCATATAACAAACAGAGG	GCTTTTTTGTGAATTCTACAAGAAC
hGAPDH	GGAGTCAACGGATTTGGT	AAGATGGTGATGGGATTTCCA
mCyp1a2	CTCCTTTAAGGAAAACCCAACCACC	ACAACACTGGGTCAGAATCTCATTG
mCyp3a11	CTAAGCAGAAGCACCGAGTGG	TTTCTGGATATCAGGGTGAGTGG

S2 Table. Altered expression of genes after 7 days at high density compared to 7 days at low density.

Fold change	Transcription factors		Phase I enzymes		Phase II enzymes				Transporters	
	NR	Others	CYP	FMO	UGT	SULT	GST	NAT	ABC	SLC
2-4	1H3 (LXRa), 1I2 (PXR), 3C2 (AR), 5A2 (LRH-1)	HNF4A	2C18, 2J2, 3A4, 3A43	3	1A6,3A1	1A1	A4		A8, C2 (MRP2), C3 (MRP3), C6 (MRP6)/C6P1/C6P2, G2	2A2 (GLUT2), 7A2 (CAT2), 15A1 (PEPT1), 16A10 (MCT10), 19A3 (THTR2), 22A18, 22A25, 23A1, 25A13 (AGC2), 25A15 (ORC1), 25A20 (CAC), 25A3, 25A33, 25A42, 30A10, 31A1, 35D1, 44A1 (CTL1), 46A3, 50A1 47A1 (MATE1)
4-6	0B2 (SHP1)		2W1, 4F3, 4F12, 8B1, 39A1		2A3	2A1		8	C6P1, G5	13A5 (NACT), 17A3 (NPT4), 22A3 (OCT3), 38A4 (ATA3)
>6	1I3 (CAR)		2A6, 2A7, 2B6, 2C8, 2C9, 2C19, 2D6/2D7, 2E1, 3A7, 4A11, 4F2, 7A1, 26A1	1, 5	1A8/1A9, 2B4, 2B15, 2B28				A6, B4 (MDR3), G8 (GBD4)	6A1 (GAT-1), 10A1 (NTCP), 17A4, 1A2 (GLT1), 22A1 (OCT1), 22A7 (OAT2), 25A47, 28A1 (CNT1), 38A3, 39A5, 51A (OST alpha), O1B1 (OATP1B1), O1B3 (OATP1B3)

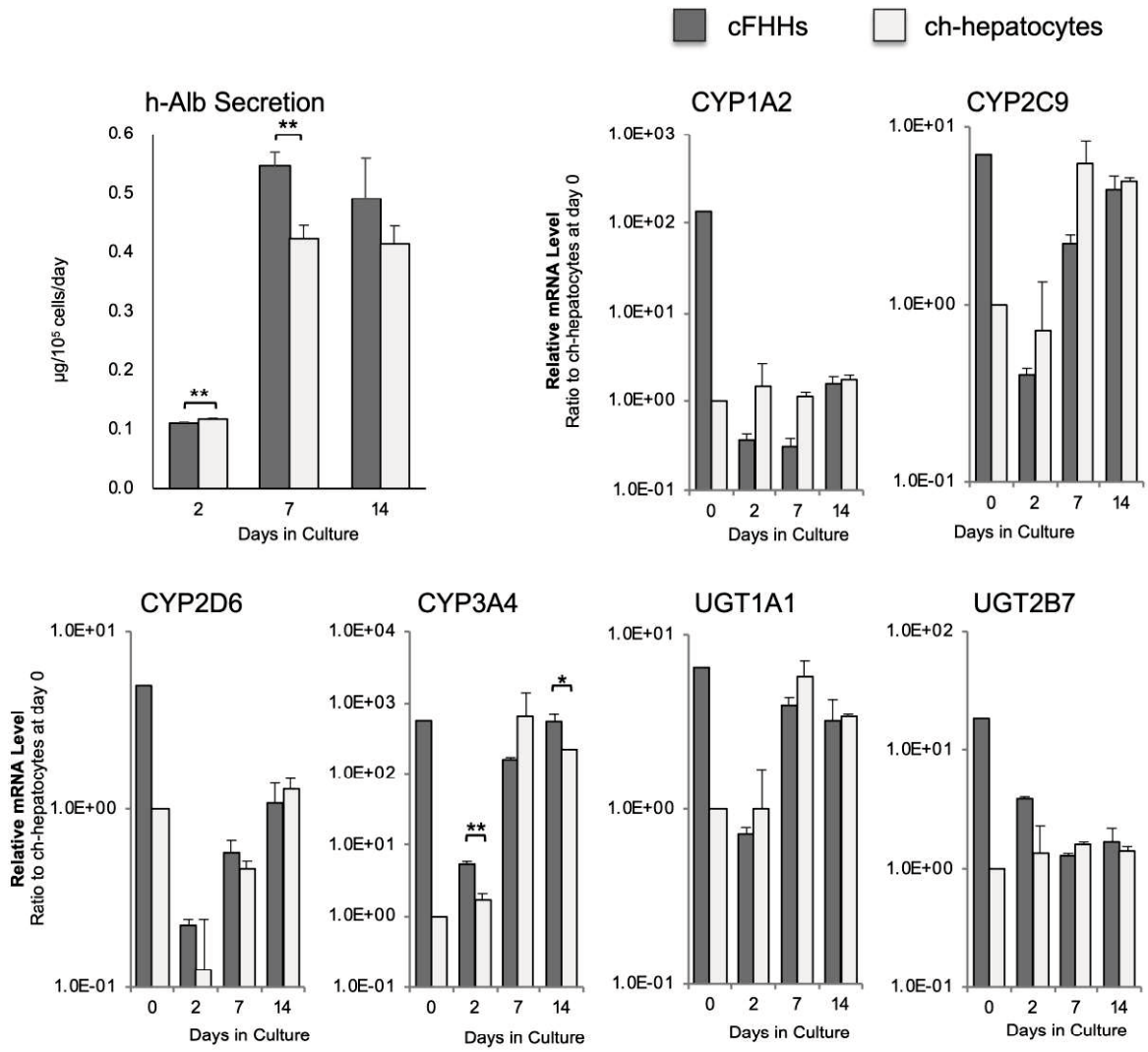

S1 Fig. h-Alb levels and gene expression levels of human phase I and II enzymes in cultured PXB-cells and original ch-hepatocytes (donor A)

PXB-cells originating from donor A and original ch-hepatocytes (donor A) were plated at 2.13×10^5 cells/cm^2 and cultured for up to 14 days. h-Alb levels in the culture supernatant were measured using ELISA. *$p < 0.05$; **$p < 0.01$ (two-tailed Student's t-test). Each gene expression level was measured by qPCR. The results represent single determination (day 0; n = 1) or the mean ± S.D. of triplicate determinations in separate wells of the culture plate (day 2, 7, and 14; n = 3) from a single experiment. The y-axis represents the relative expression level of each gene to that of the original ch-hepatocytes. Day 0 denotes the mRNA levels of isolated PXB-cells or thawed ch-hepatocytes. *$p < 0.05$; **$p < 0.01$ (two-tailed Student's t-test).

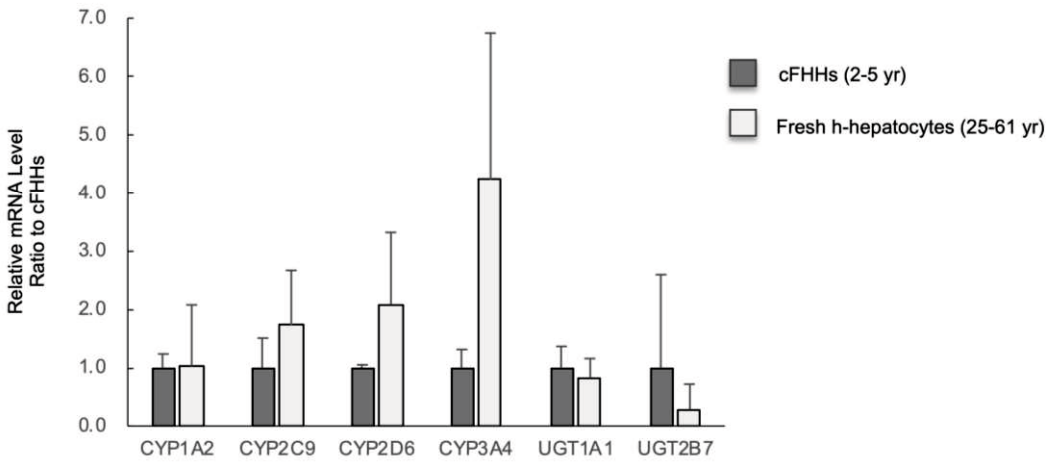

S2 Fig. Gene expression levels of human phase I and II enzymes in cFHHs and fresh adult h-hepatocytes (unplated)

cFHHs were collected from chimeric mice transplanted with cells of donor A, B, and C. Fresh adult h-hepatocytes were collected from excess normal liver tissues of surgical liver resections from 4 donors. Each gene expression level was measured by qPCR. The results indicate the relative value to the average of cFHHs normalized by value of hGAPDH. The results of cFHHs indicate the mean ± S.D. of three different animals. The results of fresh adult h-hepatocytes indicate the mean ± S.D. of four donors from 25 to 61 years of age. The y-axis represents the relative expression level of each gene to the mean value of cFHHs.

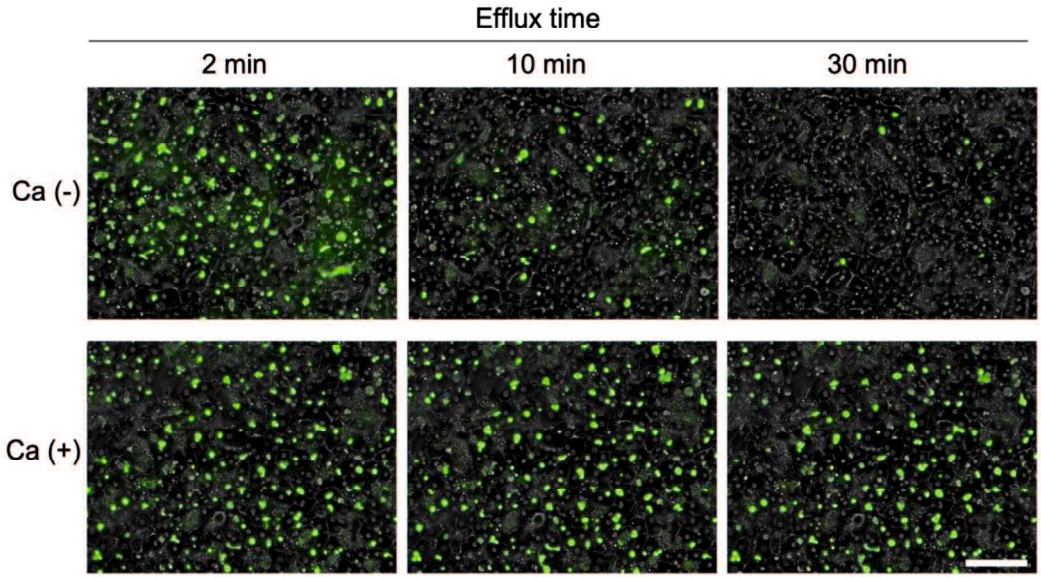

S3 Fig. MRP2 transporter activity in cFHHs.

At day 16, cFHHs were incubated with HBSS containing 1.25 μM CDFDA for 5 min, and then incubated for up to 30 min in the presence or absence of Ca^{2+}. CDF accumulation in bile canaliculi between cFHHs was observed as green spots. The bar denotes 100 μm.

IV. General conclusion

h-Hepatocytes are considered to be useful as a source of cells for drug development. It is recognized that ch-hepatocytes are the gold standard for *in vitro* studies of DMPK and toxicology [1-4]. However, the use of ch-hepatocytes is limited by lot size (at most several hundred vials from one donor), and there are individual differences among donors. Because of these limitations, researchers have been using immortalized liver-derived cell lines, such as HepG2, HepaRG, and induced pluripotent stem cell-derived hepatocytes for their *in vitro* studies [5]. Although some liver-specific functions are confirmed in these cells, many other liver functions were still significantly lower than those in primary h-hepatocytes [5-7]. This study aimed to propagate h-hepatocytes to obtain functional h-hepatocytes for drug development.

In Chapter II, I made primary cultures of h-hepatocytes in the presence of Swiss 3T3 cells and demonstrated the presence of CF-PHs. The occupancy rate of CF-PHs was~0.1%. I devised a method to propagate CF-PHs by serial sub-culturing and characterized the propagated CF-PHs. Human CF-PHs were able to be subcultured within limited passages. CF-PHs from young donors (3-month- to 12-year-old) could be passaged 7 times, Population doubling time (PDT) at passage 4 being170-220 h, and, then the cells became senescent. CF-PHs from older donors (63- to 72-year-old) were passaged only 5 times at most. They grew more slowly, their PDT at passage 4 being 650-1200 h. These results suggested that replication potential of h-CF-PHs is correlated with the age of donors. It should be emphasized that the cumulative population doubling level (CPDL) of CF-PHs from younger donors, 3-month-old and 12-months-old, were as high as 19.3 and 24.7 during 300 days, respectively. CF-PHs showed a liver epithelial cell-like morphology when they were in the growth phase and in an early phase of confluence, whereas they showed a typical hepatocyte-like morphology in condensed regions at confluence. I examined whether human CF-PHs in spheroid culture elevate differentiation-related genes. The mRNA expression level of

albumin (ALB), hepatocyte-nuclear factor 4α (HNF4α), and CYPs of CF-PHs were low in monolayer-culture. However, when these CF-PHs were cultured in spheroid, they regained the expression of mRNAs of ALB and HNF4α to a level comparable to that of the original h-hepatocytes, i.e., the cells before cultivation, and also regained a mRNA expression profile of CYPs of 2C9, 2C19, and 3A4 similar to that of original h-hepatocytes. Currently, I suppose that h-CF-PHs cultured in spheroids reexpress hepatocyte specific differentiation markers through the up-regulation of HNF4α expression. This study demonstrated the presence of CF-PHs, a highly replicative compartment of h-hepatocytes, even in the adult human liver. These CF-PHs can be serially subcultured, retaining their normal hepatocytic characteristics.

These cultures should be useful to study the cellular and molecular mechanisms of growth, differentiation, toxicity, metabolism, and carcinogenesis of human hepatocytes. However, I considered that it is difficult to obtain large number of differentiated h-hepatocytes using this method, because ratio of CF-PHs was very low (~0.1%) in h-hepatocytes.

We succeeded in propagating human hepatocytes in mouse livers by transplanting h-hepatocytes into uPA/SCID or cDNA-uPA/SCID mice via spleen. The mouse liver was replaced with h-hepatocytes at more than 70%[8, 9] . We call the mice, PXB-mice. Our previous results revealed that most genes showed comparable expression levels in the h-hepatocytes of both human and PXB-mouse livers [10]. The PXB-mouse has been used in many studies of DMPK, safety, and HBV and hepatitis C virus infections. In the case of PXB-mice, the transplanted ch-hepatocytes dramatically proliferate more than 1000-fold in the host mouse liver. Therefore, more than 10^8 hepatocytes can be isolated from a PXB-mouse (PXB-cells).

These facts indicate that PXB-mice transplanted with ch-hepatocytes derived from one donor could stably and repeatedly supply a large amount of fresh h-hepatocytes.

In Chapter III and IV, it was determined whether the PXB-mouse could be a useful source of fresh h-hepatocytes for *in vitro* drug development tests.

In Chapter III, I compared the CYP and UGT activities of ch-hepatocytes and PXB-cells. Compared with ch-hepatocytes, the CYP (1A2, 2C9, 2C19, 2D6, 2E1, 3A) activities of PXB-cells were similar or greater. Moreover, ketoprofen was more actively metabolized through glucuronide conjugates by PXB-cells than by ch-hepatocytes. I concluded that fresh and reproducible PXB-cells could be a useful tool in predicting the pharmacokinetics of chemical entities.

In general, h-hepatocytes undergo changes in cell morphology and rapidly lose their hepatic functions, such as CYP expression and ALB secretion, in traditional 2D culture model [11, 12]. To overcome this problem, several different types of culture methods have been established [13, 14]. In Chapter IV, I developed a novel culture system in which PXB-cells maintain high hepatic function for at least 21 days. In this culture system, PXB-cells were plated on type I collagen-coated plates at high density (2.13×10^5 cells/cm^2) in the dHCGM medium we previously developed [15]. h-ALB secretion, CYP3A activity, and mRNA expression levels were compared among three types of PXB-cells isolated from three PXB-mice transplanted using different donors. PXB-cells cultured at high density displayed stable production of h-ALB and CYP3A activities for at least 21 days. The mRNA expression levels of 10 of 13 CYP, UGT, and transporters were maintained at >10% of the levels of freshly isolated PXB-cells after 21 days. From 1 week, many bile canaliculi were observed between PXB-cells, and the accumulation of the MRP and BSEP in these bile canaliculi was clearly inhibited by cyclosporin A.

Several previous studies have reported that cultured cell density could affect hepatocyte-specific functions in h-hepatocytes [16], rat hepatocytes [17], and HepaRG [18]. Regardless of the culture models

and hepatocyte sources, the cell density of cultured hepatocytes might be one of the most essential factors for the maintenance of liver-specific functions *in vitro*. I predicted that the high density culture of PXB-cells should generate long-term high liver function levels. To test this hypothesis, PXB-cells were cultured at both high density and low density, and the gene expression levels were compared using microarray analysis. The mRNA expressions of 1247 genes, including phase I and II metabolic enzymes and transporter genes, were significantly up-regulated in the high density culture conditions compared to low density conditions. Nuclear receptor (NR) pathways were significantly overrepresented following pathway analysis of the 1247 genes. The mRNA expression levels of HNF4α and six NRs (LXR, PXR, AR, LRH-1, SHP1 and CAR), which are up streams of several CYP, UGT and transporter genes, were up-regulated in high density culture. The mRNA expression of HNF4α, PXR, and FXR in high density culture at 21 days were maintained at similar levels to the freshly isolated PXB-cells, while the level of CAR mRNA decreased to approximately 10% of the level in freshly isolated PXB-cells. I demonstrated that PXB-cells cultured at a high density could stably maintain several hepatic functions for long periods, using a conventional culture method with collagen-coated plates.

These results suggested PXB-cells are a valuable tool for *in vitro* drug development studies including metabolic and pharmaco-toxicological studies.

Previously, the *in vitro* culture method using induced pluripotent stem cells (iPSCs) was developed for obtaining large number of differentiated human hepatocytes [19]. This method using iPSCs requires a step for propagating undifferentiated cells and several steps for differentiation of the undifferentiated cells into hepatocytes by gene transfer or culturing them in the specified culture medium. In addition, the functions of hepatocytes obtained from iPSCs were not sufficient compared with mature human hepatocytes. On the

other hand, spheroid culture of CF-PHs and PXB-cells have high hepatic functions similar to mature human hepatocytes *in vitro*.

It was concluded that the present studies clarified the important culture conditions for supplying large number of functional human hepatocytes for research of drug discovery.

References

1) Hewitt NJ, Lechon MJ, Houston JB, Hallifax D, Brown HS, Maurel P, et al. Primary hepatocytes: current understanding of the regulation of metabolic enzymes and transporter proteins, and pharmaceutical practice for the use of hepatocytes in metabolism, enzyme induction, transporter, clearance, and hepatotoxicity studies. Drug Metab Rev. 2007;39(1):159-234. Epub 2007/03/17. doi: 10.1080/03602530601093489. PubMed PMID: 17364884.

2) Soars MG, McGinnity DF, Grime K, Riley RJ. The pivotal role of hepatocytes in drug discovery. Chem Biol Interact. 2007;168(1):2-15. Epub 2007/01/09. doi: 10.1016/j.cbi.2006.11.002. PubMed PMID: 17208208.

3) Gomez-Lechon MJ, Lahoz A, Gombau L, Castell JV, Donato MT. *In vitro* evaluation of potential hepatotoxicity induced by drugs. Curr Pharm Des. 2010;16(17):1963-77. Epub 2010/03/20. doi: 10.2174/138161210791208910. PubMed PMID: 20236064.

4) Godoy P, Hewitt NJ, Albrecht U, Andersen ME, Ansari N, Bhattacharya S, et al. Recent advances in 2D and 3D *in vitro* systems using primary hepatocytes, alternative hepatocyte sources and non-parenchymal liver cells and their use in investigating mechanisms of hepatotoxicity, cell signaling and ADME. Arch Toxicol. 2013;87(8):1315-530. Epub 2013/08/27. doi: 10.1007/s00204-013-1078-5. PubMed PMID: 23974980; PubMed Central PMCID: PMCPMC3753504.

5) Wilkening S, Stahl F, Bader A. Comparison of primary human hepatocytes and hepatoma cell line Hepg2 with regard to their biotransformation properties. Drug Metab Dispos. 2003;31(8):1035-42. Epub 2003/07/18. doi: 10.1124/dmd.31.8.1035. PubMed PMID: 12867492.

6) Sauer V, Roy-Chowdhury N, Guha C, Roy-Chowdhury J. Induced pluripotent stem cells as a source of hepatocytes. Curr Pathobiol Rep. 2014;2(1):11-20. doi: 10.1007/s40139-013-0039-2. PubMed PMID: 25650171; PubMed Central PMCID: PMCPMC4312414.

7) Nishimura M, Ueda N, Naito S. Effects of dimethyl sulfoxide on the gene induction of cytochrome P450 isoforms, UGT-dependent glucuronosyl transferase isoforms, and ABCB1 in primary culture of human hepatocytes. Biol Pharm Bull. 2003;26(7):1052-6. Epub 2003/07/05. doi: 10.1248/bpb.26.1052. PubMed PMID: 12843640.

8) Tateno C, Yoshizane Y, Saito N, Kataoka M, Utoh R, Yamasaki C, et al. Near completely humanized liver in mice shows human-type metabolic responses to drugs. Am J Pathol. 2004;165(3):901-12. Epub 2004/08/28. doi: 10.1016/s0002- 52 9440(10)63352-4. PubMed PMID: 15331414; PubMed Central PMCID: PMCPmc1618591

9) Tateno C, Kawase Y, Tobita Y. Hamamura S, Ohshita H, Yokomichi H, et al. Generation of novel chimeric mice with humanized livers by using hemizygous cDNA-uPA/SCID mice. PLoS One. 2015;10(11): e0142145. doi: 10.1371/journal.pone.0142145. PubMed PMID: 26536627.

10) Tateno C, Miya F, Wake K, Kataoka M, Ishida Y, Yamasaki C, et al. Morphological and microarray analyses of human hepatocytes from xenogeneic host livers. Lab Invest. 2013;93(1):54-71. Epub 2012/11/14. doi: 10.1038/labinvest.2012.158. PubMed PMID: 23147226.

11) Nishimura M, Ueda N, Naito S. Effects of dimethyl sulfoxide on the gene induction of cytochrome P450 isoforms, UGT-dependent glucuronosyl transferase isoforms, and ABCB1 in primary culture of human hepatocytes. Biol Pharm Bull. 2003;26(7):1052-6. Epub 2003/07/05. doi: 10.1248/bpb.26.1052. PubMed PMID: 12843640.

12) Soldatow VY, Lecluyse EL, Griffith LG, Rusyn I. *In vitro* models for liver toxicity testing. Toxicol Res (Camb). 2013;2(1):23-39. doi: 10.1039/C2TX20051A. PubMed PMID: 23495363; PubMed Central PMCID: PMCPMC3593300.

13) Chan TS, Yu H, Moore A, Khetani SR, Tweedie D. Meeting the challenge of predicting hepatic clearance of compounds slowly metabolized by cytochrome P450 using a novel hepatocyte model, HepatoPac. Drug Metab Dispos. 2013;41(12):2024-32. doi: 10.1124/dmd.113.053397. PubMed PMID: 23959596.

14) Bell CC, Hendriks DF, Moro SM, Ellis E, Walsh J, Renblom A, et al. Characterization of primary human hepatocyte spheroids as a model system for drug-induced liver injury, liver function and disease. Sci Rep. 2016;6:25187. doi: 10.1038/srep25187. PubMed PMID: 27143246; PubMed Central PMCID: PMCPMC4855186.

15) Ishida Y, Yamasaki C, Yanagi A, Yoshizane Y, Fujikawa K, Watashi K, et al. Novel robust *in vitro* hepatitis B virus infection model using fresh human hepatocytes isolated from humanized mice. Am J Pathol. 2015;185(5):1275-85. doi: 10.1016/j.ajpath.2015.01.028. PubMed PMID: 25791527.

16) Greuet J, Pichard L, Ourlin JC, Bonfils C, Domergue J, Le Treut P, et al. Effect of cell density and epidermal growth factor on the inducible expression of CYP3A and CYP1A genes in human hepatocytes in primary culture. Hepatology (Baltimore, Md). 1997;25(5):1166-75. Epub 1997/05/01. doi: 10.1002/hep.510250520. PubMed PMID: 9141435.

17) Nakazawa K, Shinmura Y, Yoshiura Y, Sakai Y. Effect of cell spot sizes on micropatterned cultures of rat hepatocytes. Biochem Eng J. 2010;53(1):85-91. doi: 10.1016/j.bej.2010.09.013.

18) Le Vee M, Jigorel E, Glaise D, Gripon P, Guguen-Guillouzo C, Fardel O. Functional expression of sinusoidal and canalicular hepatic drug transporters in the differentiated human hepatoma HepaRG cell line. Eur J Pharm Sci. 2006;28(1-2):109-17. Epub 2006/02/21. doi: 10.1016/j.ejps.2006.01.004. PubMed PMID: 16488578.

19) Takayama, K., Inamura, M., Kawabata, K., Katayama, K., Higuchi, M., Tashiro, K., Nonaka, A., Sakurai, F., Hayakawa, T. and Mizuguchi, H. (2012). Efficient generation of functional hepatocytes from human embryonic stem cells and induced pluripotent stem cells by HNF4α transduction. Molecular Therapy, 20(1), 127-137.